

DOE/BC/14994
(DE96001289)

CT IMAGING TECHNIQUES FOR TWO-PHASE AND THREE-PHASE IN-SITU SATURATION MEASUREMENTS

SUPRI TR 107 Report

By
Bakul C. Sharma
William E. Brigham
Louis M. Castanier

June 1997

Performed Under Contract No. DE-FG22-96BC14994

Stanford University
Stanford, California



National Petroleum Technology Office
U. S. DEPARTMENT OF ENERGY
Tulsa, Oklahoma

DISCLAIMER

This report was prepared as an account of work sponsored by an agency of the United States Government. Neither the United States Government nor any agency thereof, nor any of their employees, makes any warranty, expressed or implied, or assumes any legal liability or responsibility for the accuracy, completeness, or usefulness of any information, apparatus, product, or process disclosed, or represents that its use would not infringe privately owned rights. Reference herein to any specific commercial product, process, or service by trade name, trademark, manufacturer, or otherwise does not necessarily constitute or imply its endorsement, recommendation, or favoring by the United States Government or any agency thereof. The views and opinions of authors expressed herein do not necessarily state or reflect those of the United States Government.

This report has been reproduced directly from the best available copy.

Available to DOE and DOE contractors from the Office of Scientific and Technical Information, P.O. Box 62, Oak Ridge, TN 37831; prices available from (615) 576-8401.

Available to the public from the National Technical Information Service, U.S. Department of Commerce, 5285 Port Royal Rd., Springfield VA 22161

DOE/BC/14994
Distribution Category UC-122

CT Imaging Techniques For Two-Phase And Three-Phase In-Situ
Saturation Measurements

SUPRI TR 107 Report

By
Bakul C. Sharma
William E. Brigham
Louis M. Castanier

June 1997

Work Performed Under Contract No. DE-FG22-96BC14994

Prepared for
U.S. Department of Energy
Assistant Secretary for Fossil Energy

Thomas Reid, Project Manager
National Petroleum Technology Office
P.O. Box 3628
Tulsa, OK 74101

Prepared by:
Stanford University
Stanford, California

Table of Contents

	Page No.
LIST OF FIGURES	iv
LIST OF TABLES	vi
ACKNOWLEDGEMENTS	vi
ABSTRACT	vii
1. INTRODUCTION	1
2. CT IMAGING TECHNIQUE	4
2.1 The Picker's Synerview 1200X Scanner	4
2.1.1 Special Features of the Scanner	5
3. EXPERIMENTAL SETUP	6
3.1 Injection End	6
3.2 3D Steam Model	6
3.2.1 Locations of Thermocouples and Pressure Taps	10
3.3 Production End	10
4. METHODOLOGY FOR SATURATION MEASUREMENTS	11
4.1 Porosity	11
4.2 Two-Phase Saturation Measurements Using Single Energy	11
4.3 Three-Phase Saturation Measurements Using Dual Energy	12
4.4 Error Analysis	14
4.4.1 Error in Two-Phase Saturation Measurement	14
4.4.2 Errors in Three-Phase Saturation Measurements	16
5. WATER AND STEAM FLOOD EXPERIMENTS	22
5.1 Experimental Procedure	22
5.1.1 General Experimental Procedure	22

5.1.2	CT Scan Procedure	23
5.2	Saturation Calculations	28
5.3	Heat Transfer Calculations	28
6.	RESULTS and DISCUSSIONS	32
6.1	Experiments Without Using Dopant	32
6.2	Experiments Using Dopants	32
6.2.1	Waterflood Experiments	33
6.2.2	Steamflood Experiments	41
7.	CONCLUSIONS	55
8.	RECOMMENDATIONS	56
	REFERENCES	57
APPENDIX A	3D Model Operating Principles	61
APPENDIX B	Computer Program For The Pressure Transducer Calibration	78
APPENDIX C	Computer Program For Data Logging	84
APPENDIX D	Computer Program For Data Preparation For Sectional Temperature Distributions	97
APPENDIX E	Computer Programs For 2-Phase and 3-Phase Saturation Measurements	99

List of Figures

	Page No.
3.1 Schematic Flow Diagram of the Experimental Setup	7
3.2 Location of Thermocouples and Pressure Taps Along Injector Producer Cross-Section of the 3D Model	8
3.3 A-A' Cross-section of the Injection Well	9
3.4 Areal Locations of Thermocouples and Pressure Taps of 3D Model	9
5.1 Scan Slices in the 3D Model	24
5.2 Composite Wall Representation of the Insulation	24
6.1 Average Oil Saturations in the Model During Waterflood Experiments	34
6.2 Average Water Saturation Distributions in Slice 1 During Waterflood Experiment	35
6.3 Oil and Water Saturation Distributions in Slice 2 During Waterflood Experiment	36
6.4 Oil and Water Saturation Distributions in Slice 3 During Waterflood Experiment	37
6.5 Oil and Water Saturation Distributions in Slice 4 During Waterflood Experiment	38
6.6 Oil and Water Saturation Distributions in Slice 5 During Waterflood Experiment	39
6.7 Oil and Water Saturation Distributions in Slice 6 During Waterflood Experiment	40
6.8 Heat Transfer During Steamflood Experiments	42
6.9 Oil Recovery at Various Stages of the Experiments	45
6.10 Temperature and Saturation Distributions in Slice 1 During Steamflood Experiments	46
6.11 Temperature and Saturation Distributions in Slice 2 During Steamflood Experiments	47
6.12 Temperature and Saturation Distributions in Slice 3 During Steamflood Experiments	48

6.13	Temperature and Saturation Distributions in Slice 4 During Steamflood Experiments	49
6.14	Temperature and Saturation Distributions in Slice 5 During Steamflood Experiments	50
6.15	Temperature and Saturation Distributions in Slice 6 During Steamflood Experiments	51
6.16	Areal Temperature Distributions During Steamflood Experiments	52
6.17	Average Oil Saturations in the Model During Steamflood Experiments	53
6.18	Average Water Saturations in the Model During Steamflood Experiments	54
A.1	Schematic of the Control Panel	62
A.2	Valves on the Control Panel	63
A.3	Demodulators and Heater Controllers Port of the Control Panel	63
A.4	Sideview of the Control Panel	66
A.5	Schematic of Signal Connection System	67
A.6	Schematic of Injection Side Connections of 3D Model	72
A.7	Connections Schematic	74
A.8	Screen Appearance During Pressure Transducers Calibration	76
A.9	Screen Appearance During Data Logging	76

List of Tables

	Page No.
4.1 Measured CT Numbers, and the Resulting Error in the Computation of S_o	16
4.2 Typical Experimental Values of CT Numbers Used in Eqs. 4.33 and 4.42	20
4.3 Error in S_o Due to Error in CT Number Measurement	20
4.4 Error in S_g Due to Error in CT Number Measurement	20
5.1 CT Scanner Settings for Steamflood Experiments	25
6.1 Comparison of Error in S_o , Obtained Using Material Balance, With Those Using Eq. 4.23	33
6.2 Comparison of Error in S_o , Obtained Using Material Balance, With Those Using Eq. 4.33	43
6.3 Error in S_w Using Material Balance	43
A.1 Signal Connections on Signal Port 1	69
A.2 Signal Connections on Signal Port 2	70
A.3 Signal Connections on Signal Port 3	71

Acknowledgements

The author is grateful for the financial support from the U.S. Department of Energy through grant DE-FG22-96BC14994 and from the SUPRI A Industrial Affiliates Program.

Abstract

The aim of this research is to use the SUPRI 3D steam injection laboratory model to establish a reliable method for 3-phase in-situ saturation measurements, and thereafter investigate the mechanism of steamflood at residual oil saturation.

Demiral et al. (1992) designed and constructed a three dimensional laboratory model that can be used to measure temperature, pressure and heat loss data. The model is also designed so that its construction materials are not a limiting factor for CT scanning. We have used this model for our study. In this study, we saturated the model with mineral oil, and carried out waterflood until residual oil saturation. Steamflood was then carried out. A leak appeared at the bottom of the model. Despite this problem, the saturation results, obtained by using 2-phase and 3-phase saturation equations and obtained from the Cat scanner, were compared with the saturations obtained from material balance. The errors thus obtained were compared with those obtained by an error analysis carried out on the saturation equations.

This report gives details of the experimental procedures, the data acquisition and data processing computer programs, and the analysis of a steamflood experiment carried out at residual oil saturation.

1. INTRODUCTION

The aim of this research is to use the SUPRI 3D steam injection laboratory model to establish a reliable method for 3-phase in-situ saturation measurements, and thereafter investigate the mechanism of steamflood at residual oil saturation.

Computerized Tomography is a powerful tool for non-destructive measurement of variables in rock properties and fluid saturations in reservoir rocks. Many researchers have used CT scanners in the past for measurement of two-phase and three-phase fluid saturations. But most of the procedures developed are not accurate enough to be of any real help in computing saturations in three-phase displacement experiments. In most of the past studies, equations for computation of fluid saturations required the CT attenuation value of each pure component, which was assumed constant (Vinegar, 1986). This value is actually dependent on the location of the voxel in the model.

To develop a reliable method for measurement of in situ fluid saturations, we have tried to reduce all the possible sources of error. We have developed equations that no longer have pure component CT attenuation terms. Since three-phase saturation measurements require dual energy scanning at each location and time period, the time interval between the two scans at the two energy levels should be as small as possible. This condition was well satisfied in our study by using a modified fourth generation PICKER's Synerview 1200X scanner that can do the two scans at an interval of four seconds.

Although CT scanners have been used to investigate the mechanisms of some EOR processes, these experiments were mainly carried out in linear models, with only a few 3D ones (Demiral *et al.*, 1992). Linear models lead to poor representation of phenomena such as gravity override and channeling. On the other hand, CT scanners are usually not used for applications where high temperature and pressure play an important role in the recovery mechanism, as they do in thermal recovery processes. This is because the high pressures and temperatures, involved in laboratory simulation of thermal EOR methods, require metallic core holders, making it difficult to use X-ray absorption techniques. Demiral *et al.* (1992) designed and constructed a three dimensional laboratory model that can be used to measure temperature, pressure and heat loss data. The model is also designed so that its construction materials are not a limiting factor for CT scanning. We have used this model for our study.

In this study, we saturated the model with mineral oil, and carried out waterflood until residual oil saturation. Steamflood was then carried out. The saturation results, obtained by using two-phase and three-phase saturation equations, were compared with the saturations obtained from material balance. The errors thus obtained were compared with those obtained by an error analysis carried out on the saturation equations.

This report gives details of the experimental procedures, the data acquisition and data processing computer programs, and the analysis of a steamflood experiment carried out at residual oil saturation.

Invented for medical purposes (Haunsfield, 1972), X-ray Computerized Tomography has developed, both clinically and technically, at an unprecedented rate. CT scanners have been heavily used in petroleum engineering applications. The CT-scanner is a useful tool for rock description and core analysis [Bergosh *et al.* (1985), Hornapur *et al.* (1985), Hornapur *et al.* (1986), Hunt *et al.* (1988), Narayanan and Deans (1988), Gilliland and Coles (1989), Sprunt (1989), Raynaud *et al.* (1989), Fabre *et al.* (1989), Jasti *et al.* (1990), Kantzas (1990), Moss *et al.* (1990), Peters and Afzal (1992), Johns *et al.* (1993)]. These include determination of fractures and heterogeneities, bulk density and porosity measurement, visualization of fluid displacements, viscous fingering and gravity segregation, lithologic characterization, evaluation of damage in unconsolidated cores and thin section analysis of cores.

The CT can be used for determination of in-situ saturations in the porous media. Wang *et al.* (1984) studied oil saturation distribution histories in Berea sandstone cores using CT scanning. Cromwell *et al.* (1984) performed two-phase displacement experiments and were able to locate the Buckley-Leverett shock front inside the core during the displacement of mineral oil by an iodine solution in Berea sandstone and Danian chalk cores. Wang *et al.* (1985) conducted two phase immiscible displacement experiments in unconsolidated cores and used a CT scanner to view the instabilities during displacement experiments. They demonstrated the use of CT scanning for observing oil displacements in laboratory corefloods. Vinegar (1986) discussed the application of CT scanning in multiphase flow experiments. Vinegar and Wellington (1987) conducted three phase flow experiments using CT imaging techniques during CO₂ injection. They suggested dual energy scans to determine the saturations of the fluids. At high energy Compton scattering dominates the X-ray adsorption, and at low energy photoelectric absorption is dominant. Thus the two equations of CT attenuation at the two energy levels are linearly independent

and therefore solvable. They also suggested dopants to sharpen the contrast and help identify individual fluids.

Application of CT in various coreflood experiments are discussed by many researchers. CT has proved to be an excellent technic to visualize flow phenomena in porous media, especially in heterogeneous (layered) systems [Withjack *et al.* (1990), Hicks *et al.* (1992), Hove *et al.* (1990), Peters and Hardham (1990), Auzerais *et al.* (1991), Withjack *et al.* (1991), Alvestad *et al.* (1992), Hicks *et al.* (1994)]. Fransham and Jelen (1987) investigated the displacement of a viscous oil by waterflooding in a linear sandpack. Hove *et al.* (1987) investigated uncertainties associated with methods used to obtain relative-permeability data. Withjack (1988) discussed the development and application of CT scanning for the determination of rock properties and conducted miscible displacement experiments in laboratory cores. MacAllister *et al.* (1990) conducted three-phase oil/water and gas/water experiments using CT scanner to investigate the dependence of relative permeability on wettability. They concluded that some traditional thinking about measuring relative permeability may be in error and merits further investigation. Hicks and Deans (1992) discussed the feasibility and limitations of CT scanning as a method for measuring residual oil saturations on a core sample..

Demiral *et al.* (1992) used CT imaging technic together with temperature and pressure measurements to follow the steam propagation during steam and steam-foam injection experiments in a three dimensional laboratory steam injection model. They concluded that in-situ saturation measurements are quite useful to help identify the flow mechanisms in the steam-foam process, and that CT scanning has proven to be a useful tool for thermal recovery laboratory research. Sameer *et al.* (1993) carried out simulation studies and compared the simulation results with the experimental results obtained by Demiral *et al.* They concluded that there is a fairly good agreement between the experimental results and the simulator output. Studies by Demiral *et al.* and Sameer *et al.* were carried out for two-phase saturations, without any oil in the model.

In this study, observations made by above researchers were used to establish a reliable method for three-phase (oil, water, and steam) in-situ saturation measurement, and thereafter investigate the mechanism of steamflood at residual oil saturation.

2. CT IMAGING TECHNIQUE

Computed tomography is a system which combines the physics of X-rays, computer technology, and reconstructive mathematics to produce diagnostic quality cross-sectional images. The first total body CT system was used in a clinical environment in 1974. There have been several generations of CT-scanners since then. The first generation scanners had a single-beam source and a detector. Second generation scanners used rotating multiple detectors, resulting in better image quality. Third generation scanners use a rotational fan-beam geometry with the source and detectors rotating together around the object. Fourth generation scanners use a fan-beam geometry with the source rotating within a fixed ring of detectors to gain higher resolution and to improve image quality. The current fifth generation scanners use a stationary-geometry method in which both the sources and the detectors are fixed, and the data is collected without any physical movement.

2.1 The PICKER's Synerview 1200X Scanner

The Synerview 1200X is a fourth generation scanner and produces detailed cross-sectional images of excellent quality. An image appears on the video screen as a filled in circle, and the image information is in a 512 by 512 matrix. Each pixel represents a CT number which is related to the average absorption coefficient of a spatial volume within the scanned field. The volume of each pixel varies according to scanned field size and beam thickness selections. The CT numbers are compared to water, which is assigned a value of zero. CT numbers range from -1000 for air to +1000 for dense bones.

During scanning, an X-ray source is collimated to provide a thin fan beam which is received by an array of crystal detectors. X-ray photons which strike these crystals cause them to produce light, the intensity of which is proportional to the number of photons received. When an object is placed in the beam between the source and the detector array, only those photons that are not absorbed by the object reach the detectors. The values thus attained represent the beam attenuation due to passage through the object.

The detectors are in a stationary array around the gantry. The X-ray beams are always directed through a collimator as the source moves around it in a circular path. At regular time intervals the detectors are read and the resulting data is stored in a computer. After all readings for a slice have been acquired and stored in a computer, the scanner mathematically reconstructs these images for viewing.

2.1.1 Special Features of The Scanner

The scanner has some special features as listed below:

- a. Selectable scan field size: 24 or 48 cm diameter.
- b. Selectable scanning speeds: 1 to 20 seconds for 48 cm field and 2 to 20 seconds for 24 cm field
- c. Time to process data (image reconstruction): 12 to 50 seconds
- d. Selectable X-ray voltage: 80 to 140 kV in steps of 5 kV
- e. Selectable X-ray intensity: 5 to 200 mA in steps of 15 mA
- f. Selectable slice spacing: 1 to 50 mm
- g. Selectable slice thickness: 1 to 10 mm
- h. Range of displayable CT numbers: -1000 to +4000

Detailed explanation of the above parameters, and their values used in our experiments are given in Section 5.1.2.

3. EXPERIMENTAL SETUP

The main experimental setup, as shown in Fig. 3.1, consists of three parts: injection system, 3D steam model, and production equipment. This is the equipment designed by Demiral *et al.* (1992). More details may be found in Demiral's report.

3.1 Injection End

Two liquid chromatography pumps are used to inject water or oil and to feed the steam generator with distilled water.

There is also a gas flow controller which can be used to inject nitrogen at a constant rate into the model during the experiments.

3.2 3D Steam Model

The 3D rectangular box with dimensions 20x20x7.5 cm represents one fourth of a five spot pattern. A cross-section of the 3D model is shown in Fig. 3.2. Some of its important features are listed below:

- (i) The top cover is designed such that the cover can compress the sand to assure that there is no gas cap above it.
- (ii) The injection well system allows injection of 100% steam through the total depth of the well. This is done by introducing a heater cartridge within an aluminum rod through which the steam flows. Figure 3.3 shows the detailed cross-section of the injector.
- (iii) The insulation and construction sequence used is Teflon, aluminum, Fiberfrax, from inside to outside. Teflon was used in contact with the porous medium because of chemical and temperature stability. Aluminum was necessary to support the Teflon for strength under the experimental pressure and temperature conditions. Aluminum was chosen as the construction material since it absorbs less X-ray than other metallic materials. Fiberfrax was chosen as the outermost layer because it is inexpensive, has low thermal conductivity and can be applied as a putty which air dries to a semi-permanent cast.

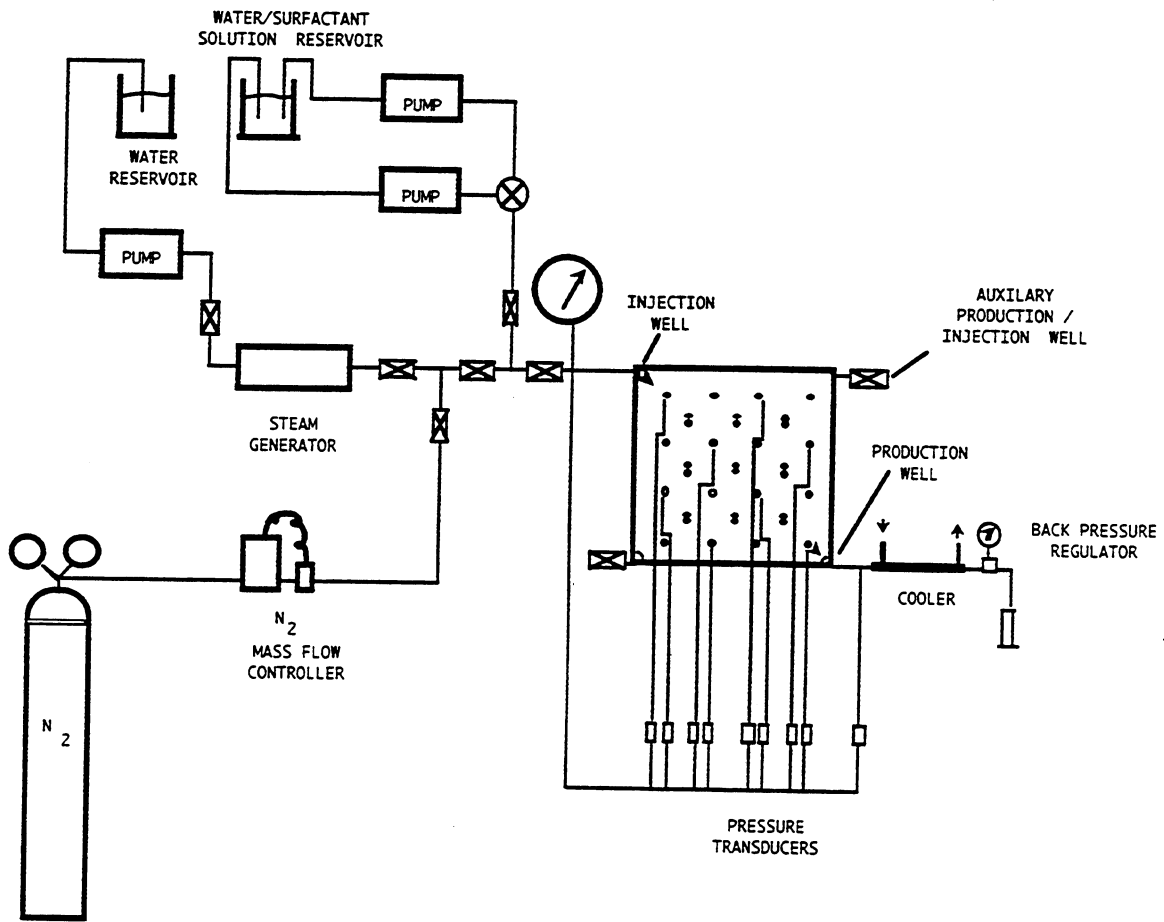


Figure 3.1: Schematic Flow Diagram of the Experimental Setup
 (Source: Demiral et al., 1992)

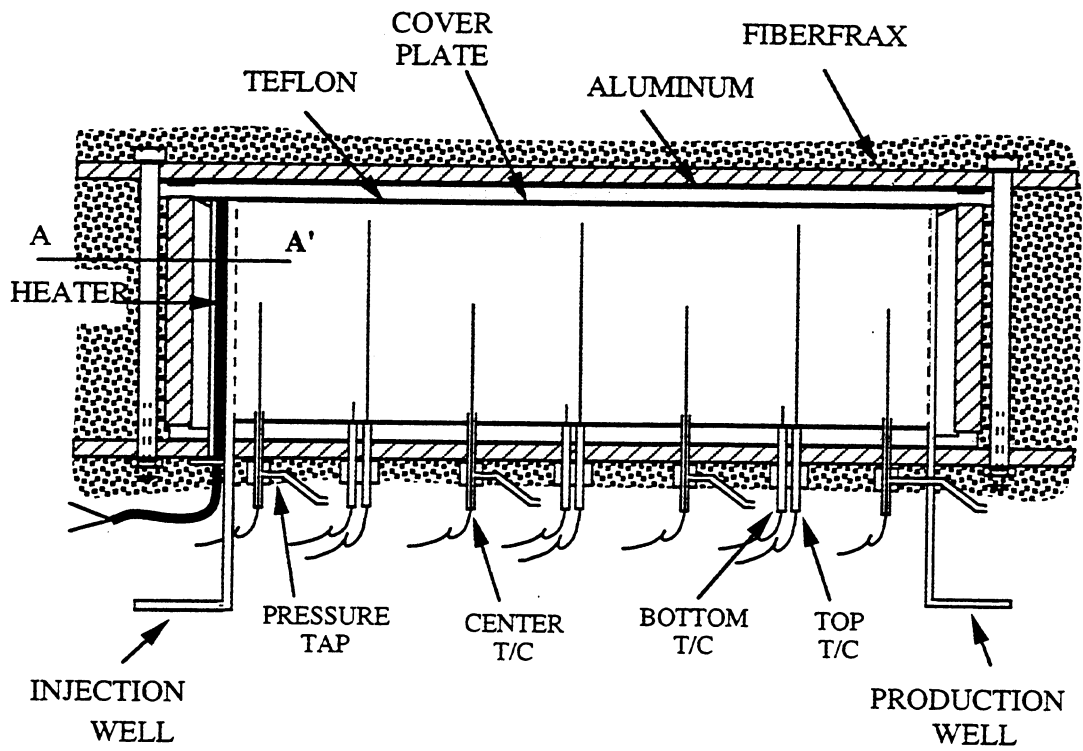


Figure 3.2: Location of Thermocouples and Pressure Taps Along Injector Producer Cross-Section of the 3D Model

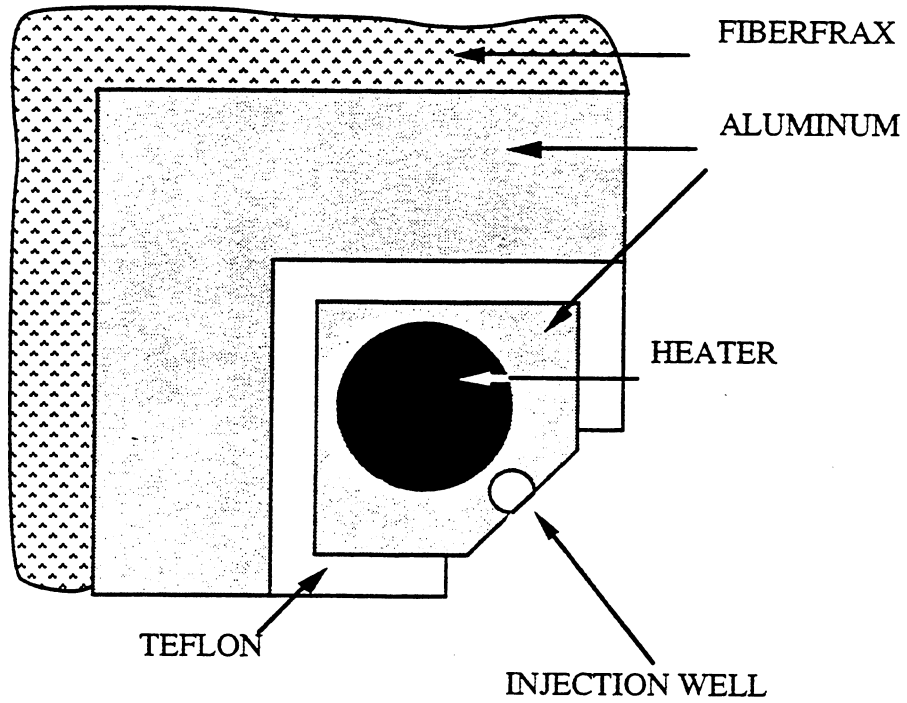


Figure 3.3: A-A' Cross-section of the Injection Well
 (Source: Demiral et al., 1992)

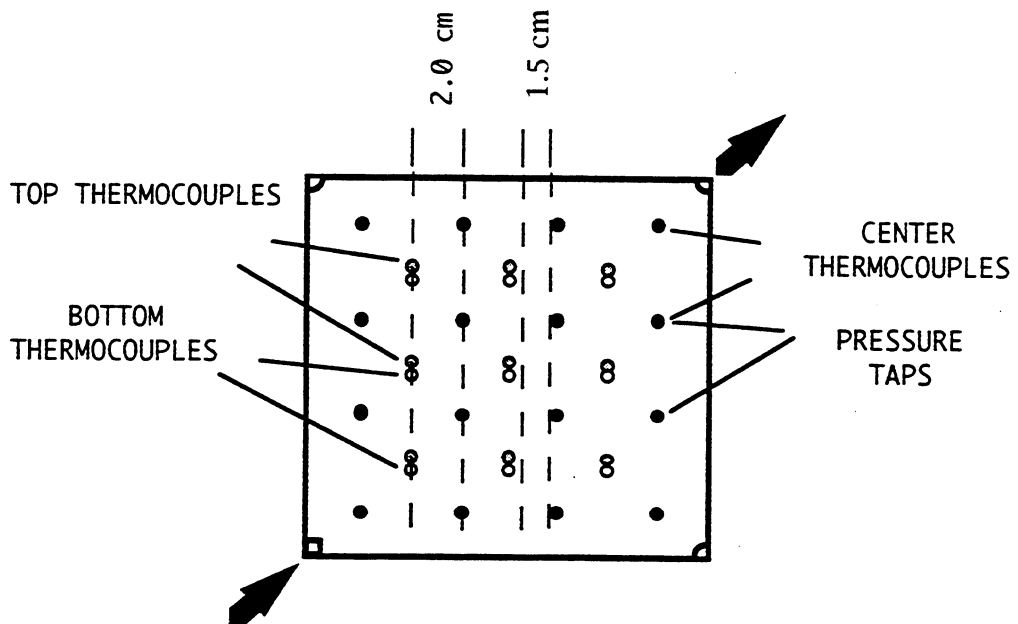


Figure 3.4: Areal Locations of Thermocouples and Pressure Taps of 3D Model
 (Source: Demiral et al., 1992)

- (iv) The pressure taps are located with the center thermocouples. A special tee fitting allows the use of thermocouple entry holes as outlets for the pressure lines.
- (v) Heat flux sensors are located at four sides and the top of the model. These were used to study the heat loss during the steam injection experiments. The general working principles of these sensors were discussed by Shallcross and Wood (1990).

3.2.1 Locations of Thermocouples and Pressure Taps

Thirty four type J thermocouples and sixteen pressure taps are distributed in the model as shown in Fig. 3.4. The sixteen center thermocouples are placed 1.5 inches from the bottom. The pressure taps are also located at the same places, but they read the pressure at the bottom of the model. Nine bottom and nine top thermocouples are placed symmetrically above and below the center line, 0.25 and 2.75 inches from the bottom of the model.

3.3 Production End

A back pressure regulator maintains a constant pressure at the producing corner of the model. A cooler is used to condense the produced steam. The volume of the liquid produced is measured at regular time intervals.

4. METHODOLOGY FOR SATURATION MEASUREMENTS

Methods were explored for measuring three-phase (steam, oil, and water) saturations using the CT scanner. While CT scanning at one X-ray energy level is adequate for porosity and two-phase saturation measurements, three-phase fluid saturation measurements require that the media be scanned at two different (dual) X-ray energy levels.

The equations for calculating porosity, and saturations using single and dual energy are given below:

4.1 Porosity

$$\emptyset = (CT_{wm} - CT_{am}) / (CT_w - CT_a) \quad (4.1)$$

where

\emptyset = Porosity

CT_{wm} = CT attenuation of 100% water saturated core, H.U.

CT_{am} = CT attenuation of dry core, H.U.

CT_w = CT attenuation of water, H.U.

CT_a = CT attenuation of air, H.U.

4.2 Two-Phase Saturation Measurements Using Single Energy

For waterflood experiments, the single energy method was used to calculate the saturations of water and oil. One of the major goals of this study was to reduce the error in the computation of saturations, which was mainly generated due to the assumption made in many past studies, that X-ray attenuation for a pure component is constant over the complete scan area. This goal was achieved by eliminating the need for pure component CT attenuation values.

For each voxel of the sample one can write the following equations, which describe the X-ray attenuation due to the combined effect of oil, water and rock matrix (all CT number measurements hereafter are made in the matrix). These equations assume that the CT saturations of a system containing both water and oil are linearly related to the saturation values.

$$CT_w S_w + CT_o S_o = CT_{wo} \quad (4.2)$$

and

$$S_w + S_o = 1 \quad (4.3)$$

where

CT_w = CT attenuation of 100% water saturated core, H.U.

CT_o = CT attenuation of 100% oil saturated core, H.U.

CT_{wo} = CT attenuation of fluid saturated core, H.U.

S_o = Saturation of oil in the matrix

S_w = Saturation of water in the matrix

By eliminating S_w from Eqs. 2 and 3, one obtains the value of S_o as:

$$S_o = \frac{CT_{wo} - CT_w}{CT_o - CT_w} \quad (4.4)$$

The only way to obtain the value of CT_o after scanning the water saturated core (to obtain CT_w) is, complete drying of the core followed by saturation of the core with oil. This process can be eliminated if we scan at S_{wc} (connate water saturation). The value of S_{wc} is easily obtained from material balance. At connate water saturation Eq. 4.2 can be written as:

$$CT_w S_{wc} + CT_o (1 - S_{wc}) = CT_{swc} \quad (4.5)$$

or

$$CT_o - CT_w = \frac{CT_{swc} - CT_w}{1 - S_{wc}} \quad (4.6)$$

where:

CT_{swc} = CT attenuation with core at connate water saturation

By eliminating CT_o from Eqs. 4.4 and 4.6, we obtain the value of S_o as:

$$S_o = \frac{(CT_{wo} - CT_w)(1 - S_{wc})}{(CT_{swc} - CT_w)} \quad (4.7)$$

4.3 Three-Phase Saturation Measurements Using Dual Energy

The equations for the dual energy case can be developed using a process similar to the single energy method. In our experiment energy levels of 100 and 140 keV were chosen. For each voxel one can write the following equations, which describe the X-ray attenuation

due to the combined effect of oil, water, steam and rock matrix:

$$(CT_w)_1 S_w + (CT_g)_1 S_g + (CT_o)_1 S_o = (CT_{wog})_1 \quad (4.8)$$

$$(CT_w)_2 S_w + (CT_g)_2 S_g + (CT_o)_2 S_o = (CT_{wog})_2 \quad (4.9)$$

$$S_w + S_o + S_g = 1 \text{ or } S_w = 1 - S_o - S_g \quad (4.10)$$

where:

- $(CT_{wog})_1$ = CT attenuation of fluid saturated core at 140 keV, H.U.
- $(CT_{wog})_2$ = CT attenuation of fluid saturated core at 100 keV, H.U.
- $(CT_w)_1$ = CT attenuation of 100% water saturated core at 140 keV, H.U.
- $(CT_w)_2$ = CT attenuation of 100% water saturated core at 100 keV, H.U.
- $(CT_g)_1$ = CT attenuation of dry core at 140 keV, H.U.
- $(CT_g)_2$ = CT attenuation of dry core at 100 keV, H.U.
- $(CT_o)_1$ = CT attenuation of 100% oil saturated core at 140 keV, H.U.
- $(CT_o)_2$ = CT attenuation of 100% oil saturated core at 100 keV, H.U.

Substituting the value of S_w from Eq. 4.10 into Eqs. 4.8 and 4.9, we get:

$$(CT_w)_1 (1 - S_o - S_g) + (CT_g)_1 S_g + (CT_o)_1 S_o = (CT_{wog})_1 \quad (4.11)$$

$$(CT_w)_2 (1 - S_o - S_g) + (CT_g)_2 S_g + (CT_o)_2 S_o = (CT_{wog})_2 \quad (4.12)$$

or

$$[(CT_g)_1 - (CT_w)_1] S_g + [(CT_o)_1 - (CT_w)_1] S_o = [(CT_{wog})_1 - (CT_w)_1] \quad (4.13)$$

$$[(CT_g)_2 - (CT_w)_2] S_g + [(CT_o)_2 - (CT_w)_2] S_o = [(CT_{wog})_2 - (CT_w)_2] \quad (4.14)$$

So, we have two equations with two unknowns S_g and S_o . Solving these equations we have the following expressions for saturations:

$$S_o = \frac{[(CT_{wog})_1 - (CT_w)_1][(CT_g)_2 - (CT_w)_2] - [(CT_{wog})_2 - (CT_w)_2][(CT_g)_1 - (CT_w)_1]}{[(CT_o)_1 - (CT_w)_1][(CT_g)_2 - (CT_w)_2] - [(CT_o)_2 - (CT_w)_2][(CT_g)_1 - (CT_w)_1]} \quad (4.15)$$

$$S_g = \frac{[(CT_{wog})_1 - (CT_w)_1][(CT_o)_2 - (CT_w)_2] - [(CT_{wog})_2 - (CT_w)_2][(CT_o)_1 - (CT_w)_1]}{[(CT_o)_2 - (CT_w)_2][(CT_g)_1 - (CT_w)_1] - [(CT_o)_1 - (CT_w)_1][(CT_g)_2 - (CT_w)_2]} \quad (4.16)$$

$$S_w = 1 - S_o - S_g \quad (4.17)$$

For the dual energy method Eq. 4.6 can be written as:

$$(CT_o)_1 - (CT_w)_1 = \frac{(CT_{swc})_1 - (CT_w)_1}{1 - S_{wc}} \quad (4.18)$$

$$(CT_o)_2 - (CT_w)_2 = \frac{(CT_{swc})_2 - (CT_w)_2}{1 - S_{wc}} \quad (4.19)$$

where:

$(CT_{swc})_1$ = CT attenuation of core at connate water saturation at 140 keV, H.U.

$(CT_{swc})_2$ = CT attenuation of core at connate water saturation at 100 keV, H.U.

Equations 4.15 and 4.16 in combination with Eqs. 4.18 and 4.19 were used for the measurement of saturations, thereby, eliminating the need for the measurement of CT attenuation values of oil saturated core (Please refer to the discussion in this regard for two phase saturation measurement).

4.4 Error Analysis

Error analysis was done on the value of oil saturation obtained at any pixel for both the two-phase saturation and the three-phase saturation cases.

4.4.1 Error in Two-Phase Saturation Measurement

From Eq. 4.4 we know that,

$$S_o = f(CT_{wo}, CT_w, CT_o)$$

Differentiating Eq. 4.4 with respect to each of the above variables, we get:

$$\frac{\delta S_o}{\delta CT_{wo}} = \frac{CT_o - CT_w}{(CT_o - CT_w)^2} \quad (4.20)$$

$$\frac{\delta S_o}{\delta CT_w} = \frac{CT_{wo} - CT_o}{(CT_o - CT_w)^2} \quad (4.21)$$

$$\frac{\delta S_o}{\delta CT_o} = \frac{CT_w - CT_{wo}}{(CT_o - CT_w)^2} \quad (4.22)$$

The total error in S_o , squared, is equal to the sum of the squares of the individual errors in S_o , as follows:

$$dS_o^2 = \left[\frac{\delta S_o}{\delta CT_{wo}} \cdot dCT_{wo} \right]^2 + \left[\frac{\delta S_o}{\delta CT_w} \cdot dCT_w \right]^2 + \left[\frac{\delta S_o}{\delta CT_o} \cdot dCT_o \right]^2 \quad (4.23)$$

where:

- dS_o = Absolute error in S_o
- dCT_{wo} = Absolute error in CT_{wo} measurement
- dCT_w = Absolute error in CT_w measurement
- dCT_o = Absolute error in CT_o measurement

The percentage error can therefore be written as:

$$\frac{100(dS_o)}{S_o}$$

Table 4.1 gives the error in S_o , using typical experimental values of CT numbers in Eq. 4.23, and assuming that the absolute error in CT number measurement is ± 1 CT unit (actual error will be smaller) at all times (Castanier, 1988).

In the following table we observe that the error in S_o due to CT_{wo} is constant at all the three oil saturations. This is because the equation for error in S_o due to CT_{wo} (Eq. 4.20) has terms that are constant throughout the experiment. Error due to CT_w increases with S_w , and error due to CT_o increases with S_o . This behavior is due to the numerators

in Eqs. 4.21 and 4.22. The total absolute error is almost the same in all the three cases, resulting in an increase in percentage error in S_o with decrease in oil saturation.

Table 4.1: Measured CT numbers, and the resulting error in the computation of S_o

S_o	expt. value of CT_{wo}	expt. value of CT_w	expt. value of CT_o	abs. err. in S_o due to CT_{wo}	abs. err. in S_o due to CT_w	abs. err. in S_o due to CT_o	absolute error in S_o	% error in S_o
0.30	256	200	400	.005	.0036	.0014	.0063	2.1
0.46	292	200	400	.005	.0027	.0023	.0061	1.3
0.89	372	200	400	.005	.0007	.0043	.0066	0.7

4.4.2 Errors in Three-Phase Saturation Measurements

From Eq. 4.15 we know that,

$$S_o = f[(CT_{wog})_1, (CT_{wog})_2, (CT_w)_1, (CT_w)_2, (CT_g)_1, (CT_g)_2, (CT_o)_1, (CT_o)_2]$$

Differentiating Eq. 4.15 with respect to each of the above variables, we get eight equations to define the error in S_o as follows:

$$\frac{\delta S_o}{\delta (CT_{wog})_1} = \frac{D[(CT_g)_2 - (CT_w)_2]}{D^2} \quad (4.24)$$

where, the term, D , is the denominator of Eq. 15, defined as follows:

$$D = [(CT_o)_1 - (CT_w)_1][(CT_g)_2 - (CT_w)_2] - [(CT_o)_2 - (CT_w)_2][(CT_g)_1 - (CT_w)_1]$$

$$\frac{\delta S_o}{\delta (CT_{wog})_2} = \frac{D[(CT_w)_1 - (CT_g)_1]}{D^2} \quad (4.25)$$

$$\frac{\delta S_o}{\delta (CT_w)_1} = \frac{D[(CT_{wog})_2 - (CT_g)_2] - N[(CT_o)_2 - (CT_g)_2]}{D^2} \quad (4.26)$$

where, the term, N , is the numerator of Eq. 4.15, defined as follows:

$$N = [(CT_{wog})_1 - (CT_w)_1][(CT_g)_2 - (CT_w)_2] - [(CT_{wog})_2 - (CT_w)_2][(CT_g)_1 - (CT_w)_1]$$

$$\frac{\delta S_o}{\delta (CT_w)_2} = \frac{D[(CT_g)_1 - (CT_{wog})_1] - N[(CT_g)_1 - (CT_o)_1]}{D^2} \quad (4.27)$$

$$\frac{\delta S_o}{\delta (CT_g)_1} = \frac{D[(CT_w)_2 - (CT_{wog})_2] - N[(CT_w)_2 - (CT_o)_2]}{D^2} \quad (4.28)$$

$$\frac{\delta S_o}{\delta (CT_g)_2} = \frac{D[(CT_{wog})_1 - (CT_w)_1] - N[(CT_o)_1 - (CT_w)_1]}{D^2} \quad (4.30)$$

$$\frac{\delta S_o}{\delta (CT_o)_1} = \frac{N[(CT_w)_2 - (CT_g)_2]}{D^2} \quad (4.31)$$

$$\frac{\delta S_o}{\delta (CT_o)_2} = \frac{N[(CT_g)_1 - (CT_w)_1]}{D^2} \quad (4.32)$$

The error in S_o , squared, is equal to the sums of the squares of the individual errors in Eqs. 4.24 through 4.32, as follows:

$$\begin{aligned} dS_o^2 = & \left[\frac{\delta S_o}{\delta (CT_{wog})_1} \cdot d(CT_{wog})_1 \right]^2 + \left[\frac{\delta S_o}{\delta (CT_{wog})_2} \cdot d(CT_{wog})_2 \right]^2 \\ & + \left[\frac{\delta S_o}{\delta (CT_w)_1} \cdot d(CT_w)_1 \right]^2 + \left[\frac{\delta S_o}{\delta (CT_w)_2} \cdot d(CT_w)_2 \right]^2 \\ & + \left[\frac{\delta S_o}{\delta (CT_g)_1} \cdot d(CT_g)_1 \right]^2 + \left[\frac{\delta S_o}{\delta (CT_g)_2} \cdot d(CT_g)_2 \right]^2 \\ & + \left[\frac{\delta S_o}{\delta (CT_o)_1} \cdot d(CT_o)_1 \right]^2 + \left[\frac{\delta S_o}{\delta (CT_o)_2} \cdot d(CT_o)_2 \right]^2 \end{aligned} \quad (4.33)$$

where:

$$\begin{aligned}
d(CT_{wog})_1 &= \text{Absolute error in } d(CT_{wog})_1 \text{ measurement} \\
d(CT_{wog})_2 &= \text{Absolute error in } d(CT_{wog})_2 \text{ measurement} \\
d(CT_w)_1 &= \text{Absolute error in } d(CT_w)_1 \text{ measurement} \\
d(CT_w)_2 &= \text{Absolute error in } d(CT_w)_2 \text{ measurement} \\
d(CT_g)_1 &= \text{Absolute error in } d(CT_g)_1 \text{ measurement} \\
d(CT_g)_2 &= \text{Absolute error in } d(CT_g)_2 \text{ measurement} \\
d(CT_o)_1 &= \text{Absolute error in } d(CT_o)_1 \text{ measurement} \\
d(CT_o)_2 &= \text{Absolute error in } d(CT_o)_2 \text{ measurement}
\end{aligned}$$

Thus Eq. 4.33 tells us the accuracy with which we can measure S_o . In a similar manner we can assess the accuracy of our measurement of S_g . From Eq. 4.16, we know that,

$$S_g = f[(CT_{wog})_1, (CT_{wog})_2, (CT_w)_1, (CT_w)_2, (CT_g)_1, (CT_g)_2, (CT_o)_1, (CT_o)_2]$$

Differentiating Eq. 4.16 with respect to each of the above variables, we again get eight equations to define the errors in S_g , as follows:

$$\frac{\delta S_g}{\delta(CT_{wog})_1} = \frac{D[(CT_o)_2 - (CT_w)_2]}{D^2} \quad (4.34)$$

$$\frac{\delta S_g}{\delta(CT_{wog})_2} = \frac{D[(CT_w)_1 - (CT_o)_1]}{D^2} \quad (4.35)$$

where, the term, D , is the denominator in Eq. 4.16, defined as follows:

$$\begin{aligned}
D &= [(CT_o)_2 - (CT_w)_2][(CT_g)_1 - (CT_w)_1] - [(CT_o)_1 - (CT_w)_1][(CT_g)_2 - (CT_w)_2] \\
\frac{\delta S_g}{\delta(CT_w)_1} &= \frac{D[(CT_{wog})_2 - (CT_o)_2] - N[(CT_g)_2 - (CT_o)_2]}{D^2} \quad (4.36)
\end{aligned}$$

where, the term, N , is the numerator on Eq. 4.16, defined as follows:

$$N = [(CT_{wog})_1 - (CT_w)_1][(CT_o)_2 - (CT_w)_2] - [(CT_{wog})_2 - (CT_w)_2][(CT_o)_1 - (CT_w)_1]$$

$$\frac{\delta S_g}{\delta (CT_w)_2} = \frac{D[(CT_o)_1 - (CT_{wog})_1] - N[(CT_o)_1 - (CT_g)_1]}{D^2} \quad (4.37)$$

$$\frac{\delta S_g}{\delta (CT_g)_1} = \frac{N[(CT_w)_2 - (CT_o)_2]}{D^2} \quad (4.38)$$

$$\frac{\delta S_g}{\delta (CT_g)_2} = \frac{N[(CT_o)_1 - (CT_w)_1]}{D^2} \quad (4.39)$$

$$\frac{\delta S_g}{\delta (CT_o)_1} = \frac{D[(CT_w)_2 - (CT_{wog})_2] - N[(CT_w)_2 - (CT_g)_2]}{D^2} \quad (4.40)$$

$$\frac{\delta S_g}{\delta (CT_o)_2} = \frac{D[(CT_{wog})_1 - (CT_w)_1] - N[(CT_g)_1 - (CT_w)_1]}{D^2} \quad (4.41)$$

The error in S_o , squared, is equal to the sums of the squares of the individual errors in Eqs. 4.34 through 4.41, as follows:

$$\begin{aligned} dS_g^2 = & \left[\frac{\delta S_g}{\delta (CT_{wog})_1} \cdot d(CT_{wog})_1 \right]^2 + \left[\frac{\delta S_g}{\delta (CT_{wog})_2} \cdot d(CT_{wog})_2 \right]^2 \\ & + \left[\frac{\delta S_g}{\delta (CT_w)_1} \cdot d(CT_w)_1 \right]^2 + \left[\frac{\delta S_g}{\delta (CT_w)_2} \cdot d(CT_w)_2 \right]^2 \\ & + \left[\frac{\delta S_g}{\delta (CT_g)_1} \cdot d(CT_g)_1 \right]^2 + \left[\frac{\delta S_g}{\delta (CT_g)_2} \cdot d(CT_g)_2 \right]^2 \\ & + \left[\frac{\delta S_g}{\delta (CT_o)_1} \cdot d(CT_o)_1 \right]^2 + \left[\frac{\delta S_g}{\delta (CT_o)_2} \cdot d(CT_o)_2 \right]^2 \end{aligned} \quad (4.42)$$

where:

$$dS_g = \text{Total Absolute error in } S_g$$

Table 4.2: Typical experimental values of CT numbers used in Eqs. 4.33 and 4.42.

S_o	$(CT_{wog})_1$	$(CT_{wog})_2$	$(CT_w)_1$	$(CT_w)_2$	$(CT_g)_1$	$(CT_g)_2$	$(CT_o)_1$	$(CT_o)_2$
0.30	239	125	200	100	-650	-750	400	250
0.21	83	-28	200	100	-650	-750	400	250
0.11	-208	-314	200	100	-650	-750	400	250

Shown below in Tables 4.3 and 4.4 are the absolute errors obtained in S_o and S_g , for a typical range of saturations, using Eqs. 4.33 and 4.42.

Table 4.3: Error in S_o due to error in CT number measurement.

S_o	abs. err. in S_o due to								total err.	
	$(CT_{wog})_1$	$(CT_{wog})_2$	$(CT_w)_1$	$(CT_w)_2$	$(CT_g)_1$	$(CT_g)_2$	$(CT_o)_1$	$(CT_o)_2$	abs.	%
0.30	.02	.02	.014	.014	0	0	.006	.006	.035	11.8
0.21	.02	.02	.012	.012	.004	.004	.004	.004	.034	16.1
0.11	.02	.02	.007	.007	.010	.010	.003	.003	.034	30.5

Table 4.4: Error in S_g due to error in CT number measurement.

S_g	abs. err. in S_g due to								total err.	
	$(CT_{wog})_1$	$(CT_{wog})_2$	$(CT_w)_1$	$(CT_w)_2$	$(CT_g)_1$	$(CT_g)_2$	$(CT_o)_1$	$(CT_o)_2$	abs.	%
0	.004	.005	.002	.003	-	-	.001	.001	.007	-
0.19	.004	.005	.002	.003	.001	.001	.001	.001	.007	3.7
0.55	.004	.005	.001	.002	.002	.002	.000	.001	.007	1.3

In Tables 4.3 and 4.4, due to reasons similar to that in two phase saturation measurement, we observe that errors in S_o and S_g due to $(CT_{wog})_1$ and $(CT_{wog})_2$ are constant at all

saturations. Similarly, errors in S_o and S_g due to $(CT_w)_1$ and $(CT_w)_2$ increase with S_w , errors due to $(CT_g)_1$ and $(CT_g)_2$ increase with S_g , and errors due to $(CT_o)_1$ and $(CT_o)_2$ increase with S_o . The total absolute error in S_o and S_g is almost the same (.034 and .007) at all the three saturations, resulting in higher error at lower saturations. We also notice that most of the error in saturation measurement is due to $(CT_{wog})_1$ and $(CT_{wog})_2$.

5. WATER AND STEAM FLOOD EXPERIMENTS

The model was initially packed with unconsolidated, -100 mesh size Ottawa sand. But, the packing did not appear to be stable. Therefore, the model was repacked with unconsolidated, 28-35 mesh size, Ottawa sand. The latter packing, with an average porosity of 30%, appeared to be stable throughout the experiment.

5.1 Experimental Procedure

The experimental procedure can most easily be discussed in two parts; general experimental procedure, and CT scanning procedure.

5.1.1 General Experimental Procedure

During the experiments the model was first saturated with distilled water, then either mineral oil with or without dopant was injected, to find out the effect of dopant on saturation measurements. The dopant used in our experiments was 1-bromo dodecane at 50% concentration during these waterflood and steamflood experiments. We considered 1-iodo dodecane as a possible dopant, but it is sensitive to light, and therefore was not used in our study, even though it is more effective in increasing the CT attenuation properties of the oil.

The oil was injected until the water saturation in the model was reduced to 0.1, the connate water saturation. At this stage waterflood was started, and the water injection rate was maintained at 6 ml/min. The waterflood was stopped when the oil production rate became less than 1% by volume of the produced fluids. The oil saturation in the model reached 0.3, the residual oil saturation.

Steamflooding was then started, and the steam was injected at a constant rate of 6 ml/min cold water equivalents. This was continued until the rate of drop of oil saturation in the model became negligible, i.e. the oil production rate became less than 1% by volume of the produced fluids. The pressure and temperature data was collected using a data logger. The masses of the produced fluids were measured every half hour using an electronic weigh balance.

During the steamflood experiments it was observed that about a quarter of steam injected leaked through a crack at the bottom of the model. This was later confirmed by the material balance and the heat balance results.

5.1.2 CT Scan Procedure

As discussed in Section 2.1, the CT scanner used in this study is a modified Picker International's Synerview 1200x scanner.

The quarter of a 5-spot model was scanned at six different locations during the experiments. These scans were taken through the 1.5 cm clearance (Fig 3.4) between the thermocouples. Fig 5.1 shows the locations of the six scan slices. All slices were scanned at dual energy level (140 keV and 100 keV), as is required for three-phase saturation measurements. The total scan time for six slices (i.e. twelve scans) is about four minutes. During the dual energy scans in this study the scanner moved the model automatically by a preset distance after scanning each slice at dual energy levels.

The model was first scanned dry after packing. The next scanning was done after saturating the sand with water. The third set of scanning was carried out with the model at connate water saturation. Thereafter scanning was done at regular intervals during waterflood and steamflood experiments.

The CT scanner settings were kept the same for all the experiments, and they are as shown in Table 5.1 on the following page. The terms used in the table are:

Calibration Mode: (ON/OFF) When turned on calibration scans are performed prior to scanning. Calibration must be performed when any of the parameters, namely, energy level, field size, slice thickness, X-ray filter, resolution, focal spot, sampling or scan angle is changed.

Scan Mode: (OFF/MAN/AUTO/DUAL) The various scan modes apply to dual energy scanning process. Primary and alternate voltage is applied to the X-ray tube in an alternating fashion. When this mode is turned off no scanning takes place. The three scan modes are:

Manual: In this mode each scan is done by depressing the start button.

Auto: In this mode the scans are initiated by the computer.

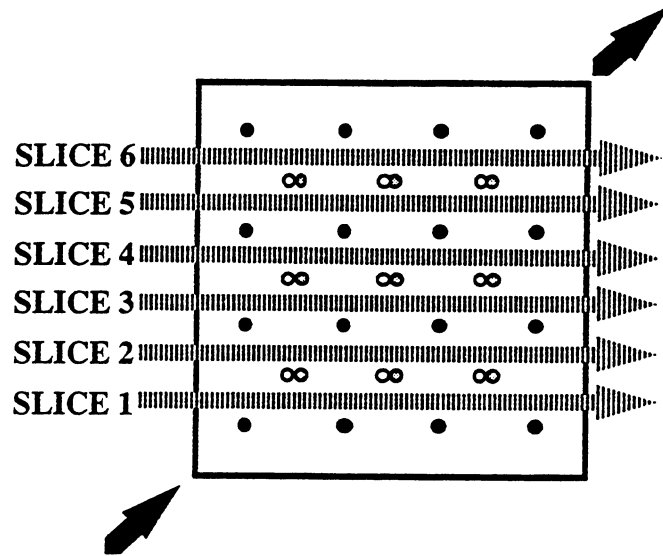


Figure 5.1: Scan Slices in the 3D Model
(Source: Demiral et al., 1992)

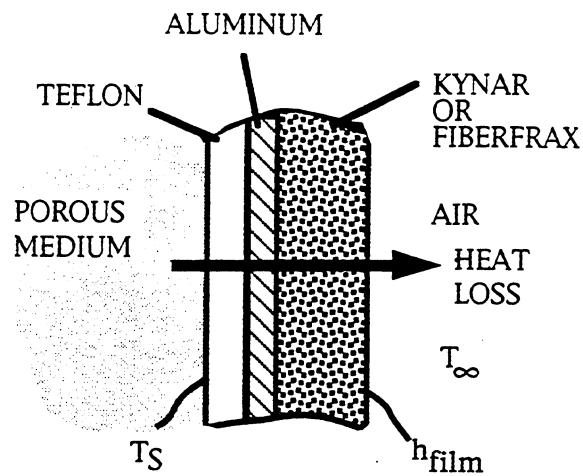


Figure 5.2: Composite Wall Representation of the Insulation
(Source: Demiral et al., 1992)

Dual: Dual mode allows for primary and alternate scans to be performed at a single location before moving the couch to the next position.

Table 5.1: CT scanner settings for steamflood experiments.

Calibration: ON/OFF	Scan Mode: DUAL	Process Mode: ON/OFF
Primary Technique	Field Size: FULL	Total Slices: 16
kV: 140	X-ray Filter: 1	Field of View: 48 cm
mA: 080	Pilot: OFF	Algorithm: o8
Recon: 2C53	Couch Index: -24 mm	Matrix: 512
Spectrum: 0F97	Speed: 03	Center X: 000o
Alternative Technique	Thickness: 05 mm	Center Y: 000o
kV: 100	Scan Rotation: 398 Deg	Image Rotation: 000 Deg
mA: 080	Resolution: HIGH	Dyn Cal: ON
Recon: 28C6	Sampling: 1024	Dyn Ref: ON
Spectrum: 1127	Focal Point: LARGE Anode Speed: LOW	

Process Mode: (ON/OFF) When process mode is turned off no image processing occurs. Otherwise, the images are processed using the variables specified in the process mode section.

Primary Technic: The primary technic is the first or the odd scan to be performed. The KV variable sets the voltage to be applied to the X-ray tube and the MA factor is the electric current applied to it. The reconstruction constant is a hex value that affects the base CT number. This value is normally calculated for a base line of 0 for water. The spectrum constant is used to correct for image bowling.

Alternate Technic: The alternate technic is the second or the even scan to be performed.

Field Size: (HALF/FULL) There are two scanning fields. Half field ranges from 6 to 24 cm and the full field from 24 to 48 cm. Large objects are scanned in full field.

X-Ray Filter: (C/1/2/3) The compensator is a filter which adjusts the concentration of the X-ray beams to conform to more unified beam wavelengths. The compensator is used with no additional filtration. Filter 1 is no added filtration to inherent filtration of 0.7 mm. Filter 2 is an additional 4.7 mm of aluminum added to the inherent. Filter 3 is 9.4 mm of added filtration.

Pilot: (OFF/HORZ/VERT) A pilot scan is a digital positioning aid that can be displayed in a horizontal or vertical view. The couch always moves out of the gantry during a pilot, regardless of the direction the couch will index during the study. It moves 256 mm in the half field and 512 mm in the full field.

Couch Index: (-50 to +50) The couch has a capability of incrementing -50 mm to +50 mm per index. If a negative number is entered, the table will move away from the gantry.

Scan Speed: (2 to 10) This is the time required for the X-ray tube to make one rotation. A scan speed of 2 produces a 2.2 second scan for the 230° scan angle, 3.2 second scan for the 360° scan and 3.6 second scan for 398° scan angle. To calculate the approximate exposure time for scans at other speeds, we multiply the factor of 1.1, 1.6 or 1.8 (depending on the scan angle being used) by the scan speed.

Thickness: (1 to 10) The slice thickness is variable from 1 to 10 mm. A slice thickness of less than 5 mm yields high spatial resolution and decreases the partial volume effect. A 5 mm slice thickness would produce a balance of contrast and spatial resolution.

Scan Rotation: (230/360/398) The scan rotation determines the degree of rotation of the X-ray tube. A scan angle of 230° produces the fastest scans. The 398° scan angle produces the highest resolution due to an overscan of 38°.

Resolution: (NORM/HIGH/UHR) Resolution pertains to the collimation of the crystal part of the detector. In normal resolution the detector aperture is 4 mm wide. Ultra high resolution (UHR) provides a detector aperture of 1.8 mm wide. This narrowing of the UHR results in increased spatial resolution.

Sampling: (512/1024) Determines the amount of data samples taken in a certain field size.

Focal Point: (SMAL/LARG) Small focal point is normally used for high spatial resolution and large is normally used for increased contrast resolution.

Anode Speed: (LOW/HIGH/AUTO) High speed is only necessary when a higher technic is used along with small focal point. Auto mode automatically chooses the proper anode speed for the technic that was selected.

Total Slices: (2 to 18) This is set for the total number of scans desired in one run.

Field of View: The field of view size is chosen for the diameter (in centimeters) of the total area to be reconstructed.

Algorithm: (1 to 12) An image algorithm is a software mathematical function that varies the amount of spatial and contrast resolution seen in an image. Spatial resolution is the ability to resolve very small objects within a given slice. Contrast resolution is the ability to resolve slight density differences within the area being examined.

Matrix: (256/512) The matrix size is the number of points or pixels across the diameter of the image used in construction of that image. The 512 matrix should be used whenever maximum resolution is desired.

Center X: (-256 to +256) This value is an offset from the center of the original scan field in the horizontal axis. It is used for specifying the center of the reconstruction circle.

Center Y: (-256 to +256) This value has the same effect as center X, except it applies in the vertical axis.

Image Rotation: (0 to 360) Reconstructed images may be rotated at any angle from 0 to 360 degrees.

Dyn Ref: (ON/OFF) On either side of the fan beam there are 5 detectors that reference and calibrate air lying at the edges of the fan beam. Dynamic reference checks each of these detectors during scanning motion and corrects for X-ray variations.

Dyn Cal: (ON/OFF) Dynamic calibration is similar to Dyn Ref except readings are used to correct for small detectors changes.

5.2 Saturation Calculations

Two-phase saturation equations as developed in Section 4.2 were used for the waterflood experiments. Three-phase saturation equations as developed in Section 4.3 were used for the steamflood experiment. Computer programs (Appendix E) were written for image processing, and a software called Photofinish was used to view the images.

5.3 Heat Transfer Calculations

The 3D model is surrounded by a composite heat insulator as shown in Fig. 5.2. The heat transfer is transient until 0.3 VP injection and thereafter attains steady state (Joshi *et al.*, 1993). Assuming that steady state heat transfer conditions prevail, and the heat transfer mechanism between the outer surface of the insulator and air is natural convection only.

Thermal resistance of this model can be written as:

$$R_t = \sum_{i=1}^3 \left[\frac{x}{kA} \right]_i + \frac{1}{h_f A} \quad (5.1)$$

Where:

- R_t = thermal resistance of the model, °F/Btu-hr⁻¹
- x = thickness of the shell, ft
- k = thermal conductivity, Btu/hr°Fft
- A = inside area, ft²
- h_f = film coefficient of heat transfer, Btu/hr°Fft²

Hence the rate of heat loss is:

$$Q_L = \frac{T_s - T_\infty}{\sum_{i=1}^3 \left[\frac{x}{kA} \right]_i + \frac{1}{h_f A}} \quad (5.2)$$

where:

T_s = inner surface temperature, °F

T_∞ = ambient temperature, °F

The cross-sectional area to heat flow for a 3D box is not constant but increases from inside to outside. Therefore the shape factor for a parallelepiped shell is used (Demiral *et al.*, 1992):

$$S = \frac{A_i}{x} + 2.16(a + b + c) + 1.2x \quad (5.3)$$

where:

A_i = inside area, ft²

a, b, c = inside dimensions, ft

x = thickness of the shell, ft

The rate of heat loss can therefore be written as:

$$Q_L = \frac{T_s - T_\infty}{\sum_{i=1}^3 \left[\frac{1}{kS} \right]_i + \frac{1}{h_f A_o}} \quad (5.4)$$

where:

S_1 = shape factor for Teflon, ft

S_2 = shape factor for aluminum, ft

S_3 = shape factor for Fiberfrax, ft

A_o = outside area of the 3D model, ft²

The total experimental rate of heat loss at any time is calculated by using the heat flux data and the equation below:

$$Q_L = \sum_{i=1}^4 [q_i A_j] + 2q_T A_T \quad (5.5)$$

where:

- q_i = instantaneous rate of heat loss from the heat flux sensors attached on the sides
- q_T = instantaneous rate of heat loss from the top heat flux sensor
- A_j = cross sectional area to heat flow adjacent to the corresponding sensor
- A_T = cross sectional area of the top surface

in Eq. 5.5, it was assumed that the rate of heat loss measured at the sensor location was the same everywhere on the side to which the sensor was attached. It was also assumed that the rate of heat loss from the top was equal to that from the bottom. This is why the term $q_T A_T$ is doubled.

The rate of heat lost to the produced fluids is:

$$Q_p = m_1 h_1 + m_2 h_2 \quad (5.6)$$

where:

- m_1 = production rate of water, lb/hr
- m_2 = production rate of oil, lb/hr
- h_1 = enthalpy of water at exit, Btu/lb
- h_2 = enthalpy of oil at exit, Btu/lb

The rate of heat input to the model is:

$$Q_i = m_s H_s \quad (5.7)$$

where:

- m_s = steam injection rate in water equivalents, lb/hr
- H_s = enthalpy of steam, Btu/lb

The overall heat balance at any time, t , can therefore be written as:

$$\int_0^t \dot{Q}_i = \int_0^t \dot{Q}_p + \int_0^t \dot{Q}_L \quad (5.8)$$

6. RESULTS and DISCUSSION

The model was initially packed with -100 mesh unconsolidated sand and scanned in a fully saturated condition. Then it was vacuumed to do dry scans. On scanning it was observed that the sand had collapsed in certain locations. So, these experiments had to be discontinued. The model was then repacked with coarser sand (28-35 mesh).

There were two sets of experiments carried out using the coarser sand. The first experiment use no dopant, and the second one was with doped mineral oil. The second experiment developed a leak at the bottom of the model. However, the experiment was completed and fluid saturations were computed as planned.

From the scanned images it was observed that the aluminum shell created a non uniform value of CT attenuation in the medium. It was also observed that there was a slight vertical displacement during the movement of the table in the horizontal direction. This led to a slight error in the saturation values obtained using the saturation equations.

6.1 Experiments Without Using Dopant

The saturation equations developed in Section 4.2 and 4.3 did not give reasonably accurate saturation values for water and oil using the scans obtained during these experiments. This was mainly because the values of CT attenuation due to oil and water in the sand were nearly the same. However, the steam saturation could be determined quite accurately because of the large difference in CT attenuation values of steam compared to those of mineral oil and water.

6.2 Experiments Using Dopants

The experiments involving doping of mineral oil were carried out successfully, and the results are discussed below in detail:

6.2.1 Waterflood Experiments

The average oil saturations (obtained from material balance and CT scanning) during the waterflood experiments are shown in Fig. 6.1. Waterflooding was stopped after 5.8 PV of water was injected. The oil saturation dropped from 0.89 to 0.30 (residual oil saturation). Table 6.1 gives the values of saturations obtained from material balance and CT scanning, experimental errors in S_o due to CT scanning, and the errors obtained using error analysis.

Table 6.1: Comparison of error in S_o , obtained using material balance, with those using Eq. 4.23.

PV Injected	S_o		Error in S_o (Expt.)		Error using Eq. 4.23	
	Mat. Bal.	CT Scan	Absolute	Percentage	Absolute	Percentage
0	0.89	0.86	0.03	3.4	0.0066	0.7
0.31	0.66	0.63	0.03	4.5		
0.72	0.53	0.56	0.03	5.7		
1.10	0.46	0.46	0	0	0.0061	1.3
1.50	0.42	0.40	0.02	4.8		
5.00	0.31	0.34	0.03	9.7		
5.80	0.30	0.28	0.02	6.7	0.0063	2.1

The values obtained by using the two-phase saturation equations developed in Section 4.2 compare well with those obtained from material balance. The saturation distributions generated using the saturation equations are shown in Figs. 6.2, 6.3, 6.4, 6.5, 6.6, and 6.7.

We also notice that some of the errors obtained in the measurement of S_o are slightly higher than the maximum expected errors using error analysis (Eq. 4.23). As discussed earlier, this could be due to the vertical displacement of the table or dense construction material of the shell.

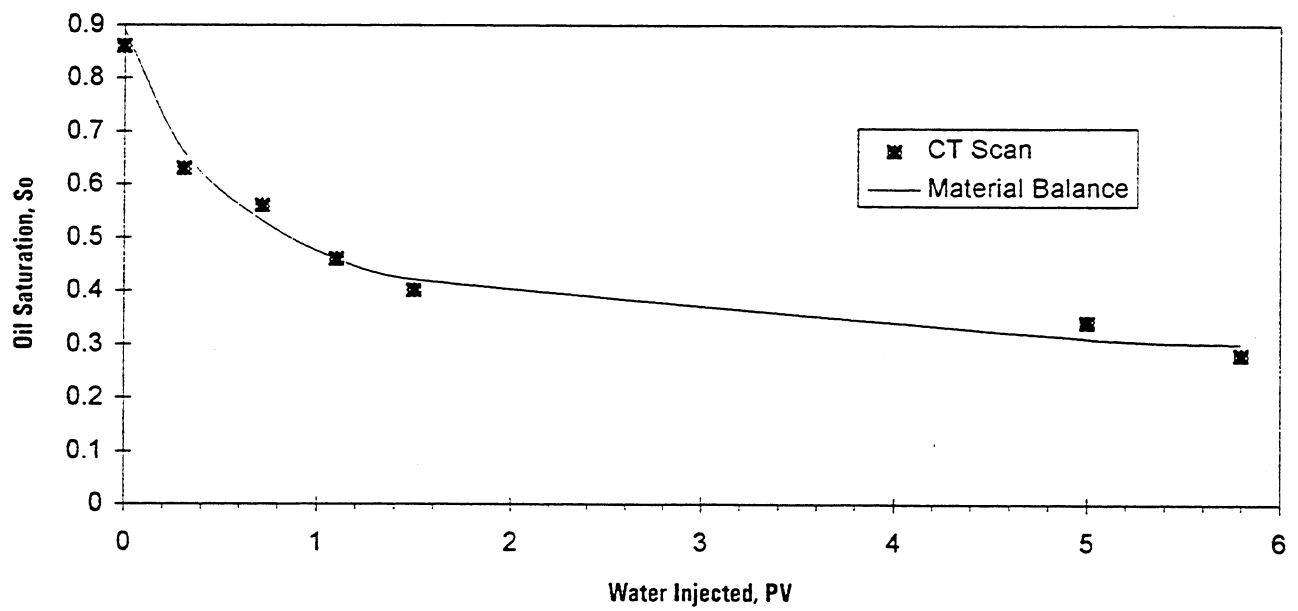
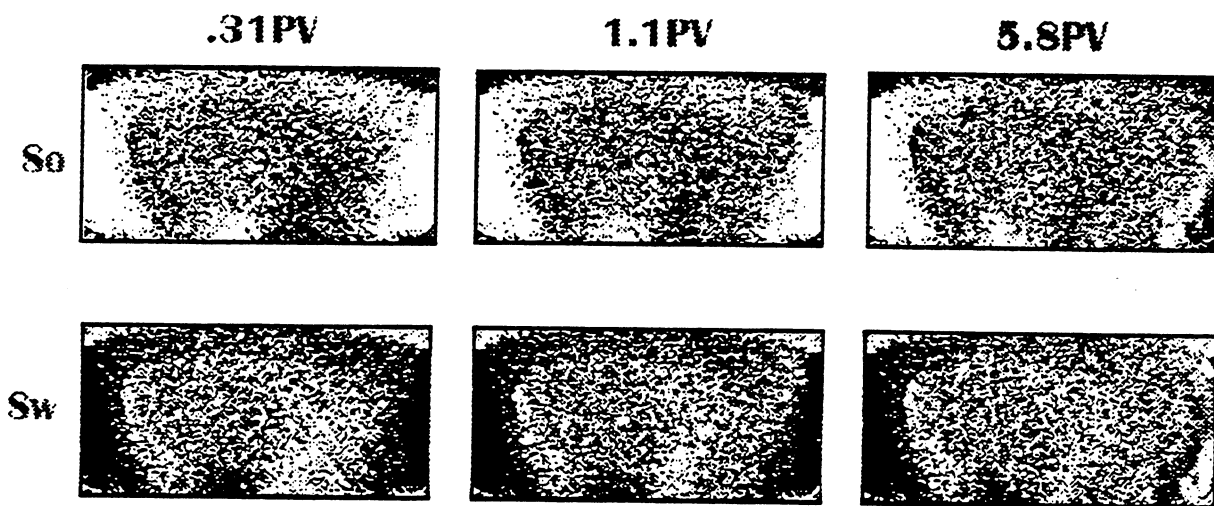


Figure 6.1: Average Oil Saturations in the Model During Waterflood Experiments



Waterflood(Slice1)

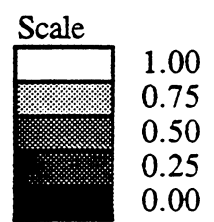
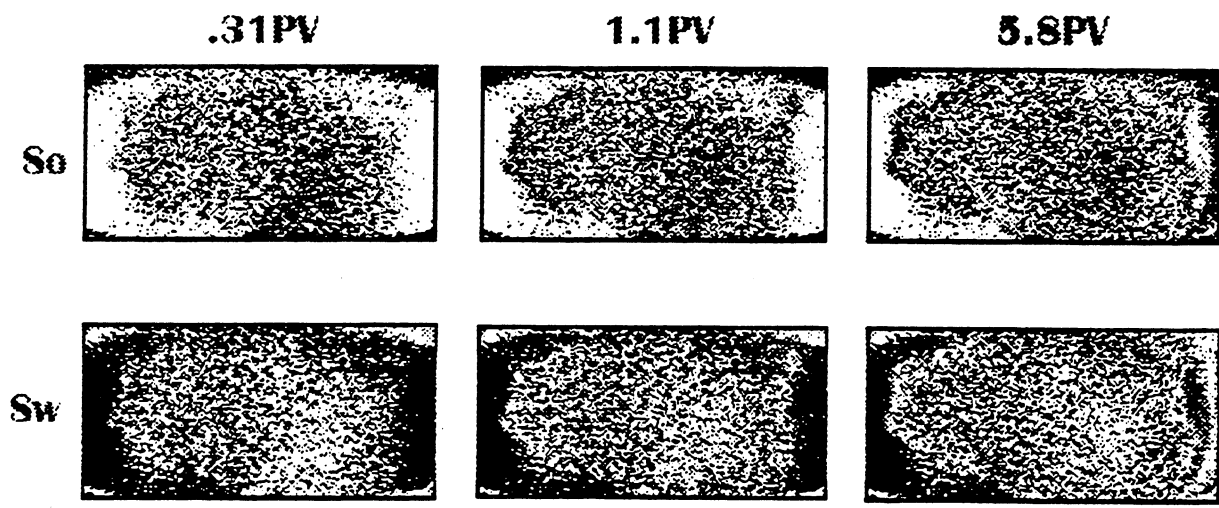


Figure 6.2: Oil and Water Saturation Distributions in Slice 1 During Waterflood Experiment



Waterflood(Slice2)

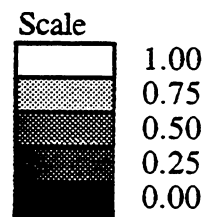
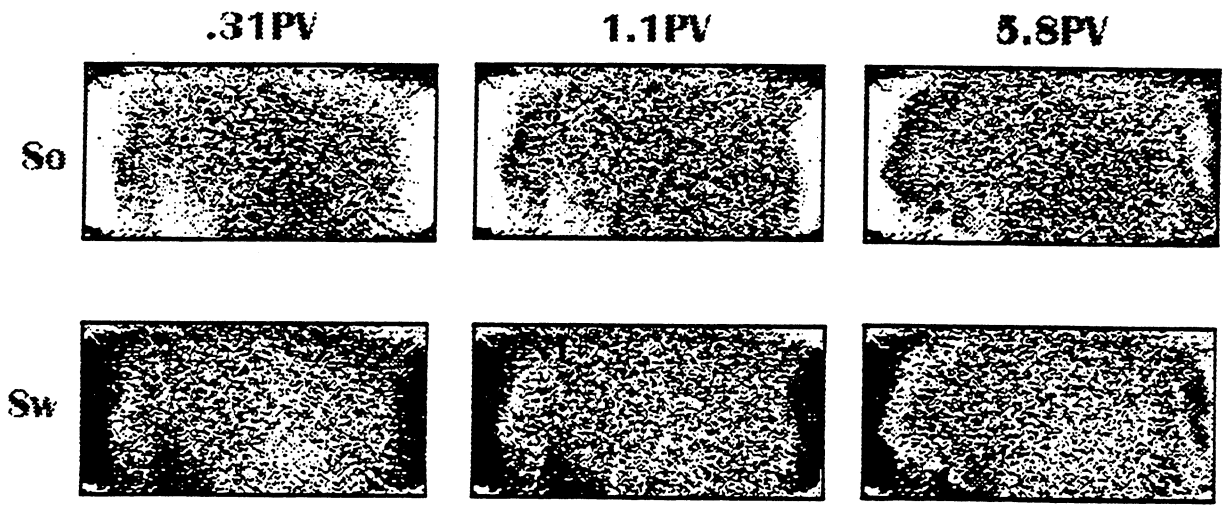


Figure 6.3: Oil and Water Saturation Distributions in Slice 2 During Waterflood Experiment



Waterflood(Slice3)

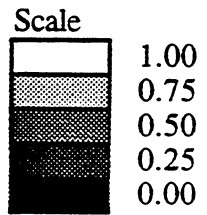
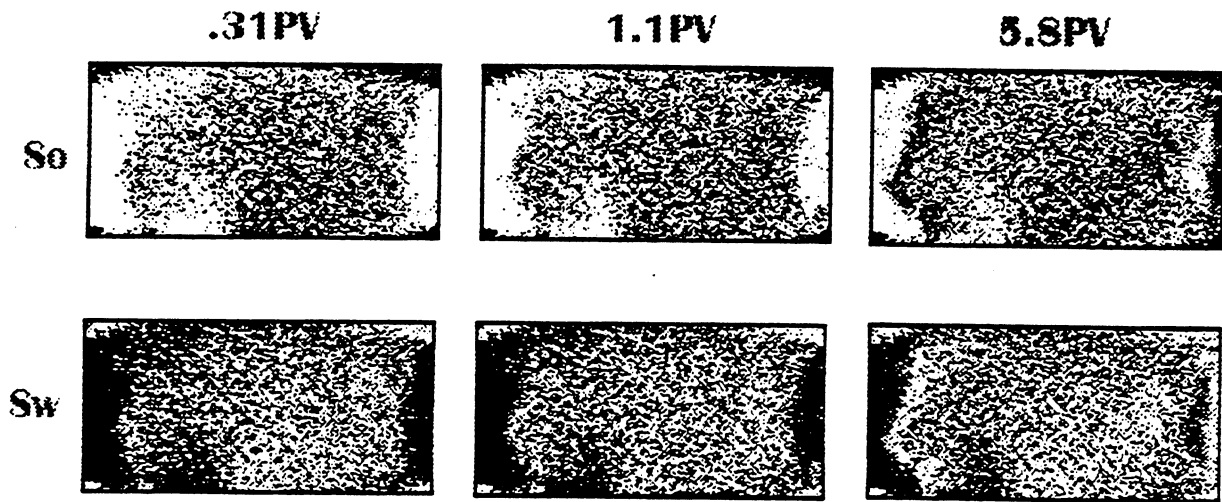


Figure 6.4: Oil and Water Saturation Distributions in Slice 3 During Waterflood Experiment



Waterflood(Slice4)

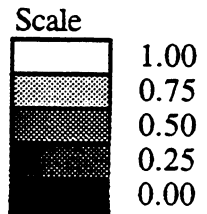


Figure 6.5: Oil and Water Saturation Distributions in Slice 4 During Waterflood Experiment

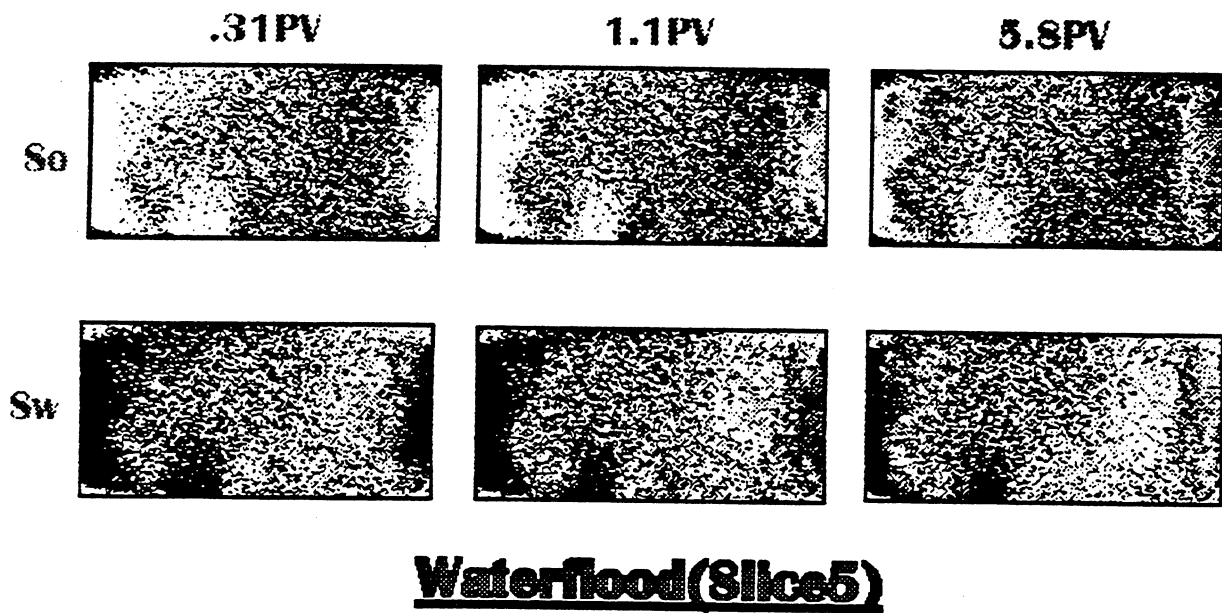
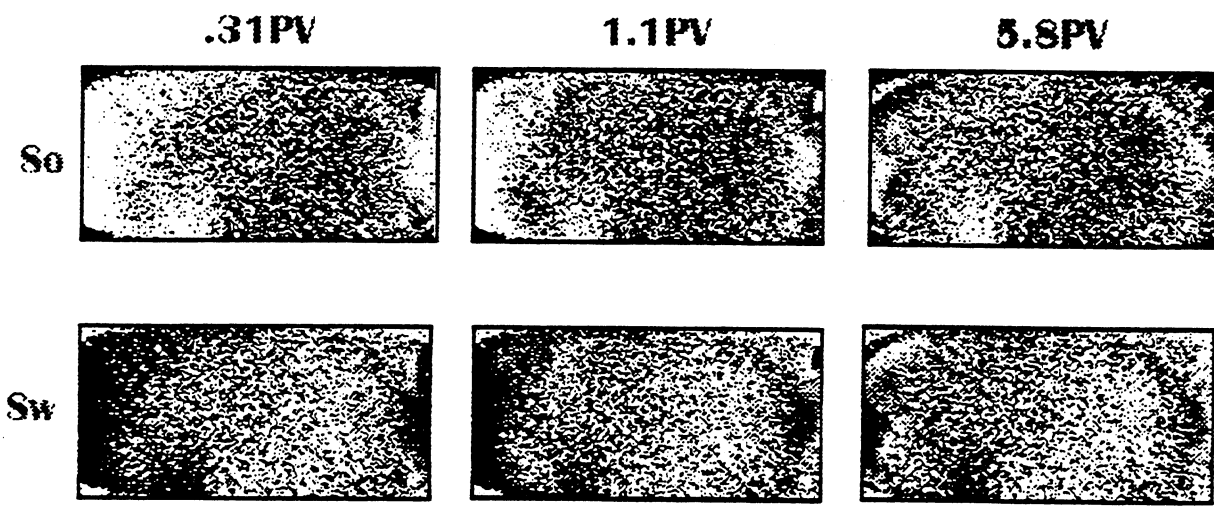


Figure 6.6: Oil and Water Saturation Distributions in Slice 5 During Waterflood Experiment



Waterflood(Slice6)

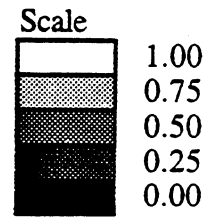


Figure 6.7: Oil and Water Saturation Distributions in Slice 6 During Waterflood Experiment

6.2.2 Steamflood Experiments

The steamflood experiments resulted in a reduction of residual oil saturation from 30% (obtained at the end of waterflood) to 11%. During the experiments it was observed that less than 1% of oil was lost through the crack at the bottom of the model. Looking at the scans we observe that before waterflooding was started oil had gone into a small area surrounding the crack. This oil was not displaced much in the insulation during the experiments due to its high viscosity. This resulted in minimizing the leak of oil. There was no evaporation loss of the oil because the boiling point of the oil is much higher than the steam temperature maintained during the steamflood experiment. However, unlike oil, large quantities of steam leaked from the system.

A heat balance history of the system is shown in Fig. 6.8. As seen, heat input with steam is much larger than the total heat in the system, i.e., the total of heat with produced fluid, heat losses from model surfaces and heat accumulation in the core. A crack at the bottom of the model has resulted in loss of a large quantity of steam and the associated heat. About 25% of the heat injected was lost continuously after 0.30 PV of steam was injected. We also observe that the heat accumulated in the core was almost steady at 700 BTU after 0.30 PV was injected. This is because 75% of this accumulated heat was heat accumulation in the sand, and the sand had reached steam temperature at 0.30 PV injection.

Figure 6.9 shows the oil recovery at various stages of the experiment. 66% of the oil was recovered at the end of waterflood, and 88% of the oil was recovered at the end of steamflood. We have shown two recovery curves for the steamflood part of the experiment. The one showing higher recovery is the effective recovery, i.e. subtracting the steam losses from the PV of steam injected.

On the following page, Table 6.2 gives the values of oil saturations obtained from material balance and CT scanning, experimental errors in S_o due to CT scanning, and the errors obtained using error analysis.

Table 6.3 on the following page gives the values of water saturations obtained from material balance and CT scanning, and experimental errors in S_w due to CT scanning.

From Table 6.2 we observe that the values of oil saturations obtained by using the three-phase saturation equations developed in Section 4.3 compare well with those obtained from material balance.

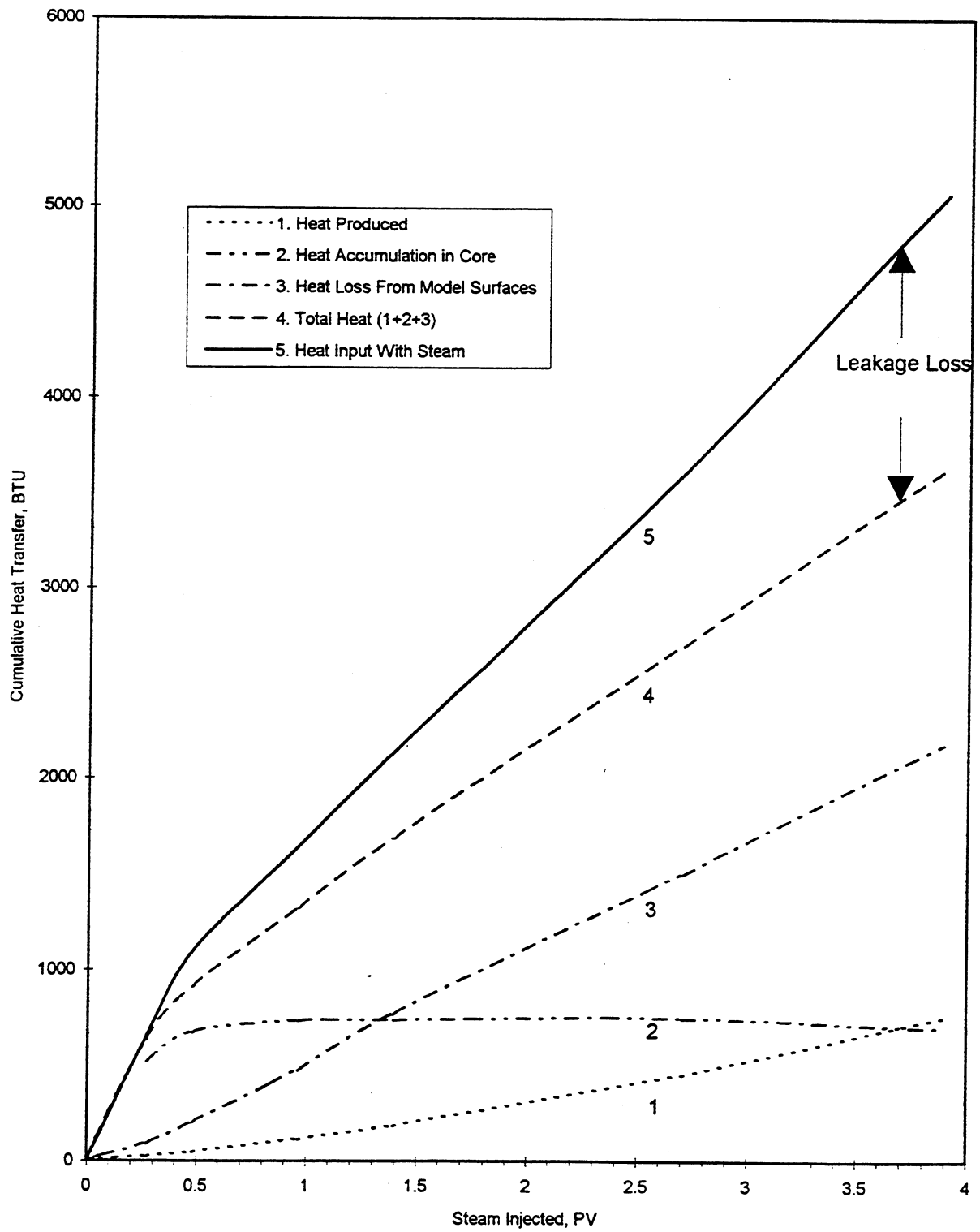


Figure 6.8: Heat Transfer During Steamflood Experiments

Table 6.2: Comparison of error in S_o , obtained using material balance, with those using Eq. 4.33.

PV Injected	S_o		Error in S_o (Expt.)		Error using Eq. 4.33	
	Mat. Bal.	CT Scan	Absolute	Percentage	Absolute	Percentage
0	0.30	0.28	0.02	6.7	0.04	11.8
0.27	0.29	0.27	0.02	6.9		
0.48	0.27	0.27	0	0		
0.96	0.24	0.26	0.02	8.3		
1.39	0.21	0.23	0.02	9.5	0.03	16.1
2.70	0.15	0.13	0.02	13.3		
3.90	0.11	0.13	0.02	18.2	0.03	30.5

Table 6.3: Error in S_w using material balance.

PV Injected	S_w		Error in S_w (Expt.)	
	Mat. Bal.	CT Scan	Absolute	Percentage
0	0.70	0.70	0	0
0.27	0.68	0.66	0.02	2.9
0.48	0.66	0.63	0.03	4.5
0.96	0.63	0.61	0.02	3.2
1.39	0.60	0.58	0.02	3.3
2.70	0.47	0.50	0.03	6.4
3.90	0.34	0.36	0.02	5.9

We also notice that some of the errors obtained in the measurement of S_o are less than the maximum expected errors using error analysis (Eq. 4.33). This result is not in agreement with the results obtained for two-phase measurements. With the data that we have, we are unable to give any reason for this behavior. Possibly, the reasoning given for error in two-phase measurement holds true for three-phase measurements too.

From Table 6.3 we observe that the values of water saturations obtained by using the three-phase saturation equations developed in Section 4.3 compare well with those obtained from material balance.

The saturation distributions shown in Figs. 6.10, 6.11, 6.12, 6.13, 6.14, and 6.15 were generated using three-phase saturation equations developed in Section 4.3. We also see that the steam saturation values match well with the sectional temperature distributions at each stage, shown directly above the sections showing steam saturation distributions. As discussed in Appendix A, these temperature distribution images were created from the temperature data obtained during the steamflood experiments. Areal temperature distributions are shown in Fig. 6.16.

The average oil saturations (obtained from material balance and CT scanning) during the steamflood experiment, obtained from material balance, are shown in Fig. 6.17. Similarly, saturations of water are shown in Fig. 6.18. From Figs. 6.17 and 6.18 we find that the saturation values obtained using the saturation equations match quite well with the saturation values obtained from material balance. This was also seen from the data in Tables 6.2 and 6.3. Steamflooding was stopped after 3.9 PV of steam was injected, when the oil production rate fell below 1% of the produced fluids. The oil saturation dropped from 0.30 to 0.11.

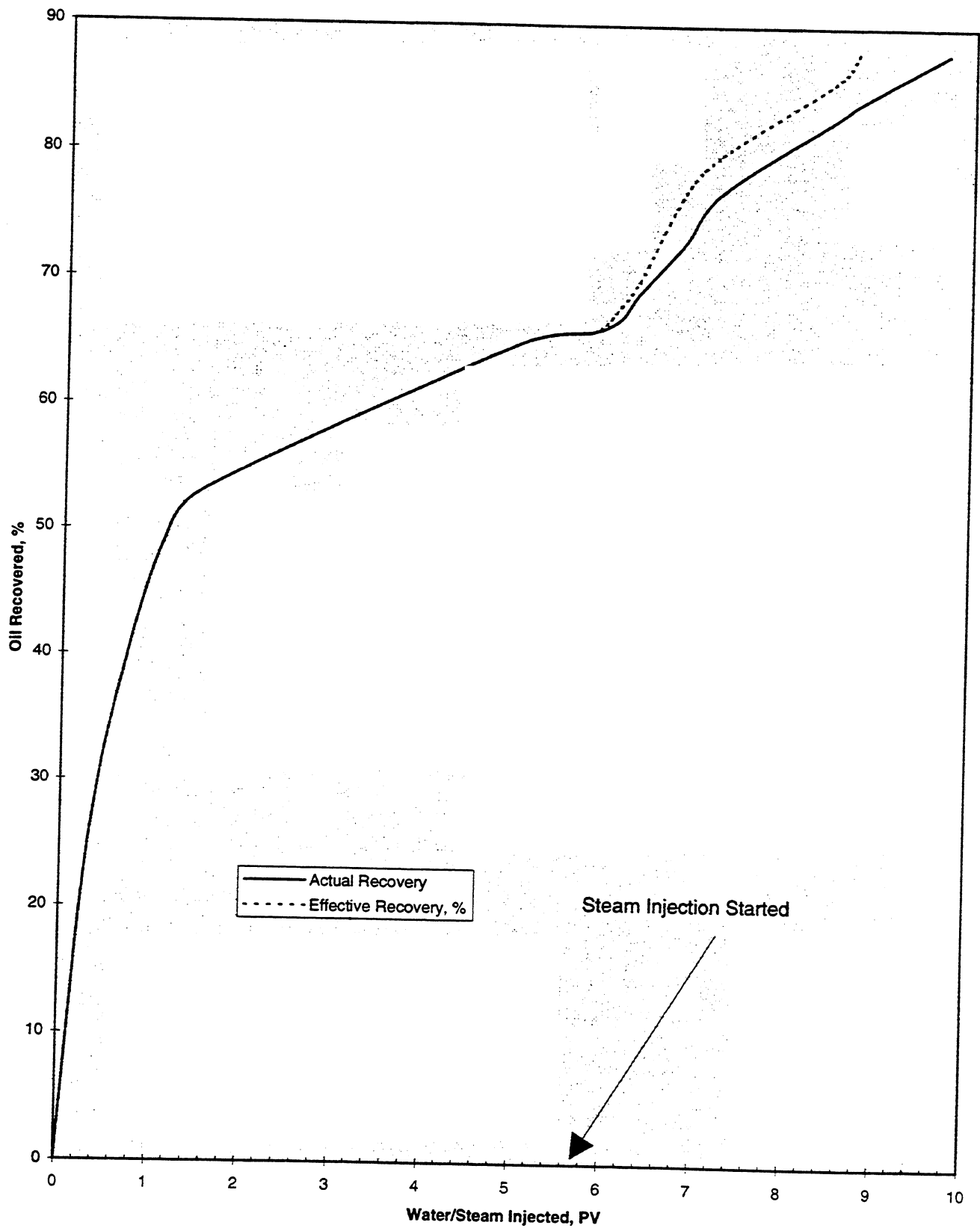
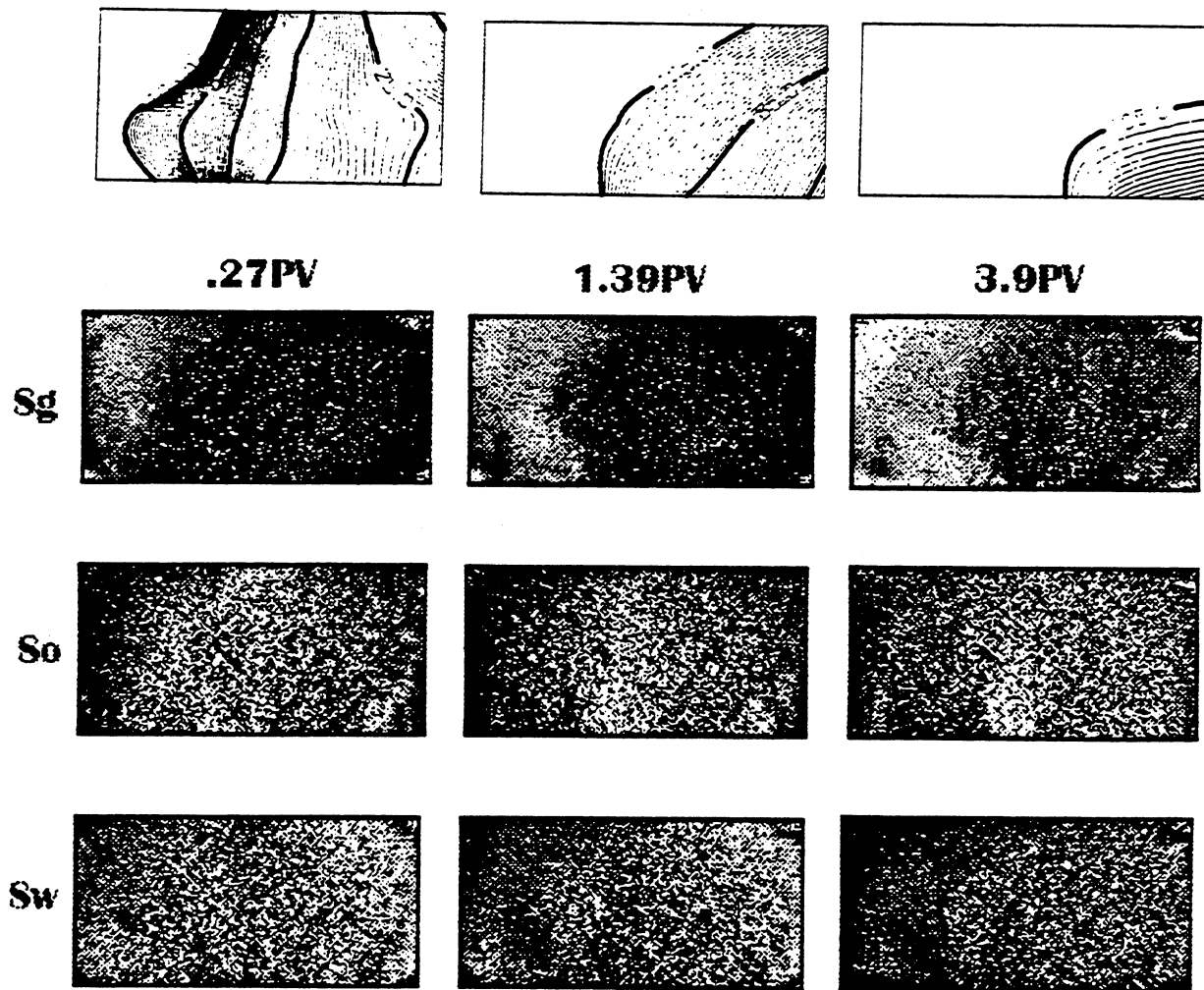


Figure 6.9: Oil Recovery at Various Stages of the Experiments



Steamflood(Slice 1)

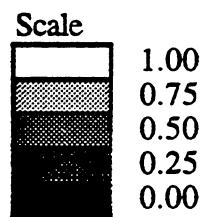
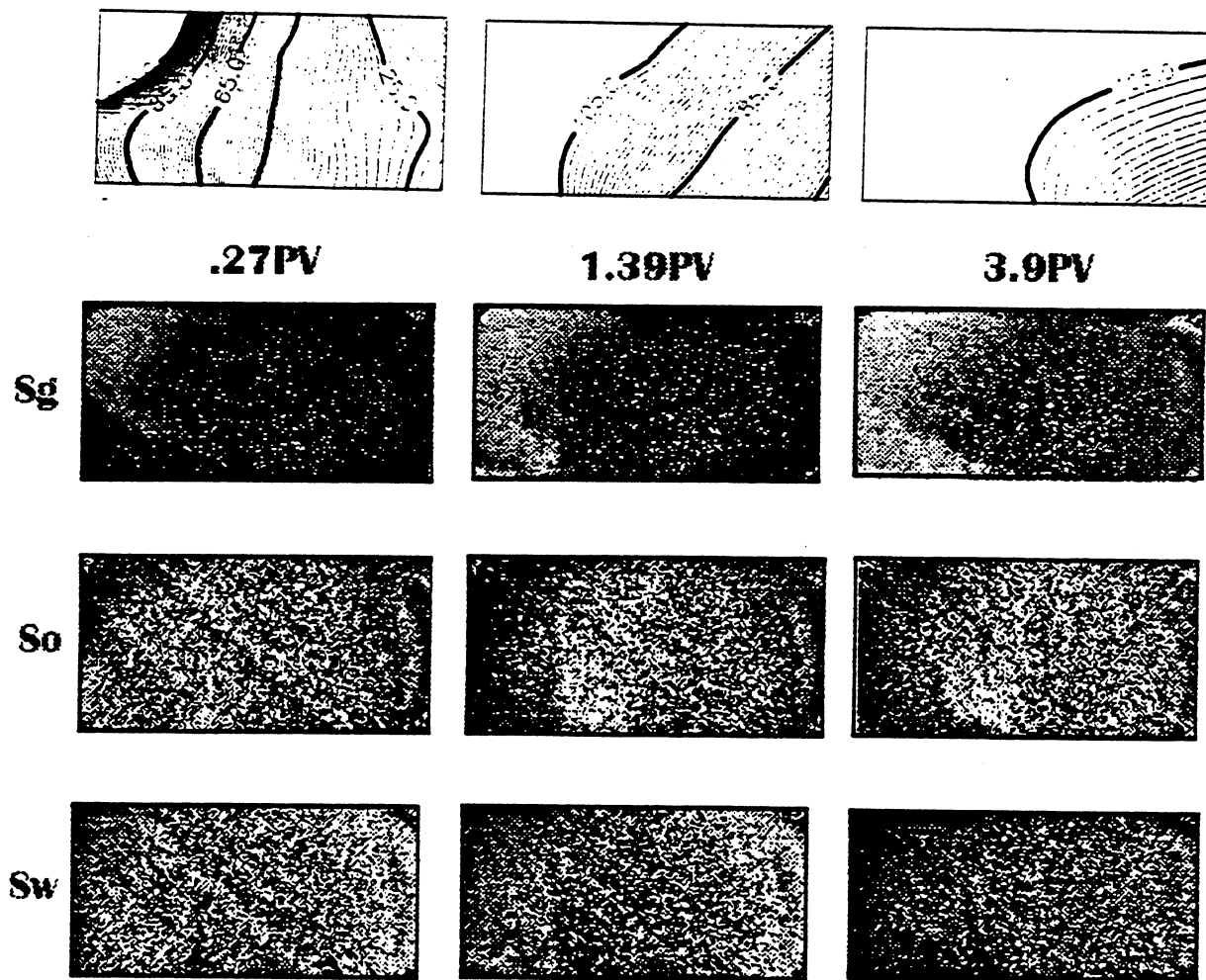


Figure 6.10: Temperature and Saturation Distributions in Slice 1 During Steamflood Experiments



Steamflood(Slice 2)

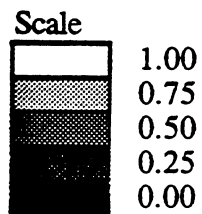
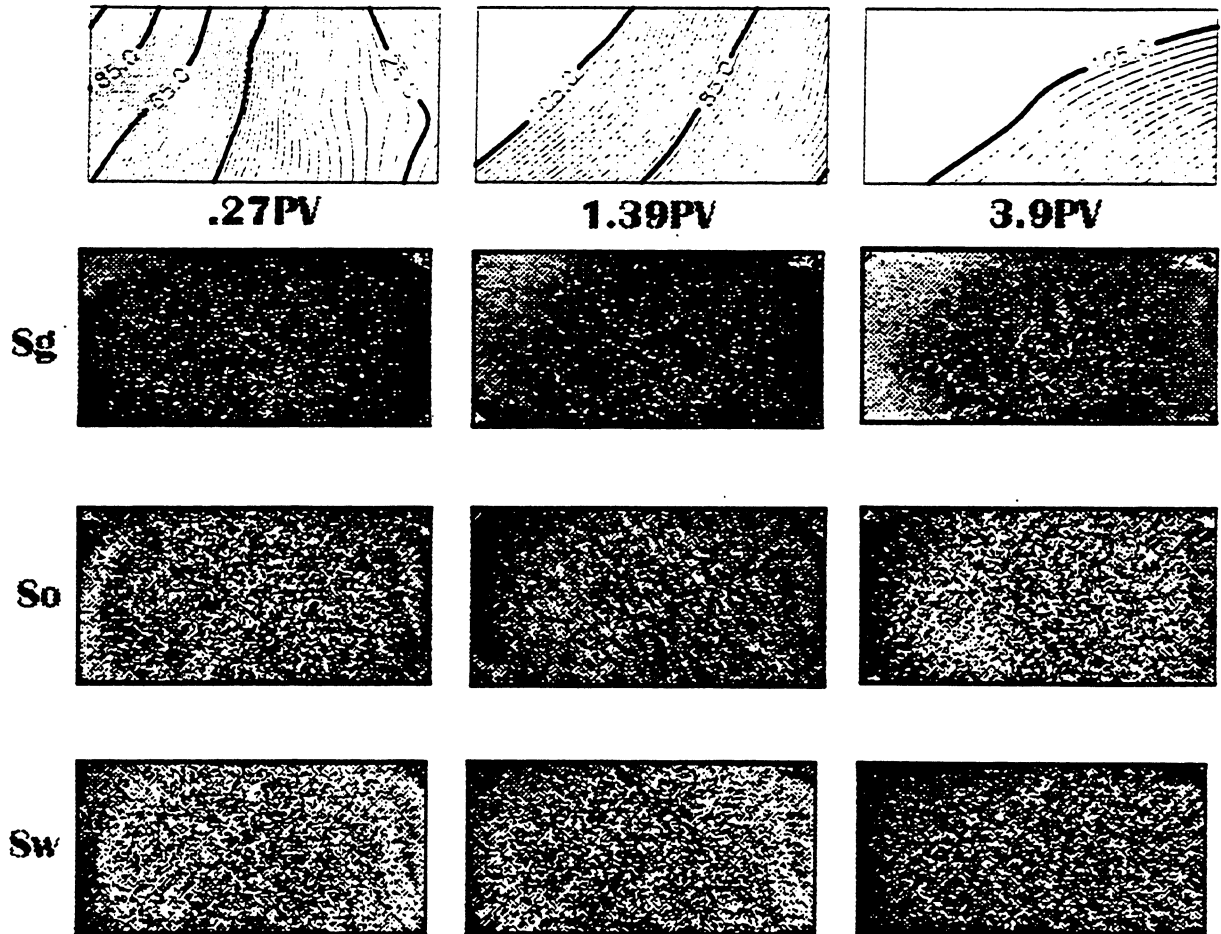


Figure 6.11: Temperature and Saturation Distributions in Slice 2 During Steamflood Experiments



Steamflood(Slice 3)

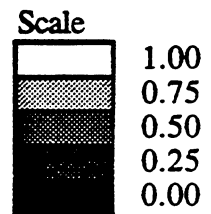
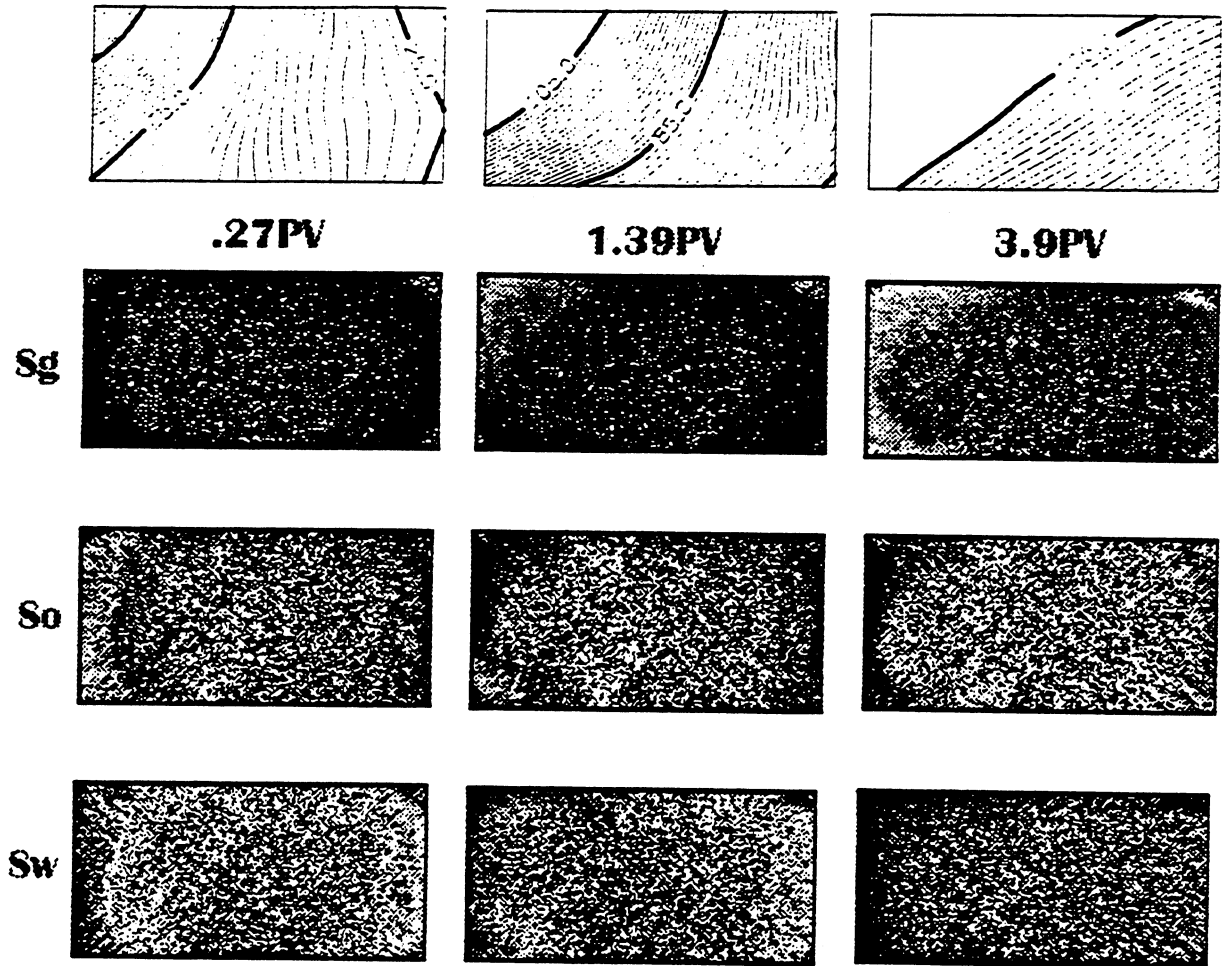


Figure 6.12: Temperature and Saturation Distributions in Slice 3 During Steamflood Experiments



Steamflood(Slice 4)

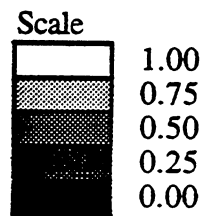
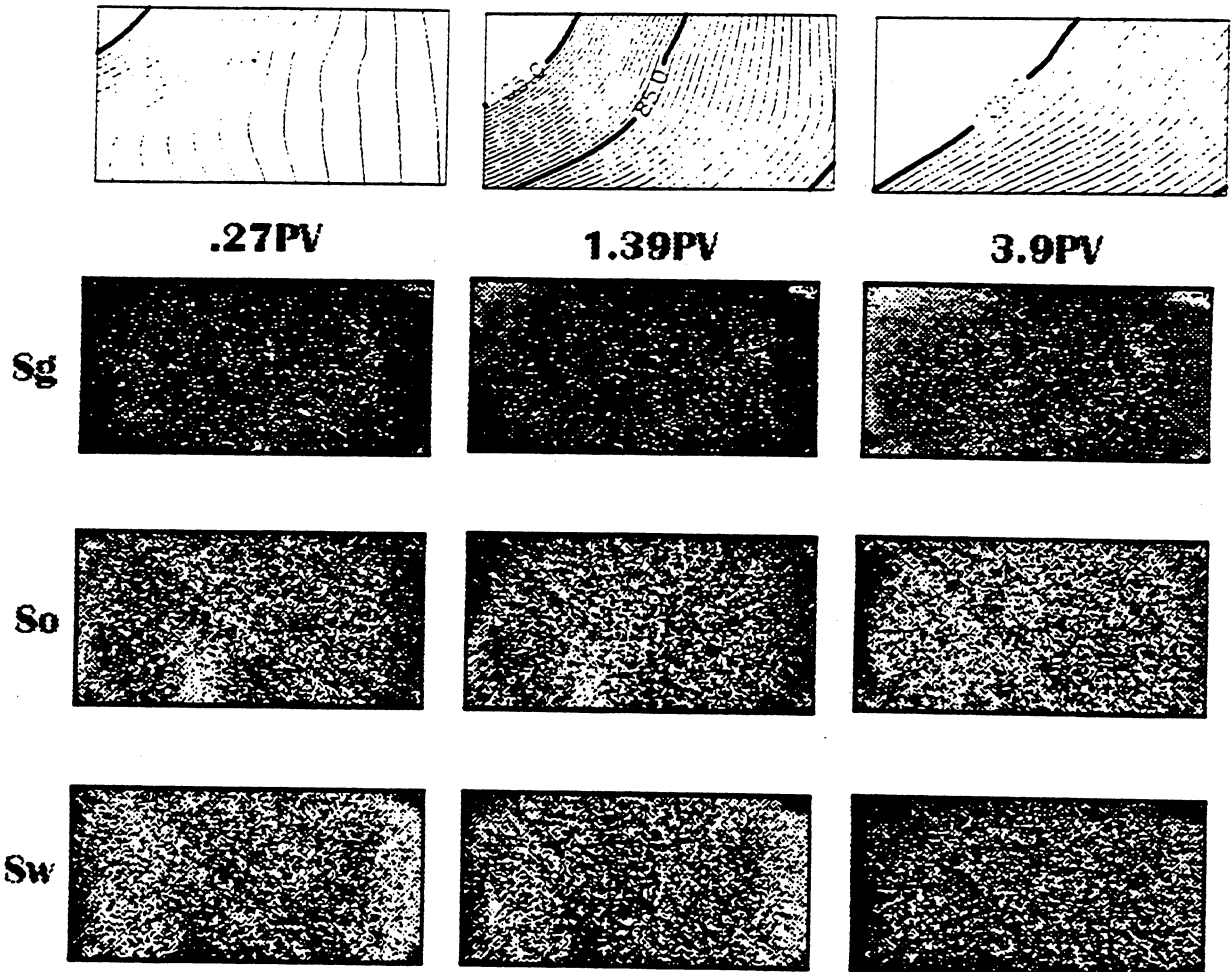


Figure 6.13: Temperature and Saturation Distributions in Slice 4 During Steamflood Experiments



Steamflood(Slice 5)

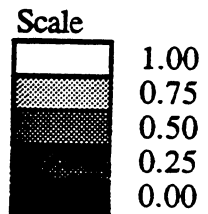
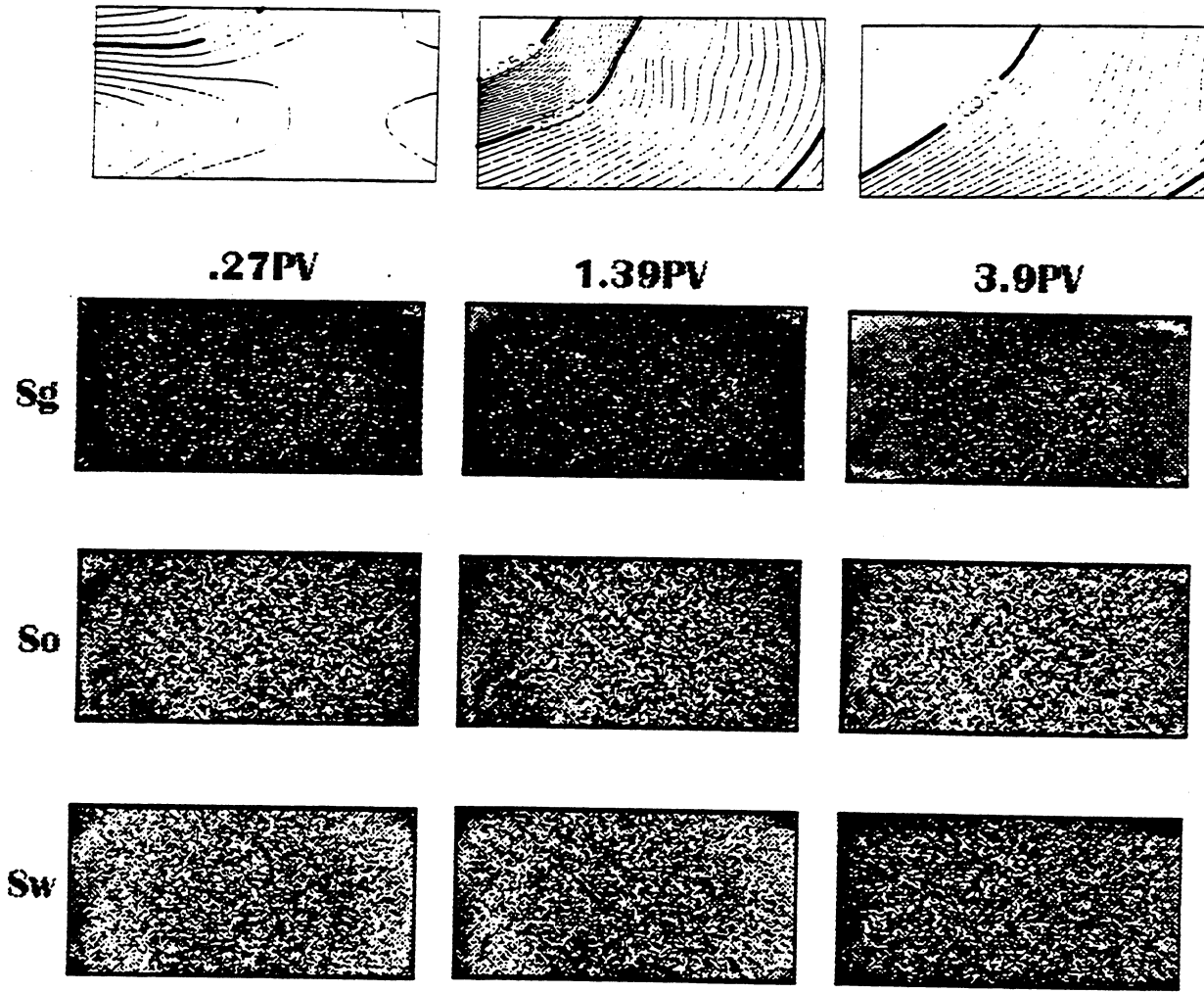


Figure 6.14: Temperature and Saturation Distributions in Slice 5 During Steamflood Experiments



Steamflood(Slice 6)

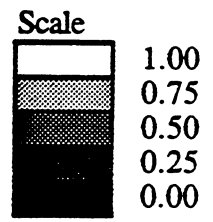


Figure 6.15: Temperature and Saturation Distributions in Slice 6 During Steamflood Experiments

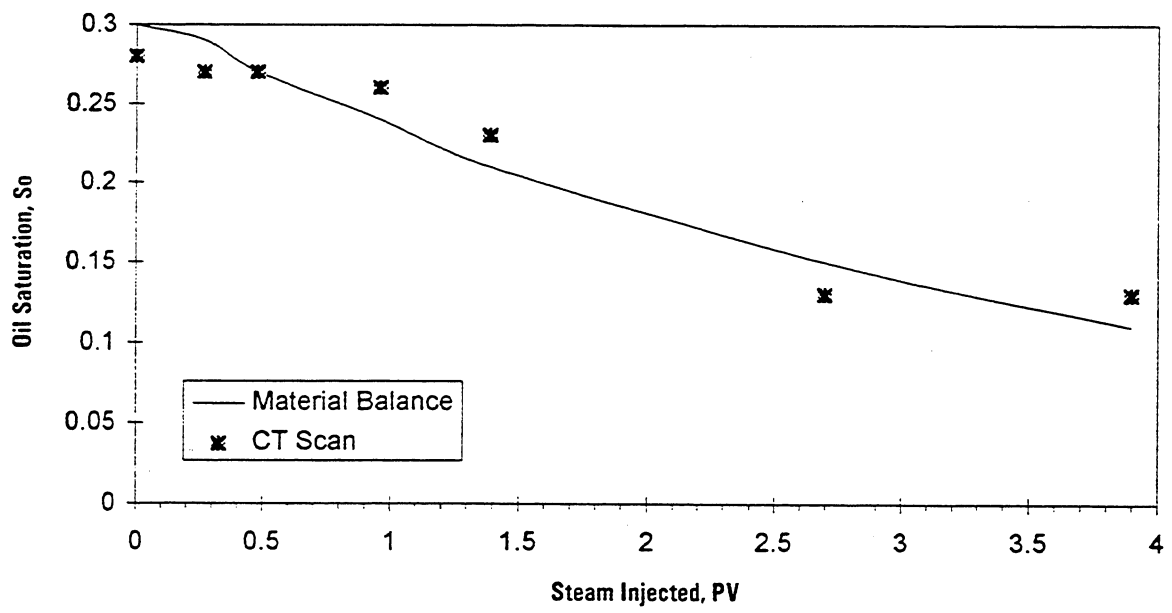


Figure 6.17: Average Oil Saturations in the Model During Steamflood Experiments

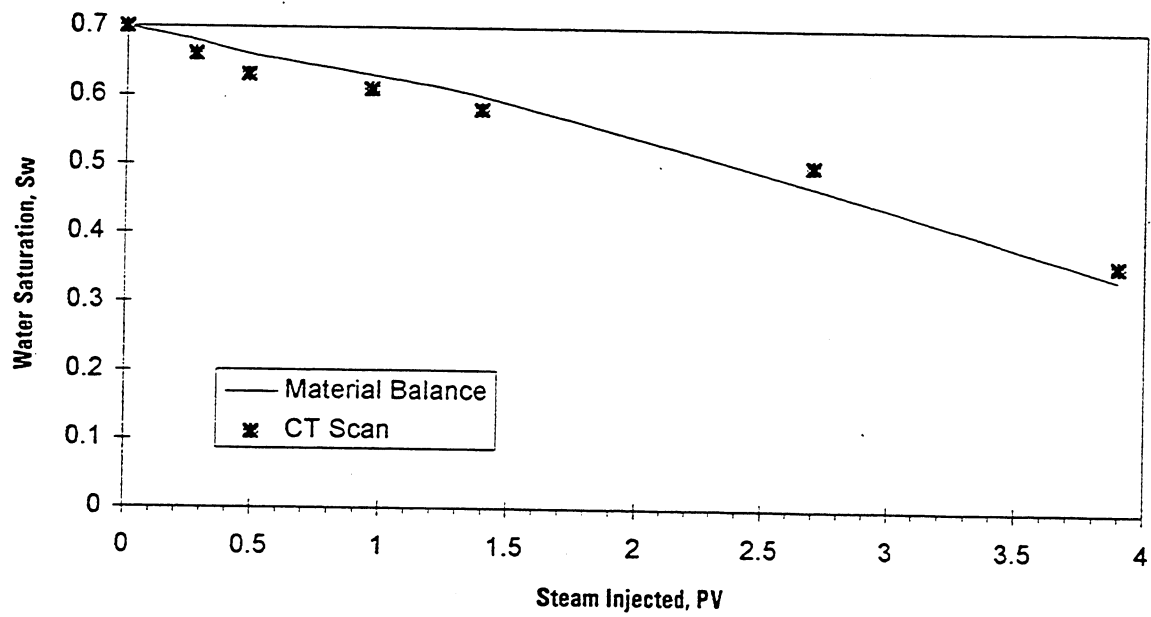


Figure 6.18: Average Water Saturations in the Model During Steamflood Experiments

7. CONCLUSIONS

The saturation equations developed in Sections 4.2 and 4.3 are found to be quite accurate for determining saturation distributions in a two-phase and three-phase system respectively, as seen from the comparison of these values with those obtained using material balance.

Fine unconsolidated sand requires very careful packing and should be used with caution.

In a three phase system it is very difficult to distinguish between oil and water saturations without doping one of the fluids.

At various stages of the steamflood experiment water vaporizes to steam and steam condenses to water. Due to this fact, doping the water is not desirable. So, the oil alone should be doped.

For oil, 1-bromo dodecane was found to be an effective and stable dopant.

8. RECOMMENDATIONS

The approach developed in this study for saturation measurements can be made more accurate and useful with changes to take care of the following problems in the system:

The aluminum body of the model creates a non uniform CT attenuation in the medium. Due to this fact, aluminum shell should be replaced with one using a less dense material.

The vertical positioning device of the scanner was not very accurate for our experimental purposes. Measures should be taken to take care of this problem. One of the ways is to install a laser positioning device for vertical positioning.

REFERENCES

- [1] Haunsfield, G.N.: "A Method of and Apparatus for Examinations of a Body by Radiation Such as X- or Gamma- Radiation," British Patent No. 1,283,915, London (1972).
- [2] Bergosh, J. L., Marks, T. R. and Mitkus, A. F.: "New Core Analysis Techniques for Naturally Fractured Reservoirs," SPE 13653, paper presented at the 58th Annual California Regional Meeting, Bakersfield (March 27-29, 1985).
- [3] Honarpour, M. M., Cromwell, V., Hatton, D. and Satchwell, R.: "Reservoir Rock Descriptions Using Computed Tomography (CT)," SPE 14272, paper presented at the 60th Annual Technical Conference and Exhibition of the SPE, Las Vegas (Sept. 22-25, 1985).
- [4] Honarpour, M. M., McGee, K. R., Crocker, M. E., Maerefat, N. L. and Sharma, B.: "Detailed Core Description of a Dolomite Sample from the Upper Madison Limestone Group," SPE 15174, paper presented at the Rocky Mountain Regional Meeting, Billings (May 19-21, 1986).
- [5] Hunt, P. K., Engler, P. and Bajsarowicz, C.: "Computed Tomography as a Core Analysis Tool: Applications, Instrument Evaluation, and Image Improvement Techniques," *SPEFE* (Sept. 1988) pp. 1203-1210.
- [6] Narayanan, K. and Deans, H. A.: "A Flow Model Based on the Structure of Heterogeneous Porous Media," SPE 18328, paper presented at the 63rd Annual Technical Conference and Exhibition of the SPE, Houston (Oct. 2-5, 1988).
- [7] Gilliland, R. E. and Coles, M.E.: "Use of CT Scanning in the Investigation of Damage to Unconsolidated Cores," SCA 8902, paper presented at the SCA 1989 Annual Technical Conference, New Orleans (Aug. 2-3, 1989).
- [8] Sprunt, E. S.: "Arun Core Analysis: Special Procedures for Vuggy Carbonates," *The Log Analyst* (Sept.-Oct., 1989) pp. 353-362.
- [9] Raynaud, S., Fabre, D., Mazerolle, F., Geraud, Y. and Latiere, H.J.: "Analysis of the Internal Structure of Rocks and Characterization of Mechanical Deformation by a Non-Destructive Method: X-Ray Tomodensitometry," *Tectonophysics* 159 (1989) pp. 149-159.
- [10] Fabre, D., Mazerolle, F. and Raynaud, S.: "X-Ray Density Tomography: A Tool to Characterize Pores and Cracks in Rocks," *Rock at Great Depth, Proceedings of the International Symposium of Rock Mechanics, Pau, France* (Aug. 28-31, 1989).
- [11] Jasti, J., Jesion, G. and Feldkamp, L.: "Microscopic Imaging of Porous Media Using X-Ray Computer Tomography," SPE 20495, presented at the 65th Annual Technical Conference and Exhibition of the SPE, New Orleans (Sept. 23-26, 1990).

- [12] Kantzas, A.: "Investigation of Physical Properties of Porous Rocks and Fluid Flow Phenomena in Porous Media Using Computer Assisted Tomography," *InSitu* 14, No. 1 (1990) pp. 77-132.
- [13] Moss, R. M., Pepin, G.P. and Davis, L. A.: "Direct Measurement of the Constituent Porosities in a Dual Porosity Matrix," SCA 9003, paper presented at the SCA 1990 Annual Technical Conference, Houston (Aug. 2-3, 1990).
- [14] Peters, E. J. and Afzal, N.: "Characterization of Heterogeneities in Permeable Media With Computer Tomography Imaging," *Jour. Pet. Sci. Engr.* 7 (1992) pp. 283-296.
- [15] Johns, R. A., Steude, J. S., Castanier, L. M. and Roberts, P. V.: "Nondestructive Measurements of Fracture Aperture in Crystalline Rock Cores Using X Ray Computed Tomography," *JGR* 98 (Feb. 1993) pp. 1889-1900.
- [16] Wang, S. Y., Ayril, S. and Gryte, C.C.: "Computer-Assisted Tomography for the Observation of Oil Displacement in Porous Media," *SPEJ* (Feb. 1984) pp. 53-55.
- [17] Cromwell, V., Kortum, D. J. and Bradley, D.J.: "The Use of a Medical Computer Tomography (CT) System to Observe Multiphase Flow in Porous Media," SPE 13098, paper presented at the 59th Annual Technical Conference and Exhibition of the SPE, Houston (Sept. 16-19, 1984).
- [18] Wang, S. Y., Huang, Y. B., Pereira, V. and Gryte, C. C.: "Application of Computed Tomography to Oil Recovery from Porous Media," *Appl. Optics* 24, No. 23 (Dec. 1, 1985) pp. 4021-4027.
- [19] Vinegar, H. J.: "X-Ray CT and NMR Imaging of Rocks," *JPT* (March, 1986) pp. 257-259.
- [20] Vinegar, H. J., and Wellington, S. L.: "Tomographic Imaging of Three-Phase Flow Experiments," *Rev. Sci. Instru.* (Jan. 1987) pp. 96-107.
- [21] Fransham, P. B., and Jelen, J.: "Displacement of Heavy Oil Visualized by CAT Scan," *The Journal of Canadian Petroleum Technology* (May-June, 1987) pp. 42-47.
- [22] Hove, A. O., Ringen, J. K. and Read, P. A.: "Visualization of Laboratory Corefloods With the Aid of Computerized Tomography of X-Rays," *SPE Reservoir Engineering* (May 1987) pp. 148-154.
- [23] Withjack, E. M.: "Computed Tomography for Rock-Property Determination and Fluid-Flow Visualization," *SPEFE* (Dec. 1988) pp. 696-704.
- [24] Withjack, E. M., Graham, S. K. and Yang, C-T.: "Determination of Heterogeneities and Miscible Displacement Characteristics in Corefloods by CT Scanning," SPE 20490, paper presented at the 65th Annual Technical Conference and Exhibition of the SPE, New Orleans (Sept. 23-26, 1990).

- [25] Hicks, Jr., P. J., Deans, H. A. and Narayanan, K.: "Distribution of Residual Oil Saturations in Heterogeneous Carbonate Cores Using X-Ray CT," *SPEFE* (Sept. 1992) pp. 235-239.
- [26] MacAllister, D. J., Miller, K. C., Graham, S. K. and Yang, C-T.: "Application of X-Ray CT Scanning to the Determination of Gas-Water Relative Permeabilities," SPE 20494, paper presented at the 65th Annual Technical Conference and Exhibition of the SPE, New Orleans (Sept. 23-26, 1990).
- [27] Hove, A. O., Nilsen, V. and Leknes, J.: "Visualization of Xantham Flood Behavior in Core Samples by Means of X-Ray Tomography," *SPEFE* (Nov. 1990) pp. 475-480.
- [28] Peters, E. J., and Hardham, W. D.: "Visualization of Fluid Displacements in Porous Media Using Computed Tomography Imaging," *Jour. Pet. Sci. Engr.* 4 (1990) pp. 155-168.
- [29] Auzeais, F. M., Dussan, V. and Reischer, A. J.: "Computed Tomography for the Quantitative Characterization of Flow Through a Porous Medium," SPE 22595, paper presented at the 66th Annual Technical Conference and Exhibition of the SPE, Dallas (Oct. 6-9, 1991).
- [30] Withjack, E. M., Graham, S. K. and Yang, C-T.: "CT Determination of Heterogeneities and Miscible Displacement Characteristics," *SPEFE* (Dec. 1991) pp. 447-452.
- [31] Hicks Jr., P. J. and Deans, H. A.: "Effect of Permeability Distribution on Miscible Displacement in a Heterogeneous Carbonate Core," Petroleum Society of CIM Paper 92-10, presented at the 1992 Annual Technical Conference of Petroleum Society of CIM, Calgary, Alberta, Canada (June 7-10, 1992).
- [32] Alvestad, J., Gilje, E., Hove, A. O., Langeland O., Maldal T. and Schilling, B. E. R.: "Coreflood Experiments With Surfactant Systems for IOR: Computer Tomography and Numerical Modelling," *Jour. Pet. Sci. Engr.* 7 (1992) pp. 155-171.
- [33] Hicks, Jr., P. J., Narayanan, K. and Deans, H. A.: "An Experimental Study of Miscible Displacements in Heterogeneous Carbonate Cores Using X-Ray CT," *SPEFE* (March 1994) pp. 55-60.
- [34] Demiral, B. M. R., Castanier, L. M. and Brigham, W. E.: "CT Imaging of Steam and Steam/Foam Laboratory Experiments," SPE paper presented at the 66th Annual Technical Conference and Exhibition of the SPE, Dallas (Oct. 6-9, 1991).
- [35] Shallcross, D. C. and Wood, D.G.: "The Accurate Measurements of Heat Flux Using Thin Film Heat Flux Sensors with Application to Petroleum Engineering," DOE Fossil Energy Report SUPRI TR 74 DOE/BC/14126-20 (July 1990).
- [36] Castanier, L. M.: "Introduction to Computerized X-ray Tomography for Petroleum Research," US Department of Energy Technical Report DOE/BC/14126-7 (April 1988).

- [37] Sameer, J. and Castanier, L. M.: "Computer Modeling of a Three-Dimensional Steam Injection Experiment," DOE Fossil Energy Report SUPRI TR 94, DE-FG22-93BC14899 (June 1993).

APPENDIX A. 3D MODEL OPERATING PRINCIPLES

A.1 Control Panel

The control panel is mounted on a roller cart. The necessary electrical and tubing connections must be made prior to an experiment. The details of these connections are shown in the following sections. The schematic drawing of the control panel is shown in Fig A.1.

A.1.1 Injection Control

The injection end has two Constametric pumps. One is used to inject water to the steam generator, or directly to the 3D model. The other one is used to inject either water or oil to the 3D model. Both of these pumps are used to clean and resaturate the model in preparation for the experiments. The injection end also has a N₂ mass flow controller to inject nitrogen at a constant rate. The valves which direct the injection fluids to specific tubings are discussed below. These valves are labeled by letters A through F in Fig A.2 and their use is discussed below. All, except Valve F, are three-way valves.

Valve A: This valve directs water coming from Pump 2 either to the steam generator or to the 3D model.

Valve B: This valve directs water or oil to the 3D model, or to Valve C. The main purpose of this valve is to allow us to apply different injection schemes during the experiments. If it is on the water side, we can inject additives and steam (from Valve C) simultaneously to the model. If it is on the other direction, injection of the steam or additives can only be made alternately through Valve C.

Valve C: This valve allows the injection of either steam from the steam generator, or oil/cold water coming from Valve B.

Valve D: This valve either directs steam to the 3D model via Valve C, or puts it in a by-pass cycle. The by-pass line lets steam flow through a condenser before the steam injection experiment starts. Or alternatively, it allows additive injection during the experiment.

Valve E: The main line to this valve comes from the nitrogen mass controller. This valve directs nitrogen to the main injection line, or to the vent.

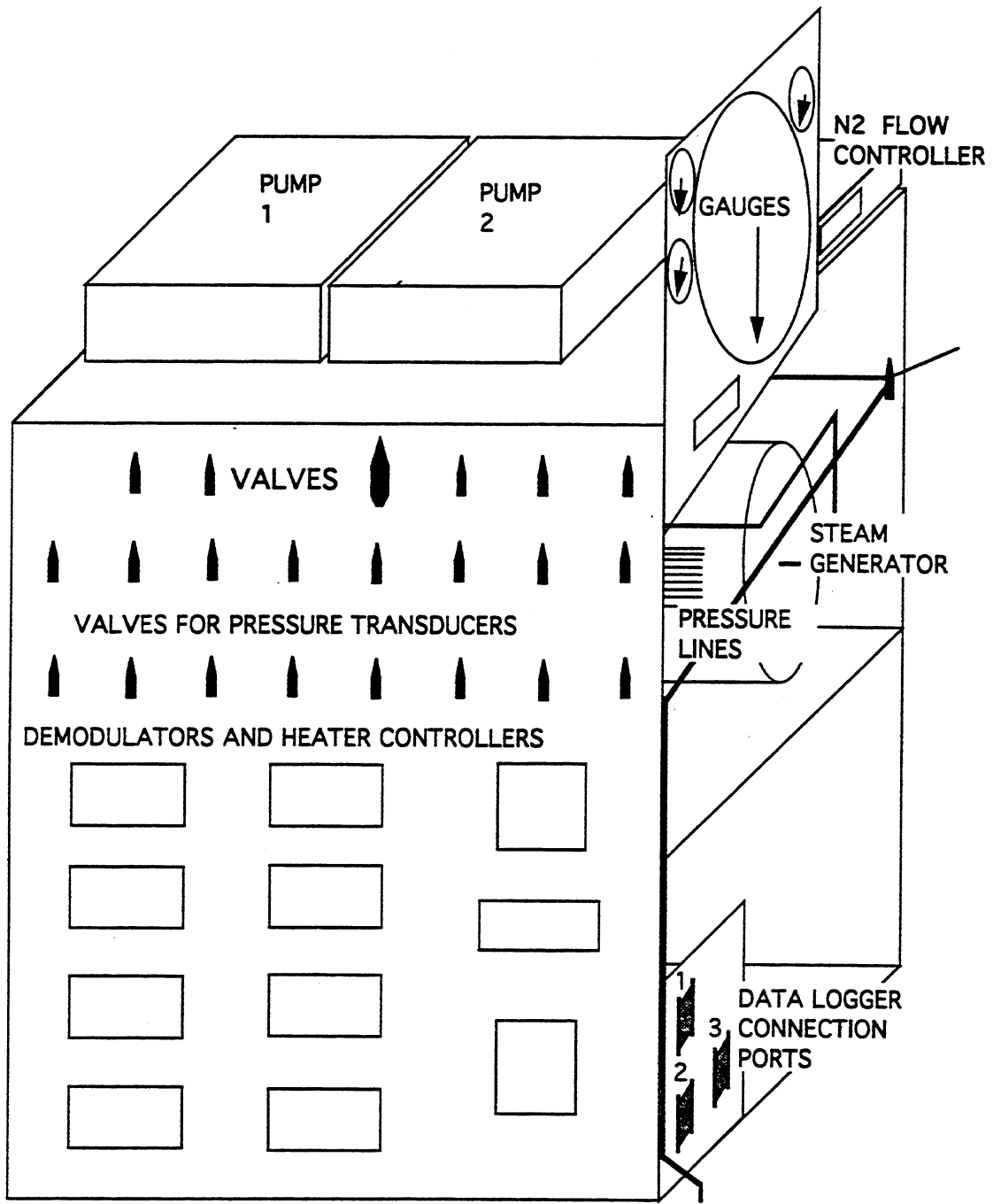


Figure A.1: Schematic of the Control Panel
 (Source: Demiral et al., 1992)

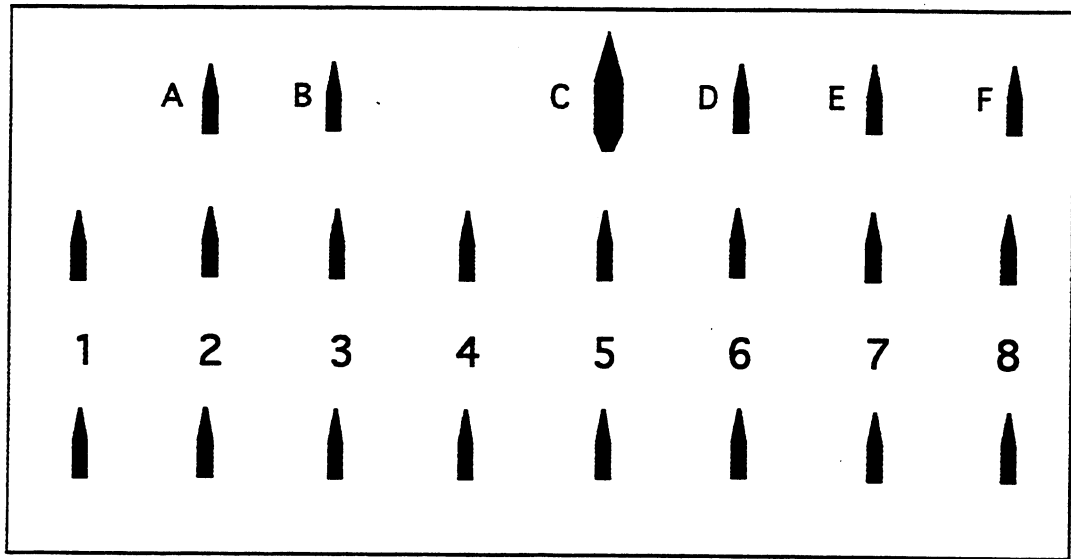


Figure A.2: Valves on the Control Panel
 (Source: Demiral et al., 1992)

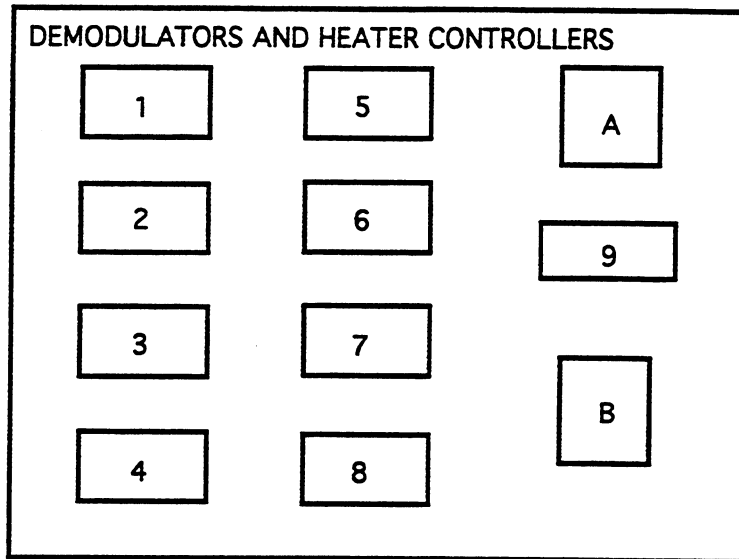


Figure A.3: Demomodulators and Heater Controllers Part of
 the Control Panel
 (Source: Demiral et al., 1992)

Valve F: This valve is used to relieve pressure from the main line.

A.1.2 Pressure Lines

The pressure lines allow us to make tubing connections between the eight pressure lines coming from the pressure taps, and the lines from the production end of the 3D model. The tubing used for pressure lines is high pressure high temperature nylon, 1/16 inch in diameter. Celesco differential pressure transducers, with 25 psi plates, are used for pressure measurements.

A.1.3 Valves for Pressure Transducer

These valves are numbered as pairs from 1 to 8 on Fig. A.2. The upper valve at each pair controls direction of fluid coming from the pressure taps on the 3D model. These valves have two directions, as either ΔP or Loop. The bottom valves control the pressure lines coming from the injection corner of the 3D model. They also have two directions, as either ΔP or Vent. When both valves of a pair are at the ΔP position, we can read the differential pressure between this pressure tap and the injection corner of the 3D model. When the top valve is at the ΔP position and the bottom one is at the Vent position, we read absolute pressure at this tap. When the top one is at Loop and the bottom one is at Vent, the pressure transducer for this tap should read zero. These valves are also used to calibrate the pressure transducers before each experiment.

A.1.4 Demodulators and Heater Controllers

There are nine demodulators for the pressure transducers. They are used for calibrating transducer signals. Fig. A.3 shows the demodulators numbered from 1 to 9. The ninth one is for the back pressure transducer which is located on the side of the control panel (Fig. A.3). Two heater controllers are labeled A and B in Fig. A.3. Heater A is used to control the temperature of the steam generator, and Heater B controls the injection well temperature.

A.1.5 Gauges

The gauges are mainly located on the top section of the side of the control panel as shown in Fig. A.4. The ones used for reading injection pressures of nitrogen, steam and water are 100 psi gauges. The gauge located at the center is a precise Heise gauge with a range of 500 psi. This gauge shows the pressure in the main injection line. There is also a pressure indicator on the production line.

A.1.6 Data Logger Connection Ports

Data Logger connection ports are provided to connect the signals coming from the 3D model to the HP data logger which collects the data during the experiments. They are located at the left bottom of the side of the control panel as shown in Fig. A.4. While making connections the numbers on the ports should match those on the ribbon cables. The ribbon cables which come from the HP data logger are located in the computer room adjacent to the CT scanner.

A.2 Prerun Routine

In this section the basic routine that is followed before each run is explained. Prerun routine is a four-step procedure: 1. Signal connections, 2. Injection side connections, 3. Production side connections, and 4. Pressure line connections.

A.2.1 Signal Connections

The signal connection system is shown in Fig. A.5. Three sets of ribbon cable connect the HP data logger, in the computer room, to the control panel in the CT room.

One end of each of these ribbon cables is mounted on the wall in the computer room. The connections to the multiplexer boards of the HP data logger are made by a set of cables with one end permanently soldered to the boards. The definition of each signal and, its

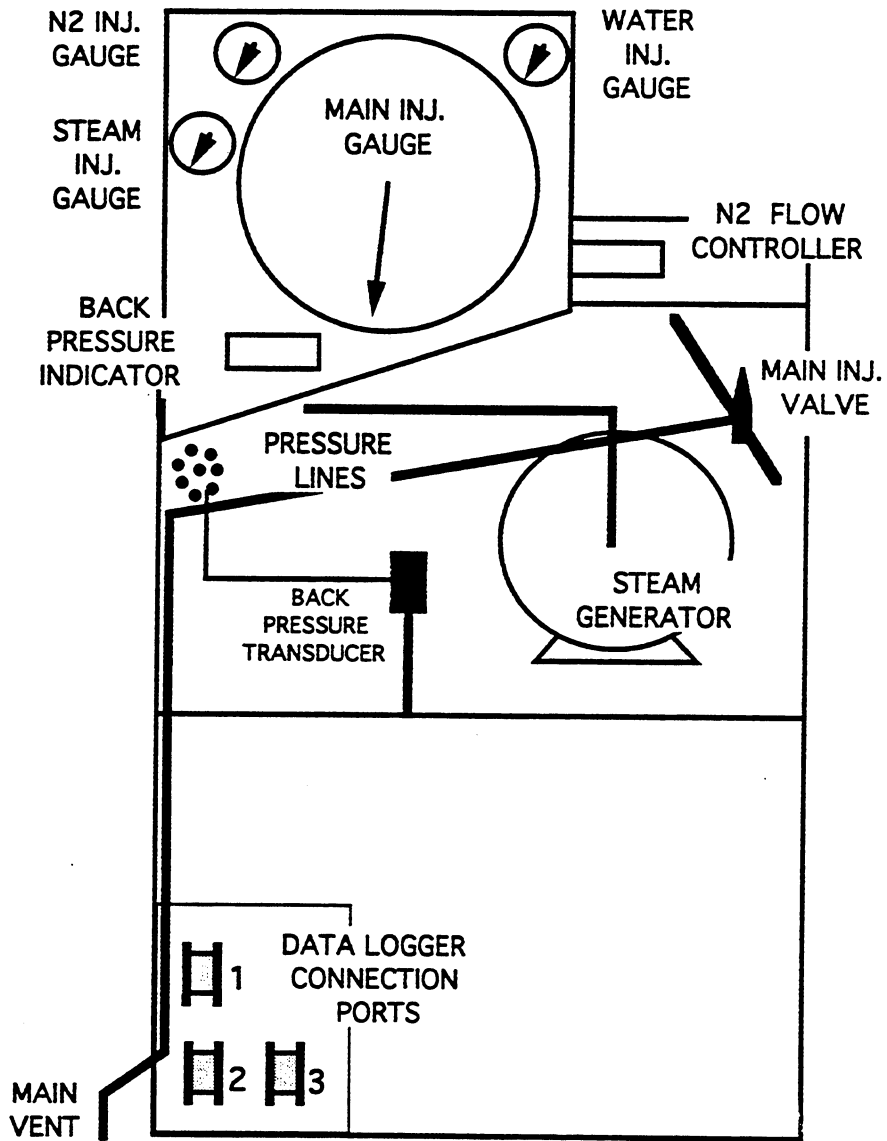


Figure A.4: Sideview of the Control Panel
 (Source: Demiral et al., 1992)

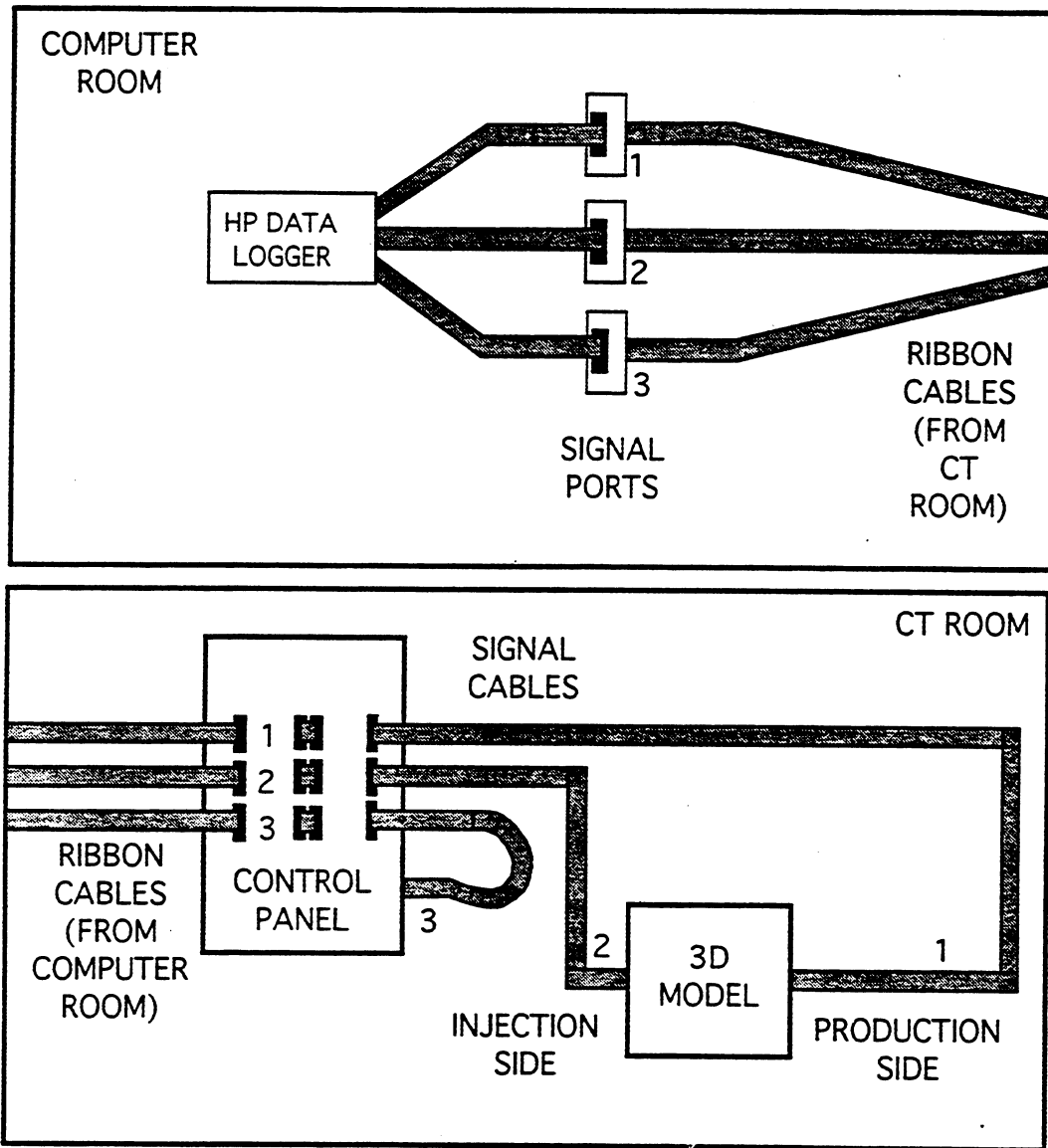


Figure A.5: Schematic of Signal Connection System
 (Source: Demiral et al., 1992)

connection location on the signal ports, channel number on the multiplexers and in the computer program, are shown in Tables A.1, A.2, and A.3.

The other ends of the ribbon cables are plugged into the data logger connection ports on the control panel.

The procedure below should be followed before each run:

1. Plug in the Ribbon Cables from the HP data logger to the matching signal ports on the wall.
2. Plug in the Ribbon Cables from the signal ports to the connection ports on the control panel. The numbers must match.
3. Plug in the three sets of signal cables coming from the 3D model and from the control panel, as follows:

Signal cable Number 1 is from the production side of the 3D model

Signal cable Number 2 is from the injection side of the model

Signal cable Number 3 is from the control panel.

A.2.2 Injection Side Connections

The schematic top view of the 3D model shown in Fig.A.6 is used to explain the necessary connections to be made before each run, at the injection side of the model. They are,

1. Bring the control panel close to the left side of the front table of the CT scanner.
2. Connect one end (C1 in Figure A.6) of the injection line to the main outlet of the control panel. Then connect the other end (C2) to the common side of the three-way injection valve (V1) of the 3D model.
3. Connect the main vent line to the other end of the same valve (V1).
4. Connect Line 4 to C4. This line is for a reference pressure for the pressure transducers.
5. Plug in signal Cable 2 to the matching port on the control panel.

Table A.1: Signal Connections on Signal Port 1
(Source: Demiral et al., 1992)

CABLE NO / CHANNEL NO	SIGNAL PORT CHANNEL NO	DATA LOGGER MULTIPX NO / CHANNEL NO	COMPUTER CODE CHANNEL NO	SIGNAL DEFINITION
3 / 1	+ 1 -2	1 / 00	00	Back Pressure Transducer
3 / 2	+ 3 -4	1 / 01	01	Pressure Transducer # 1
3 / 3	+ 5 -6	1 / 02	02	Pressure Transducer # 2
3 / 4	+ 7 -8	1 / 03	03	Pressure Transducer # 3
3 / 5	+ 9 -10	1 / 04	04	Pressure Transducer # 4
3 / 6	+11 -12	1 / 05	05	Pressure Transducer # 5
3 / 7	+13 -14	1 / 06	06	Pressure Transducer # 6
3 / 8	+15 -16	1 / 07	07	Pressure Transducer # 7
3 / 9	+17 -18	1 / 08	08	Pressure Transducer # 8
	+19 -20	1 / 09	09	
	+21 -22	1 / 10	10	
	+23 -24	1 / 11	11	
	+25 -26	1 / 12	12	
	+27 -28	1 / 13	13	
	+29 -30	1 / 14	14	
	+31/ 32	1 / 15	15	
	+33 -34	1 / 16	16	
	+35 -36	1 / 17	17	
	+37 -38	1 / 18	18	
	+39 -40	1 / 19	19	
2 / 1	+41 -42	2 / 00	20	Injection Well Thermocouple
2 / 2	+43 -44	2 / 01	21	Sandpack Thermocouple # 1
2 / 3	+45 -46	2 / 02	22	Sandpack Thermocouple # 2
1 / 1	+47 -48	2 / 03	23	Sandpack Thermocouple # 3
1 / 2	+49 -50	2 / 04	24	Sandpack Thermocouple # 4

Table A.2: Signal Connections on Signal Port 2
(Source: Demiral et al., 1992)

CABLE NO / CHANNEL NO	SIGNAL PORT CHANNEL NO	DATA LOGGER MULTIPX NO / CHANNEL NO	COMPUTER CODE CHANNEL NO	SIGNAL DEFINITION
2 / 4	+ 1 - 2	2 / 05	25	Sandpack Thermocouple # 5
2 / 5	+ 3 - 4	2 / 06	26	Sandpack Thermocouple # 6
1 / 3	+ 5 - 6	2 / 07	27	Sandpack Thermocouple # 7
2 / 6	+ 7 - 8	2 / 08	28	Sandpack Thermocouple #
2 / 7	+ 9 -10	2 / 09	29	Sandpack Thermocouple # 9
1 / 4	+11 -12	2 / 10	30	Sandpack Thermocouple # 10
2 / 8	+13 -14	2 / 11	31	Sandpack Thermocouple # 11
2 / 9	+15 -16	2 / 12	32	Sandpack Thermocouple # 12
1 / 5	+17 -18	2 / 13	33	Sandpack Thermocouple # 13
1 / 6	+19 -20	2 / 14	34	Sandpack Thermocouple # 14
2 / 11	+21 -22	2 / 15	35	Sandpack Thermocouple # 15
2 / 12	+23 -24	2 / 16	36	Sandpack Thermocouple # 16
1 / 9	+25 -26	2 / 17	37	Sandpack Thermocouple # 17
2 / 10	+27 -28	2 / 18	38	Sandpack Thermocouple # 18
1 / 7	+29 -30	2 / 19	39	Sandpack Thermocouple # 19
1 / 8	+31 -32	3 / 00	40	Sandpack Thermocouple # 20
2 / 14	+33 -34	3 / 01	41	Sandpack Thermocouple # 21
2 / 15	+35 -36	3 / 02	42	Sandpack Thermocouple # 22
1 / 10	+37 -38	3 / 03	43	Sandpack Thermocouple # 23
1 / 11	+39 -40	3 / 04	44	Sandpack Thermocouple # 24
2 / 16	+41 -42	3 / 05	45	Sandpack Thermocouple # 25
1 / 14	+43 -44	3 / 06	46	Sandpack Thermocouple # 26
1 / 12	+45 -46	3 / 07	47	Sandpack Thermocouple # 27
2 / 17	+47 -48	3 / 08	48	Sandpack Thermocouple # 28
1 / 13	+49 -50	3 / 09	49	Sandpack Thermocouple # 29

Table A.3: Signal Connections on Signal Port 3
(Source: Demiral et al., 1992)

CABLE NO / CHANNEL NO	SIGNAL PORT CHANNEL NO	DATA LOGGER MULTIPX NO / CHANNEL NO	COMPUTER CODE CHANNEL NO	SIGNAL DEFINITION
1 / 15	+ 1 - 2	3 / 10	50	Sandpack Thermocouple # 30
2 / 18	+ 3 - 4	3 / 11	51	Sandpack Thermocouple # 31
2 / 13	+ 5 - 6	3 / 12	52	Sandpack Thermocouple # 32
1 / 16	+ 7 - 8	3 / 13	53	Sandpack Thermocouple # 33
1 / 17	+ 9 -10	3 / 14	54	Sandpack Thermocouple # 34
3 / 22	+11 -12	3 / 15	55	Injection Line Thermocouple
1 / 20	+13 -14	3 / 16	56	Production Line Thermocouple
3 / 24	+15 -16	3 / 17	57	Steam Generator Thermocouple
3 / 25	+17 -18	3 / 18	58	Cold Junction Thermocouple
	+19 -20	3 / 19	59	
	+21 -22	4 / 00	60	
2 / 25	+23 -24	4 / 01	61	Heat Flux Sensor # 1
1 / 25	+25 -26	4 / 02	62	Heat Flux Sensor # 2
1 / 23	+27 -28	4 / 03	63	Heat Flux Sensor # 3
2 / 23	+29 -30	4 / 04	64	Heat Flux Sensor # 4
2 / 21	+31/ 32	4 / 05	65	Heat Flux Sensor # 5
	+33 -34	4 / 06	66	
2 / 24	+35 -36	4 / 07	67	Heat Flux Sensor Thermocouple # 1
1 / 24	+37 -38	4 / 08	68	Heat Flux Sensor Thermocouple # 2
1 / 22	+39 -40	4 / 09	69	Heat Flux Sensor Thermocouple # 3
2 / 22	+41 -42	4 / 10	70	Heat Flux Sensor Thermocouple # 4
2 / 20	+43 -44	4 / 11	71	Heat Flux Sensor Thermocouple # 5
	+45 -46	4 / 12	72	
	+47 -48	4 / 13	73	
	+49 -50		74	

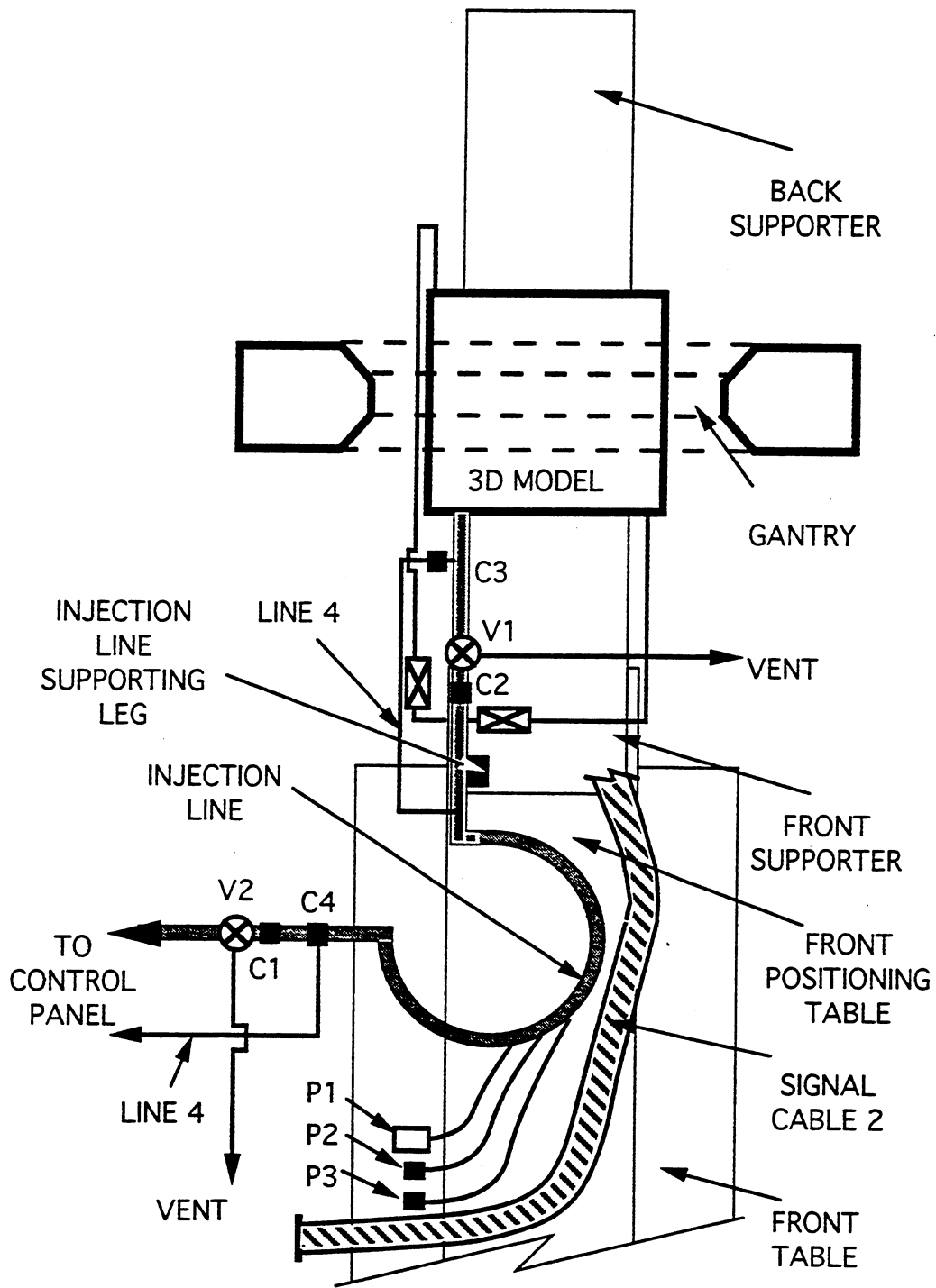


Figure A.6: Schematic of Injection Side Connections of 3D Model
 Source: Demiral et al., 1992)

6. Plug in wellbore heater power line (P1), wellbore heater thermocouple (P2), and injection line thermocouple to the corresponding plugs coming from the control panel.

A.2.3 Production Side Connections

In the production side of the 3D model following connections have to be made:

1. Plug in signal Cable 1 to its matching port on the control panel. Signal Cable 1 should be extended on the floor around the left side of the gantry.
2. Connect cooling water inlet and outlet lines to locations C1 and C2, shown in Figure A.7.
3. Connect production line to sample collector at V1, shown in Figure A.7.

A.2.4 Pressure Line Connections

The pressure lines numbered and labeled 1 to 9 are located at the injection side of the 3D model. These lines should be connected to the matching fittings on the CT side of the control panel before each experiment. The reference pressure line is also located at the same place, and the other end of Line 4 (Fig. A.6) should be connected there.

A.3 Computer Programs

Two types of data logging programs are used. One is for pressure transducer calibration and the other for data gathering during an experiment. Areal and sectional temperature distributions are plotted using another computer program and GRIDCON.

A.3.1 Pressure Transducer Calibration Program

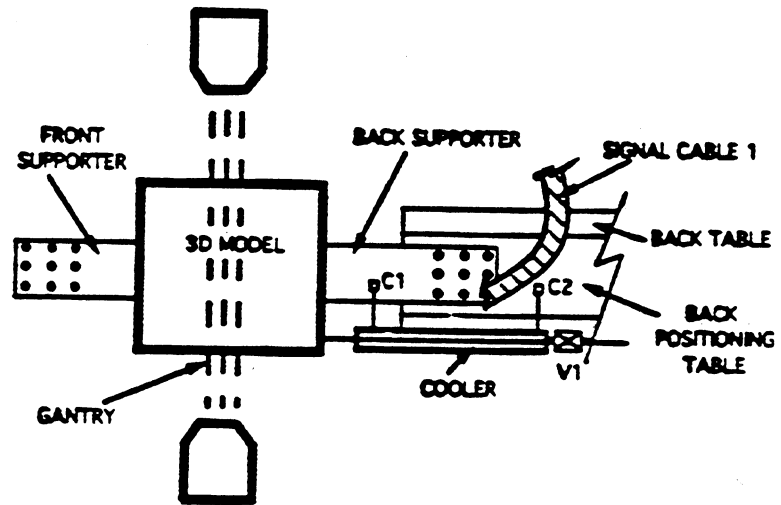


Figure A.7 Connections Schematic

The program for calibration of pressure transducers, "PRES3DCL.BAS", is written in basic. The program listing can be found in Appendix B. When the program is run, the screen looks like the one shown in Fig. A.8.

While running this program, demodulators are used to calibrate the pressure transducers. The zero knob on each demodulator is for zero adjustment when there is no pressure difference across the transducer, with its upper and bottom valves at the Vent position. The span knob is for pressure value adjustment after applying a pre-selected absolute pressure (maximum of 25 psi) over the transducer, with the upper valve at ΔP and the bottom valve at the Vent position on the transducer.

A.3.2 Data Logging Program

"STEAM3D.BAS", the data logging program is also written in BASIC. The program listing can be found in Appendix C. The output screen looks like the one shown in Fig. A.9. The program scans data every 30 seconds, writes them on an assigned datafile, and displays them on the screen. The color of the temperature values keep changing with increase in temperature, enabling the user to visually follow steam propagation in the 3D model.

A.3.3 Areal Temperature Distribution

Three level areal temperature data are prepared for the time steps corresponding to the times of scans of each slice. A software, called GRIDCON, is used to digitize these data and create gridded areal temperature distributions for the top, center and bottom of the model at the required times.

A.3.4 Sectional Temperature Distribution

The output data from the data logging program is used as input data for "Sections.f", a program written in FORTRAN, to generate sectional temperature data corresponding to the scan slice locations. The program listing can be found in Appendix D. This data is also

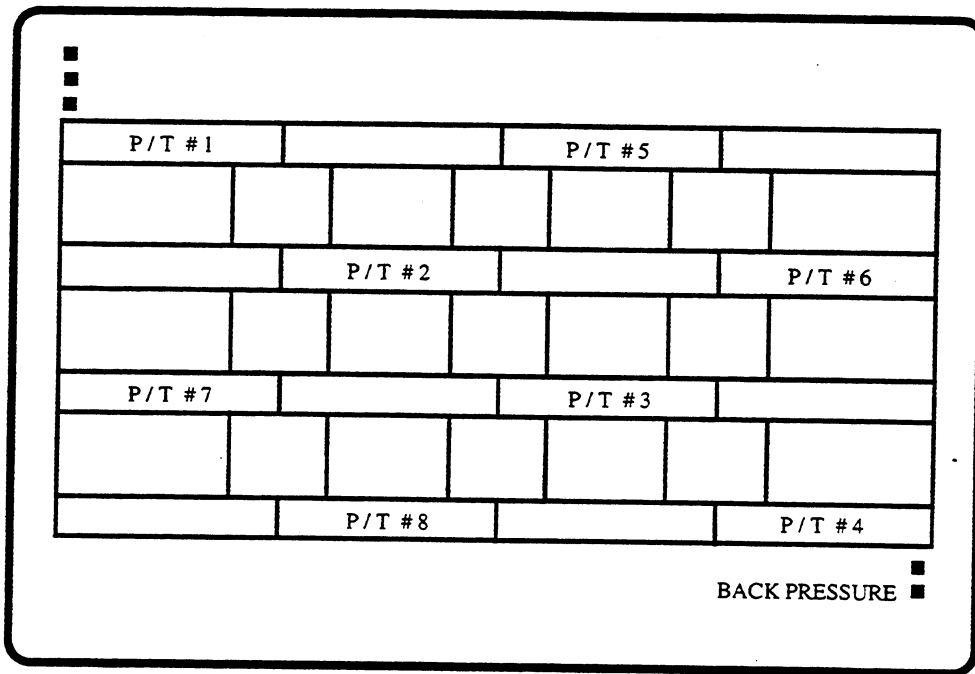
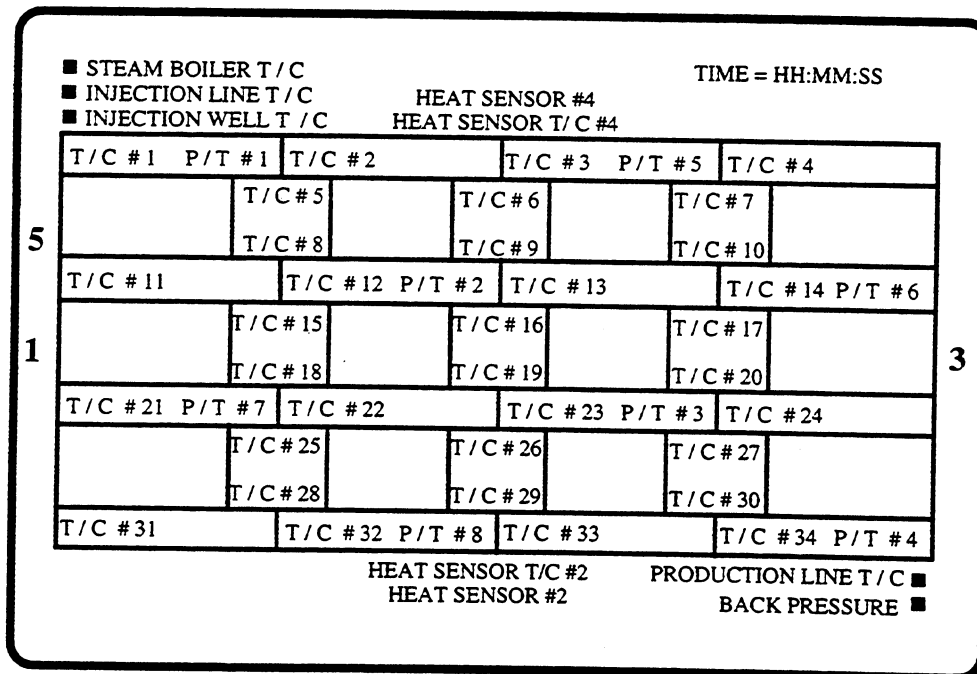


Figure A.8: Screen Appearance During Pressure Transducers Calibration
(Source: Demiral et al., 1992)



1 HEAT SENSOR #1
HEAT SENSOR T/C #1 3 HEAT SENSOR #3
HEAT SENSOR T/C #3 5 HEAT SENSOR #5
HEAT SENSOR T/C #5

Figure A.9: Screen Appearance During Data Logging
(Source: Demiral et al., 1992)

digitized, as above, using GRIDCON, creating gridded sectional temperature distributions at the required times for each slice.

APPENDIX B. COMPUTER PROGRAM FOR THE PRESSURE TRANSDUCER CALIBRATION

File Name: PRES3DCL.BAS

This program is available on the PC located in the combustion lab. Follow the steps below in order to run this program:

- (i) at C:\ type SET PCIB=C:\BAKUL
- (ii) at C:\ type cd sharma
- (iii) at C:\sharma type GWbasic
- (iv) then load "pres3dcl.bas"

```
1 '
2 ' Lines 5-570 are for initialization of the Data Logger
3 ' Lines 580-1000 are to draw 3D model on the screen
4 '
5 ' Copyright Hewlett-Packard 1984, 1985
10 '
15 ' Set up program for MS-DOS HP-IB I/O Library
20 ' For use independent of the PC instrument bus system
25 '
30 DEF SEG
35 CLEAR ,&HFE00
40 I=&HFE00
45 '
50 ' PCIB.DIR$ represents the directory where the library files
55 ' are located
60 ' PCIB is an environment variable which should be set from MS-DOS
65 ' i.e. A:> SET PCIB=A:\LIB
70 '
75 ' If there is insufficient environment space a direct assignment
80 ' can be made here, i.e
85 ' PCIB.DIR$ = "A:\LIB"
90 ' Using the environment variable is the preferred method
95 '
100 PCIB.DIR$ = ENVIRON$("PCIB")
105 I$ = PCIB.DIR$ + "\PCIBILC.BLD"
110 BLOAD I$,&HFE00
115 CALL I(PCIB.DIR$, I%, J%)
120 PCIB.SEG = I%
125 IF J%=0 THEN GOTO 160
130 PRINT "Unable to load.";
135 PRINT " (Error #";J%;")"
140 STOP
145 '
150 ' Define entry points for setup routines
155 '
160 DEF SEG = PCIB.SEG
```

```

165 O.S = 5
170 C.S = 10
175 I.V = 15
180 I.C = 20
185 L.P = 25
190 LD.FILE = 30
195 GET.MEM = 35
200 L.S = 40
205 PANELS = 45
210
215 Establish error variables and ON ERROR branching
220
225 DEF.ERR = 50
230 PCIB.ERR$ = STRING$(64,32)
235 PCIB.NAMES$ = STRING$(16,32)
240 CALL DEF.ERR(PCIB.ERR,PCIB.ERR$,PCIB.NAMES$,PCIB.GLBERR)
245 PCIB.BASERR = 255
250 ON ERROR GOTO 410
255
260 J=-1
265 I$=PCIB.DIR$+"HPIB.SYN"
270 CALL O.S(I$)
275 IF PCIB.ERR<>0 THEN ERROR PCIB.BASERR
280
285 Determine entry points for HP-IB Library routines
290
295 I=0
300 CALL I.V(I,IOABORT,IOCLEAR,IOCONTROL,IOENTER)
305 IF PCIB.ERR<>0 THEN ERROR PCIB.BASERR
310 CALL I.V(I,IOENTERA,IOENTERS,IOEOI,IOEOL)
315 IF PCIB.ERR<>0 THEN ERROR PCIB.BASERR
320 CALL I.V(I,IOGETTERM,IOLLOCKOUT,IOLOCAL,IOMATCH)
325 IF PCIB.ERR<>0 THEN ERROR PCIB.BASERR
330 CALL I.V(I,IOOUTPUT,IOOUTPUTA,IOOUTPUTS,IOPPOLL)
335 IF PCIB.ERR<>0 THEN ERROR PCIB.BASERR
340 CALL I.V(I,IOPPOLL,IOPELLU,IOREMOTE,IORESET)
345 IF PCIB.ERR<>0 THEN ERROR PCIB.BASERR
350 CALL I.V(I,IOSEND,IOSPOLL,IOSTATUS,IOTIMEOUT)
355 IF PCIB.ERR<>0 THEN ERROR PCIB.BASERR
360 CALL I.V(I,IOTRIGGER,IODMA,J,J)
365 IF PCIB.ERR<>0 THEN ERROR PCIB.BASERR
370 CALL C.S
375 I$=PCIB.DIR$+"HPIB.PLD"
380 CALL L.P(I$)
385 IF PCIB.ERR<>0 THEN ERROR PCIB.BASERR
390 GOTO 475
395
400 Error handling routine
405
410 IF ERR=PCIB.BASERR THEN GOTO 425

```

```

415 PRINT "BASIC error #";ERR;" occurred in line ";ERL
420 STOP
425 TMPERR = PCIB.ERR
430 IF TMPERR = 0 THEN TMPERR = PCIB.GLBERR
435 PRINT "PC Instrument error #";TMPERR;" detected at line ";ERL
440 PRINT "Error: ";PCIB.ERR$
445 STOP
450
455 COMMON declarations are needed if your program is going to chain
460 to other programs. When chaining, be sure to call DEF.ERR as
465 well upon entering the chained-to program
470
475 COMMON PCIB.DIR$,PCIB.SEG
480 COMMON LD.FILE,GET.MEM,PANELS,DEF.ERR
485 COMMON PCIB.BASERR,PCIB.ERR,PCIB.ERR$,PCIB.NAMES$, PCIB.GLBERR
490 COMMON IOABORT,IOCLEAR,IOCONTROL,IOENTER,IOENTERA,
IOENTERS, IOEOI,IOEOL,IOGETTERM,IOLLOCKOUT,IOLLOCAL,
IOMATCH,IOOUTPUT,IOOUTPUTA,IOOUTPUTS,IOPPOLL, IOPPOLLC,
IOPPOLLU,IOREMOTE,IORESET,IOSEND,IOSPOLL,IOSTATUS,
IOTIMEOUT,IOTRIGGER,IODMA
495
500 FALSE = 0
505 TRUE = NOT FALSE
510 NOERR = 0
515 EUNKNOWN = 100001!
520 ESEL = 100002!
525 ERANGE = 100003!
530 ETIME = 100004!
535 ECTRL = 100005!
540 EPASS = 100006!
545 ENUM = 100007!
550 EADDR = 100008!
555 COMMON FALSE, TRUE, NOERR, EUNKNOWN, ESEL, ERANGE, ETIME,
ECTRL, EPASS, ENUM, EADDR
560
565 End Program Set-up
570 User program can begin anywhere past this point
580 COLOR 14,0
590 CLS
670 LOCATE 4,8:PRINT " ":LOCATE 4,9:PRINT STRING$(63," ")
680 LOCATE 4,72:PRINT " "
690 LOCATE 4,9:PRINT " "
700 FOR I=5 TO 21
710 LOCATE I,8:PRINT " ":LOCATE I,72:PRINT " "
720 NEXT
730 LOCATE 21,8:PRINT " ":LOCATE 21,9:PRINT STRING$(63," "):
740 LOCATE 21,72:PRINT " "
750 FOR I=6 TO 18 STEP 5
760 LOCATE I,8:PRINT " ":LOCATE I,9:PRINT STRING$(63," "):LOCATE I,72:
PRINT " "

```

```

770 LOCATE I+3,8:PRINT " ":LOCATE I+3,9:PRINT STRING$(63," "):
LOCATE I+3,72:PRINT " "
780 NEXT I
790 FOR I=5 TO 21 STEP 5
800 FOR J=24 TO 56 STEP 16
810 LOCATE I,J:PRINT " "
820 NEXT J:NEXT I
830 FOR J=24 TO 56 STEP 16
840 LOCATE 4,J:PRINT " "
850 LOCATE 21,J:PRINT " "
860 NEXT J
870 FOR I=6 TO 17 STEP 5
880 FOR J=24 TO 56 STEP 16
890 LOCATE I,J:PRINT " "
900 LOCATE I+3,J:PRINT " "
910 NEXT J:NEXT I
920 FOR I=6 TO 17 STEP 5
930 FOR J=20 TO 61 STEP 16
940 LOCATE I,J:PRINT " "
950 LOCATE I,J+8:PRINT " "
960 LOCATE I+3,J:PRINT " "
970 LOCATE I+3,J+8:PRINT " "
980 NEXT J:NEXT I
990 FOR I=7 TO 18 STEP 5
991 FOR J=20 TO 61 STEP 16
992 LOCATE I,J:PRINT " "
993 LOCATE I,J+8:PRINT " "
994 LOCATE I+1,J:PRINT " "
995 LOCATE I+1,J+8:PRINT " "
996 NEXT J:NEXT I
997 LOCATE 21,71:PRINT " "
998 LOCATE 22,71:PRINT " "
999 '
1000 '
1001 ' PRESSURE TRANSDUCER CALIBRATION PROGRAM
1002 ' NOVEMBER 1989
1003 '
1005 ' INITIALIZE TIMER
1010 TIMES$="00:00:00"
1070 OPTION BASE 1
1075 ' SET UP ARRAYS
1080 DIM P0(5),P1(5),P2(5),P3(5),P4(5),P5(5),P6(5),P7(5),P8(5)
1200 ' Initialize Data Logger
1210 ISC=7
1220 DEV=709
1230 CALL IORESET (ISC)
1250 TIMEOUT = 5
1255 MAXI=5
1260 CALL IOTIMEOUT (ISC, TIMEOUT)
1280 CALL IOCLEAR (ISC)

```

```

1300 CALL IOREMOTE (ISC)
1310 CODE$="SISO1VA0VF1VS0"
1320 LENGTH=LEN(CODE$)
1330 CALL IOOUTPUTS (DEV,CODE$,LENGTH)
1340 '
1362 ' BEGIN DATA LOGGING
1363 '
1364 ' READ CHANNEL 0 (BACK PRESSURE TRANSDUCER)
1365 '
1440 CODE$="AC0VN5"
1448 LENGTH=6
1450 CALL IOOUTPUTS (DEV,CODE$,LENGTH)
1455 CALL IOENTERA (DEV,P0(1),MAXI,ACTUAL)
1456 '
1460 ' READ CHANNEL 1 TO 8 (SYSTEM PRESSURE TRANSDUCERS)
1461 '
1465 CODE$="AC1"
1470 LENGTH=3
1475 CALL IOOUTPUTS (DEV,CODE$,LENGTH)
1480 CALL IOENTERA (DEV,P1(1),MAXI,ACTUAL)
1490 CODE$="AC2"
1495 CALL IOOUTPUTS (DEV,CODE$,LENGTH)
1500 CALL IOENTERA (DEV,P2(1),MAXI,ACTUAL)
1510 CODE$="AC3"
1515 CALL IOOUTPUTS (DEV,CODE$,LENGTH)
1520 CALL IOENTERA (DEV,P3(1),MAXI,ACTUAL)
1530 CODE$="AC4"
1535 CALL IOOUTPUTS (DEV,CODE$,LENGTH)
1540 CALL IOENTERA (DEV,P4(1),MAXI,ACTUAL)
1550 CODE$="AC5"
1555 CALL IOOUTPUTS (DEV,CODE$,LENGTH)
1560 CALL IOENTERA (DEV,P5(1),MAXI,ACTUAL)
1570 CODE$="AC6"
1575 CALL IOOUTPUTS (DEV,CODE$,LENGTH)
1580 CALL IOENTERA (DEV,P6(1),MAXI,ACTUAL)
1585 CALL IOOUTPUTS (DEV,CODE$,LENGTH)
1590 CODE$="AC7"
1595 CALL IOOUTPUTS (DEV,CODE$,LENGTH)
1600 CALL IOENTERA (DEV,P7(1),MAXI,ACTUAL)
1610 CODE$="AC8"
1615 CALL IOOUTPUTS (DEV,CODE$,LENGTH)
1620 CALL IOENTERA (DEV,P8(1),MAXI,ACTUAL)
2110 '
2115 ' AVERAGE VALUES FOR THE MV PRESSURE VALUES
2116 '
2120 AP0=(P0(1)+P0(2)+P0(3)+P0(4)+P0(5))/5!
2130 AP1=(P1(1)+P1(2)+P1(3)+P1(4)+P1(5))/5!
2140 AP2=(P2(1)+P2(2)+P2(3)+P2(4)+P2(5))/5!
2150 AP3=(P3(1)+P3(2)+P3(3)+P3(4)+P3(5))/5!
2160 AP4=(P4(1)+P4(2)+P4(3)+P4(4)+P4(5))/5!

```

```

2170 AP5=(P5(1)+P5(2)+P5(3)+P5(4)+P5(5))/5!
2175 AP6=(P6(1)+P6(2)+P6(3)+P6(4)+P6(5))/5!
2180 AP7=(P7(1)+P7(2)+P7(3)+P7(4)+P7(5))/5!
2190 AP8=(P8(1)+P8(2)+P8(3)+P8(4)+P8(5))/5!
2200 PB=2.5*AP0
2210 PT1=2.5*AP1
2220 PT2=2.5*AP2
2230 PT3=2.5*AP3
2240 PT4=2.5*AP4
2250 PT5=2.5*AP5
2260 PT6=2.5*AP6
2270 PT7=2.5*AP7
2280 PT8=2.5*AP8
4500
4510 PRINTING THE RESULTS ON SCREEN
4511
4525 COLOR 12,0
4550 LOCATE 5,9:PRINT "PT#1
4560 LOCATE 15,9:PRINT "PT#7
4570 LOCATE 10,25:PRINT "PT#2
4580 LOCATE 20,25:PRINT "PT#8
4590 LOCATE 5,41:PRINT "PT#5
4600 LOCATE 15,41:PRINT "PT#3
4610 LOCATE 10,57:PRINT "PT#6
4620 LOCATE 20,57:PRINT "PT#4
4630 LOCATE 23,57:PRINT "BP"
5000 LOCATE 5,15:PRINT USING "####.##";PT1
5010 LOCATE 15,15:PRINT USING "####.##";PT7
5020 LOCATE 10,31:PRINT USING "####.##";PT2
5030 LOCATE 20,31:PRINT USING "####.##";PT8
5040 LOCATE 5,47:PRINT USING "####.##";PT5
5050 LOCATE 15,47:PRINT USING "####.##";PT3
5060 LOCATE 10,63:PRINT USING "####.##";PT6
5070 LOCATE 20,63:PRINT USING "####.##";PT4
5080 LOCATE 23,63:PRINT USING "####.##";PB
5800 GOTO 1340
5980 END

```

APPENDIX C. COMPUTER PROGRAM FOR DATA LOGGING

File Name: STEAM3D.BAS

This program is available on the PC located in the combustion lab. Follow the steps below in order to run this program:

- (i) at C:\ type SET PCIB=C:\BAKUL
- (ii) at C:\ type cd sharma
- (iii) at C:\sharma type GWbasic
- (iv) then load "steam3d.bas"

```
1 '
2 ' Lines 5-570 are for initialization of Data-Logger
3 ' Lines 570-1000 are to draw the 3D model on the screen
4 '
5 ' Copyright Hewlett-Packard 1984, 1985
10 '
15 ' Set up program for MS-DOS HP-IB I/O Library
20 ' For use independent of the PC instrument bus system
25 '
30 DEF SEG
35 CLEAR ,&HFE00
40 I=&HFE00
45 '
50 ' PCIB.DIR$ represents the directory where the library files
55 ' are located
60 ' PCIB is an environment variable which should be set from MS-DOS
65 ' i.e. A:> SET PCIB=A:\LIB
70 '
75 ' If there is insufficient environment space a direct assignment
80 ' can be made here, i.e
85 ' PCIB.DIR$ = "A:\LIB"
90 ' Using the environment variable is the preferred method
95 '
100 PCIB.DIR$ = ENVIRON$("PCIB")
105 IS = PCIB.DIR$ + "\PCIBILC.BLD"
110 BLOAD IS,&HFE00
115 CALL I(PCIB.DIR$, I%, J%)
120 PCIB.SEG = I%
125 IF J%=0 THEN GOTO 160
130 PRINT "Unable to load.";
135 PRINT " (Error #";J%;")"
140 STOP
145 '
150 ' Define entry points for setup routines
155 '
160 DEF SEG = PCIB.SEG
165 O.S = 5
170 C.S = 10
```

```

175 I.V = 15
180 I.C = 20
185 L.P = 25
190 LD.FILE = 30
195 GET.MEM = 35
200 L.S = 40
205 PANELS = 45
210 '
215 ' Establish error variables and ON ERROR branching
220 '
225 DEF.ERR = 50
230 PCIB.ERR$ = STRING$(64,32)
235 PCIB.NAMES$ = STRING$(16,32)
240 CALL DEF.ERR(PCIB.ERR,PCIB.ERR$,PCIB.NAMES$,PCIB.GLBERR)
245 PCIB.BASERR = 255
250 ON ERROR GOTO 410
255 '
260 J=-1
265 I$=PCIB.DIR$+"HPIB.SYN"
270 CALL O.S(I$)
275 IF PCIB.ERR<>0 THEN ERROR PCIB.BASERR
280 '
285 ' Determine entry points for HP-IB Library routines
290 '
295 I=0
300 CALL I.V(I,IOABORT,IOCLEAR,IOCONTROL,IOENTER)
305 IF PCIB.ERR<>0 THEN ERROR PCIB.BASERR
310 CALL I.V(I,IOENTERA,IOENTERS,IOEOI,IOEOL)
315 IF PCIB.ERR<>0 THEN ERROR PCIB.BASERR
320 CALL I.V(I,IOGETTERM,IOLLOCKOUT,IOLOCAL,IOMATCH)
325 IF PCIB.ERR<>0 THEN ERROR PCIB.BASERR
330 CALL I.V(I,IOOUTPUT,IOOUTPUTA,IOOUTPUTS,IOPPOLL)
335 IF PCIB.ERR<>0 THEN ERROR PCIB.BASERR
340 CALL I.V(I,IOPPOLL,IOREMOTE,IORESET)
345 IF PCIB.ERR<>0 THEN ERROR PCIB.BASERR
350 CALL I.V(I,IOSEND,IOSPOLL,IOSTATUS,IOTIMEOUT)
355 IF PCIB.ERR<>0 THEN ERROR PCIB.BASERR
360 CALL I.V(I,IOTRIGGER,IODMA,J,J)
365 IF PCIB.ERR<>0 THEN ERROR PCIB.BASERR
370 CALL C.S
375 I$=PCIB.DIR$+"HPIB.PLD"
380 CALL L.P(I$)
385 IF PCIB.ERR<>0 THEN ERROR PCIB.BASERR
390 GOTO 475
395 '
400 ' Error handling routine
405 '
410 IF ERR=PCIB.BASERR THEN GOTO 425
415 PRINT "BASIC error #";ERR;" occurred in line ";ERL
420 STOP

```

```

425  TMPERR = PCIB.ERR
430  IF TMPERR = 0 THEN TMPERR = PCIB.GLBERR
435  PRINT "PC Instrument error #";TMPERR;" detected at line ";ERL
440  PRINT "Error: ";PCIB.ERR$
445  STOP
450
455  COMMON declarations are needed if your program is going to chain
460  to other programs. When chaining, be sure to call DEF.ERR as
465  well upon entering the chained-to program
470
475  COMMON PCIB.DIR$,PCIB.SEG
480  COMMON LD.FILE,GET.MEM,PANELS,DEF.ERR
485  COMMON PCIB.BASERR,PCIB.ERR,PCIB.ERR$,PCIB.NAMES$,
    PCIB.GLBERR
490  COMMON IOABORT,IOCLEAR,IOCONTROL,IOENTER,IOENTERA,
    IOENTERS,IOEOL,IOEOL,IOGETTERM,IOLLOCKOUT,IOLLOCAL,
    IOMATCH,IOOUTPUT,IOOUTPUTA,IOOUTPUTS,IOPPOLL,IOPPOLLC,
    IOPPOLLU,IOREMOTE,IORESET,IOSEND,IOSPOLL,IOSTATUS,
    IOTIMEOUT,IOTRIGGER,IODMA
495
500  FALSE  = 0
505  TRUE   = NOT FALSE
510  NOERR  = 0
515  EUNKNOWN = 100001!
520  ESEL   = 100002!
525  ERANGE = 100003!
530  ETIME  = 100004!
535  ECTRL  = 100005!
540  EPASS  = 100006!
545  ENUM   = 100007!
550  EADDR  = 100008!
555  COMMON FALSE, TRUE, NOERR, EUNKNOWN, ESEL, ERANGE, ETIME,
    ECTRL, EPASS, ENUM, EADDR
560
565  End Program Set-up
570  User program can begin anywhere past this point
575  KEY OFF
585  CLS
595  GOSUB 10000
600  LOCATE 1,9:PRINT " "
610  LOCATE 1,50:PRINT "TIME = "
650  LOCATE 2,9:PRINT " "
660  LOCATE 3,9:PRINT " "
670  LOCATE 4,8:PRINT " ":LOCATE 4,9:PRINT STRING$(63," ")
680  LOCATE 4,72:PRINT " "
690  LOCATE 4,9:PRINT " "
700  FOR I=5 TO 21
710  LOCATE I,8:PRINT " ":LOCATE I,72:PRINT " "
720  NEXT
730  LOCATE 21,8:PRINT " ":LOCATE 21,9:PRINT STRING$(63," ")

```

```

740 LOCATE 21,72:PRINT " "
750 FOR I=6 TO 18 STEP 5
760 LOCATE I,8:PRINT " ":LOCATE I,9:PRINT STRING$(63," "):LOCATE I,72:
    PRINT " "
770 LOCATE I+3,8:PRINT " ":LOCATE I+3,9:PRINT STRING$(63," "):
    LOCATE I+3,72:PRINT " "
780 NEXT I
790 FOR I=5 TO 21 STEP 5
800 FOR J=24 TO 56 STEP 16
810 LOCATE I,J:PRINT " "
820 NEXT J:NEXT I
830 FOR J=24 TO 56 STEP 16
840 LOCATE 4,J:PRINT " "
850 LOCATE 21,J:PRINT " "
860 NEXT J
870 FOR I=6 TO 17 STEP 5
880 FOR J=24 TO 56 STEP 16
890 LOCATE I,J:PRINT " "
900 LOCATE I+3,J:PRINT " "
910 NEXT J:NEXT I
920 FOR I=6 TO 17 STEP 5
930 FOR J=20 TO 61 STEP 16
940 LOCATE I,J:PRINT " "
950 LOCATE I,J+8:PRINT " "
960 LOCATE I+3,J:PRINT " "
970 LOCATE I+3,J+8:PRINT " "
980 NEXT J:NEXT I
990 FOR I=7 TO 18 STEP 5
991 FOR J=20 TO 61 STEP 16
992 LOCATE I,J:PRINT " "
993 LOCATE I,J+8:PRINT " "
994 LOCATE I+1,J:PRINT " "
995 LOCATE I+1,J+8:PRINT " "
996 NEXT J:NEXT I
997 LOCATE 21,71:PRINT " "
998 LOCATE 22,71:PRINT " "
999 KEY OFF
1000 ' 3 D M O D E L
1010 ' STEAM INJECTION DATA LOGGING PROGRAM
1020 ' B I R O L D E M I R A L
1030 ' JULY 1990
1040 ' REVISED IN DECEMBER 1994 by BAKUL SHARMA
1050 '
1060 '
1070 ' INITIALIZE TIMER
1080 ' TIMES$="00:00:00"
1090 ' SET UP ARRAYS
1100 ' OPTION BASE 1
1110 ' DIM PT(90),TC(1000),APT(9),ATC(40),T(40),AT(5)
1120 ' DIM HF1(50),HF2(50),HF3(50),HF4(50),HF5(50)

```

```

1130 DIM HT1(50),HT2(50),HT3(50),HT4(50),HT5(50)
1140 '
1150 ' N O M E N C L A T U R E
1160 '
1170 ' PT = Signal From Pressure Transducers
1180 ' TC = Signal From Thermocouples
1190 ' APT = Average Pressure Values, mv
1200 ' ATC = Average Temperature Values, mv
1205 ' T = Average Temperature Values, deg C
1210 ' HF1 = Signal From Heat Flux Sensor #1
1220 ' HF2 = Signal From Heat Flux Sensor #2
1230 ' HF3 = Signal From Heat Flux Sensor #3
1240 ' HF4 = Signal From Heat Flux Sensor #4
1250 ' HF5 = Signal From Heat Flux Sensor #5
1260 ' HT1 = Signal From Heat Flux Sensor Thermocouple #1
1270 ' HT2 = Signal From Heat Flux Sensor Thermocouple #2
1280 ' HT3 = Signal From Heat Flux Sensor Thermocouple #3
1290 ' HT4 = Signal From Heat Flux Sensor Thermocouple #4
1300 ' HT5 = Signal From Heat Flux Sensor Thermocouple #5
1310 ' AHF1 = Average Heat Flux Value at #1
1320 ' AHF2 = Average Heat Flux Value at #2
1330 ' AHF3 = Average Heat Flux Value at #3
1340 ' AHF4 = Average Heat Flux Value at #4
1350 ' AHF5 = Average Heat Flux Value at #5
1360 ' AHT1 = Average Temperature at #1
1370 ' AHT2 = Average Temperature at #2
1380 ' AHT3 = Average Temperature at #3
1390 ' AHT4 = Average Temperature at #4
1400 ' AHT5 = Average Temperature at #5
1405 ' AT = Average Temperature Values for AHT's, deg C
1435 '
1440 ' INITIALIZE DATA LOGGER
1450 '
1460 ISC=7
1470 DEV=709
1475 CALL IORESET(ISC)
1480 CALL IOTIMEOUT(ISC,TIMEOUT)
1490 CALL IOCLEAR(ISC)
1495 CALL IOREMOTE(ISC)
1500 CODE$="SISO1SD1VA0VF1VS0AF00AL99"
1510 LENGTH=LEN(CODE$)
1520 CALL IOOUTPUTS(DEV,CODE$,LENGTH)
1523 ON TIMER (30) GOSUB 1530
1524 TIMER ON
1525 GOTO 1525
1526 END
1530 '
1540 ' BEGIN DATA LOGGING
1550 '
1560 ' READ CHANNEL 00 (BACK PRESSURE TRANSDUCER)

```

```

1565 '
1570 '
1580 CODE$="AC00VN10VR5"
1590 LENGTH=LEN(CODE$)
1600 MAXI=10
1605 ACTUAL=10
1610 CALL IOOUTPUTS(DEV,CODE$,LENGTH)
1620 CALL IOENTERA(DEV,PT(1),MAXI,ACTUAL)
1630 '
1640 ' READ CHANNELS 01 TO 08 (PRESSURE TRANSDUCERS)
1650 '
1660 CODE$="ASVN10"
1670 LENGTH=LEN(CODE$)
1680 FOR I=1 TO 8
1690 CALL IOOUTPUTS(DEV,CODE$,LENGTH)
1700 CALL IOENTERA(DEV,PT(10*I+1),MAXI,ACTUAL)
1710 NEXT I
1720 '
1730 ' READ CHANNEL 20 (INJECTION WELL THERMOCOUPLE)
1740 CODE$="AC20VN3VR1"
1750 LENGTH=LEN(CODE$)
1760 MAXI=3
1765 ACTUAL=3
1770 CALL IOOUTPUTS(DEV,CODE$,LENGTH)
1775 CALL IORESET(ISC)
1776 TIMEOUT=5
1780 CALL IOENTERA(DEV,TC(1),MAXI,ACTUAL)
1790 '
1800 ' READ CHANNELS 21 TO 58 (SANDPACK,INJECTION LINE,
1810 '           BOILER AND REFERENCE
1820 '           THERMOCOUPLES)
1830 '
1840 CODE$="ASVN3"
1850 LENGTH=5
1855 MAXI=3
1856 ACTUAL=3
1860 FOR I=1 TO 38
1870 CALL IOOUTPUTS(DEV,CODE$,LENGTH)
1880 CALL IOENTERA(DEV,TC(3*I+1),MAXI,ACTUAL)
1890 NEXT I
1900 '
1910 ' READ CHANNELS 61 TO 65 (HEAT FLUX SENSORS, 10 READING
1920 '           PER TRIGGER, 5 TRIGGERS)
1930 '
1940 FOR I=0 TO 4
1950 MAXI=10
1955 ACTUAL=10
1960 CODE$="AC61VR1VN10"
1970 LENGTH=LEN(CODE$)
1980 CALL IOOUTPUTS(DEV,CODE$,LENGTH)

```

```

1990 CALL IOENTERA(DEV,HF1(10*I+1),MAXI,ACTUAL)
2000 CODE$="AC62VR1VN10"
2010 CALL IOOUTPUTS(DEV,CODE$,LENGTH)
2020 CALL IOENTERA(DEV,HF2(10*I+1),MAXI,ACTUAL)
2030 CODE$="AC63VR1VN10"
2040 CALL IOOUTPUTS(DEV,CODE$,LENGTH)
2050 CALL IOENTERA(DEV,HF3(10*I+1),MAXI,ACTUAL)
2060 CODE$="AC64VR1VN10"
2070 CALL IOOUTPUTS(DEV,CODE$,LENGTH)
2080 CALL IOENTERA(DEV,HF4(10*I+1),MAXI,ACTUAL)
2090 CODE$="AC65VR1VN10"
2100 CALL IOOUTPUTS(DEV,CODE$,LENGTH)
2110 CALL IOENTERA(DEV,HF5(10*I+1),MAXI,ACTUAL)
2120 '
2130 ' READ CHANNELS 67 TO 71 (HEAT FLUX SENSOR
2140 '         THERMOCOUPLES, 3 READINGS
2150 '         PER TRIGGER, 5 TRIGGERS)
2160 '
2170 MAXI=3
2175 ACTUAL=3
2180 CODE$="AC67VN3"
2190 LENGTH=LEN(CODE$)
2200 CALL IOOUTPUTS(DEV,CODE$,LENGTH)
2210 CALL IOENTERA(DEV,HT1(3*I+1),MAXI,ACTUAL)
2220 CODE$="AC68VN3"
2230 CALL IOOUTPUTS(DEV,CODE$,LENGTH)
2240 CALL IOENTERA(DEV,HT2(3*I+1),MAXI,ACTUAL)
2250 CODE$="AC69VN3"
2260 CALL IOOUTPUTS(DEV,CODE$,LENGTH)
2270 CALL IOENTERA(DEV,HT3(3*I+1),MAXI,ACTUAL)
2280 CODE$="AC70VN3"
2290 CALL IOOUTPUTS(DEV,CODE$,LENGTH)
2300 CALL IOENTERA(DEV,HT4(3*I+1),MAXI,ACTUAL)
2310 CODE$="AC71VN3"
2320 CALL IOOUTPUTS(DEV,CODE$,LENGTH)
2330 CALL IOENTERA(DEV,HT5(3*I+1),MAXI,ACTUAL)
2340 NEXT I
2350 '
2360 ' CALCULATE AVERAGE PRESSURE SIGNALS
2370 '
2380 FOR I=1 TO 9
2390 APT(I)=0
2400 NEXT I
2410 FOR J=0 TO 8
2420 FOR I=1 TO 10
2430     APT(J+1)=APT(J+1)+PT(I+J*10)/10!
2440 NEXT I
2450 NEXT J
2451 '
2452 ' CALCULATE REAL PRESSURE VALUES IN PSI'S

```

```

2453 '
2454 FOR I=1 TO 9
2455 APT(I)=APT(I)*2.5
2456 NEXT I
2460 '
2470 ' CALCULATE AVERAGE TEMPERATURE SIGNALS
2480 '
2490 FOR I=1 TO 39
2500 ATC(I)=(TC(3*I-2)+TC(3*I-1)+TC(3*I))/3!
2510 NEXT I
2520 '
2530 ' CALCULATE AVERAGE VALUES FOR HEAT FLUX INTERMS OF VOLTS
2540 '
2550 AHF1=0:AHF2=0:AHF3=0:AHF4=0:AHF5=0
2560 FOR I=1 TO 50
2570 AHF1=AHF1+HF1(I)*20
2580 AHF2=AHF2+HF2(I)*20
2590 AHF3=AHF3+HF3(I)*20
2600 AHF4=AHF4+HF4(I)*20
2610 AHF5=AHF5+HF5(I)*20
2620 NEXT I
2630 '
2640 ' CALC. AVERAGE VALUES FOR HEAT FLUX SENSOR THERMOCOUPLES
2650 '
2660 AHT1=0:AHT2=0:AHT3=0:AHT4=0:AHT5=0
2670 FOR I=1 TO 15
2680 AHT1=AHT1+HT1(I)/15!
2690 AHT2=AHT2+HT2(I)/15!
2700 AHT3=AHT3+HT3(I)/15!
2710 AHT4=AHT4+HT4(I)/15!
2720 AHT5=AHT5+HT5(I)/15!
2730 NEXT I
2790 '
2800 ' CALL SUBROUTINE TO CONVERT TYPE-J THERMOCOUPLE SIGNAL
2810 ' TO TEMPERATURE (DEG C) USING CHANNEL 58 AS THE COLD
2820 ' JUNCTION REFERENCE
2830 '
2840 FOR I=1 TO 38
2850 EMF=(ATC(I)-ATC(39))*1000!
2860 GOSUB 6000
2870 T(I)=TEMP
2880 NEXT I
2890 EMF=-ATC(39)*1000!
2900 GOSUB 6000
2910 T(39)=TEMP
2920 '
2930 ' CALL SUBROUTINES TO CONVERT TYPE-T THERMOCOUPLE SIGNALS
2940 ' TO TEMPERATURE (DEG C) FOR HEAT FLUX SENSOR
THERMOCOUPLES
2950 ' USING THE TYPE-J SIGNAL FROM COLD JUNCTION REFERENCE

```

```

2960 '
3000 TEMP=T(39)
3010 GOSUB 8000
3020 ET=EMF
3030 EMF=AHT1*1000+ET
3040 GOSUB 7000
3050 AT(1)=TEMP
3060 EMF=AHT2*1000+ET
3070 GOSUB 7000
3080 AT(2)=TEMP
3090 EMF=AHT3*1000+ET
3100 GOSUB 7000
3110 AT(3)=TEMP
3120 EMF=AHT4*1000+ET
3130 GOSUB 7000
3140 AT(4)=TEMP
3150 EMF=AHT5*1000+ET
3160 GOSUB 7000
3170 AT(5)=TEMP
4500 '
4510 ' PRINTING THE RESULTS ON SCREEN
4520 '
4530 COLOR 15,0
4540 LOCATE 1,58:BEEP:PRINT USING "\  \";TIMES
4550 COLOR 2,0
4551 K=38:GOSUB 9000
4560 LOCATE 1,11:PRINT USING "###.##";T(38)
4561 K=36:GOSUB 9000
4570 LOCATE 2,11:PRINT USING "###.##";T(36)
4571 K=1:GOSUB 9000
4580 LOCATE 3,11:PRINT USING "###.##";T(1)
4581 K=37:GOSUB 9000
4590 LOCATE 22,65:PRINT USING "###.##";T(37)
4595 COLOR 5,0:LOCATE 23,64:PRINT USING "###.###";APT(1)
4600 '
4610 COLOR 12,0
4620 I=2
4630 FOR J=5 TO 20 STEP 5
4631 K=I:GOSUB 9000
4640 LOCATE J,9:PRINT USING "###.##";T(I)
4641 K=I+1:GOSUB 9000
4650 LOCATE J,25:PRINT USING "###.##";T(I+1)
4651 K=I+2:GOSUB 9000
4660 LOCATE J,41:PRINT USING "###.##";T(I+2)
4661 K=I+3:GOSUB 9000
4670 LOCATE J,57:PRINT USING "###.##";T(I+3)
4680 I=I+10
4690 NEXT J
4700 COLOR 10,0
4710 I=6

```

```

4720 FOR J=7 TO 17 STEP 5
4721 K=I:GOSUB 9000
4730 LOCATE J,21:PRINT USING "###.##";T(I)
4731 K=I+1:GOSUB 9000
4740 LOCATE J,37:PRINT USING "###.##";T(I+1)
4741 K=I+2:GOSUB 9000
4750 LOCATE J,53:PRINT USING "###.##";T(I+2)
4760 I=I+10:NEXT J
4770 COLOR 9,0
4780 I=9
4790 FOR J=8 TO 18 STEP 5
4791 K=I:GOSUB 9000
4800 LOCATE J,21:PRINT USING "###.##";T(I)
4801 K=I+1:GOSUB 9000
4810 LOCATE J,37:PRINT USING "###.##";T(I+1)
4811 K=I+2:GOSUB 9000
4820 LOCATE J,53:PRINT USING "###.##";T(I+2)
4830 I=I+10:NEXT J
4840 COLOR 5,0
4850 LOCATE 5,16:PRINT USING "###.#####";APT(2)
4860 LOCATE 15,16:PRINT USING "###.#####";APT(8)
4870 LOCATE 10,32:PRINT USING "###.#####";APT(3)
4880 LOCATE 20,32:PRINT USING "###.#####";APT(9)
4890 LOCATE 5,48:PRINT USING "###.#####";APT(6)
4900 LOCATE 15,48:PRINT USING "###.#####";APT(4)
4910 LOCATE 10,64:PRINT USING "###.#####";APT(7)
4920 LOCATE 20,64:PRINT USING "###.#####";APT(5)
4930 COLOR 13,0
4940 LOCATE 2,37:PRINT USING "##.###";AHF4
4945 K=40:T(K)=AT(4):GOSUB 9000
4950 LOCATE 3,37:PRINT USING "###.##";AT(4)
4960 K=40:T(K)=AT(2):GOSUB 9000
4979 LOCATE 22,37:PRINT USING "###.##";AT(2)
4980 COLOR 13,0:LOCATE 23,37:PRINT USING "##.###";AHF2
4990 LOCATE 12,1:PRINT USING "##.###";AHF1
5000 K=40:T(K)=AT(1):GOSUB 9000
5010 LOCATE 13,1:PRINT USING "###.##";AT(1)
5020 COLOR 13,0:LOCATE 12,73:PRINT USING "##.###";AHF3
5030 K=40:T(K)=AT(3):GOSUB 9000
5040 LOCATE 13,73:PRINT USING "###.##";AT(3)
5050 COLOR 13,0:LOCATE 8,1:PRINT USING "##.###";AHF5
5060 K=40:T(K)=AT(5):GOSUB 9000
5070 LOCATE 9,1:PRINT USING "###.##";AT(5)
5500 '
5510 ' PRINTING THE RESULTS ON DATA FILE A:THREEDIM.DAT
5520 '
5530 PRINT #1, USING "\ \";TIMES$
5540 PRINT #1, USING "###.## ###.## ###.## ###.## ###.##";T(38),
T(36),T(1),T(37),T(39)
5550 PRINT #1, USING "###.## ###.## ###.## ###.##";T(2),T(3),T(4),T(5)

```

```

5560 PRINT #1, USING "###.## ###.## ###.##";T(6),T(7),T(8)
5570 PRINT #1, USING "###.## ###.## ###.##";T(9),T(10),T(11)
5580 PRINT #1, USING "###.## ###.## ###.##";T(12),T(13),T(14),T(15)
5590 PRINT #1, USING "###.## ###.## ###.##";T(16),T(17),T(18)
5600 PRINT #1, USING "###.## ###.## ###.##";T(19),T(20),T(21)
5610 PRINT #1, USING "###.## ###.## ###.##";T(22),T(23),T(24),T(25)
5620 PRINT #1, USING "###.## ###.## ###.##";T(26),T(27),T(28)
5630 PRINT #1, USING "###.## ###.## ###.##";T(29),T(30),T(31)
5640 PRINT #1, USING "###.## ###.## ###.##";T(32),T(33),T(34),T(35)
5650 PRINT #1, USING "###.##### ###.##### ###.##### ###.#####
###.##### ###.#####";APT(1),APT(2),APT(3),APT(4),APT(5),
APT(6),APT(7),APT(8)
5660 PRINT #1, USING "##.### ##.### ##.### ##.### ##.###";AHF1,AHF2,
AHF3,AHF4,AHF5
5670 PRINT #1, USING "###.## ###.## ###.## ###.## ###.##";AHT1,AHT2,
AHT3,AHT4,AHT5
5680 RETURN
5690 END
6000 '
6010 ' TYPE-J THERMOCOUPLE CONVERSION PROGRAM mV to deg C
6020 '
6030 IERR=0
6040 IF EMF<3.556 THEN TEMP=-.00426+EMF*(19.8555+EMF*(-
.22977+.0126037*EMF)):
GOTO 6120
6050 IF EMF<10.237 THEN TEMP=.44759+EMF*(19.4947+EMF*(-
.13669+.0042424*EMF)):
GOTO 6120
6060 IF EMF<17.467 THEN TEMP=4.04157+EMF*(18.4682+EMF*(-
.03744+.00102*EMF)):
GOTO 6120
6070 IF EMF<25.285 THEN TEMP=19.70136+EMF*(15.839+EMF*(.11042-
.0017662*EMF)):
GOTO 6120
6080 IF EMF<33.437 THEN TEMP=24.3252+EMF*(15.0696+EMF*(.14958-
.0023976*EMF)):
GOTO 6120
6090 IF EMF<38.171 THEN TEMP=-89.9797+EMF*(25.2779+EMF*(-
.15467+.0006286*EMF)):
GOTO 6120
6100 TEMP=1219.255+EMF*(-71.5862+EMF*(2.2309-.018928*EMF))
6110 IF EMF < -.995 OR EMF > 42.922 THEN IERR=1
6120 RETURN
7000 '
7010 ' TYPE-T THERMOCOUPLE CONVERSION PROGRAM mV to deg C
7020 '
7030 IERR=0
7040 IF EMF<3.44 THEN TEMP=-.01102+EMF*(25.887+EMF*(-
.69704+.025629*EMF)):
GOTO 7080

```

```

7050 IF EMF<7.3 THEN TEMP=1.0147+EMF*(25.1566+EMF*(-
      .53147+.014117*EMF)):
      GOTO 7080
7060 TEMP=3.32158+EMF*(24.14043+EMF*(-.38292+.006906*EMF))
7070 IF EMF < -.005 OR EMF > 11.5 THEN IERR=1
7080 RETURN
8000 '
8010 ' TYPE-T THERMOCOUPLE CONVERSION PROGRAM deg C TO mV
8020 '
8030 IERR=0
8040 EMF=.00103+TEMP*(.038596+.000041*TEMP)
8050 IF TEMP < 10 OR TEMP > 30 THEN IERR=1
8060 RETURN
9000 '
9010 ' COLOR ADJUSMENT WITH RESPECT TO TEMPERATURE
9020 '
9030 IF T(K)<=50!, THEN COLOR 2,0
9040 IF T(K)>50! AND T(K)<=60!, THEN COLOR 2,0
9050 IF T(K)>60! AND T(K)<=70!, THEN COLOR 10,0
9060 IF T(K)>70! AND T(K)<=80!, THEN COLOR 3,0
9070 IF T(K)>80! AND T(K)<=90!, THEN COLOR 11,0
9080 IF T(K)>90! AND T(K)<=100!, THEN COLOR 14,0
9090 IF T(K)>100! AND T(K)<=110!, THEN COLOR 6,0
9100 IF T(K)>110! AND T(K)<=120!, THEN COLOR 12,0
9110 IF T(K)>120!, THEN COLOR 4,0
9120 RETURN
9130 END
10000 COLOR 9,0
10010 LOCATE 3,19:PRINT " ":LOCATE 3,20:PRINT STRING$(42," "):
      LOCATE 3,62:PRINT " "
10015 LOCATE 4,19:PRINT " ":LOCATE 4,62:PRINT " "
10020 LOCATE 5,19:PRINT " ":LOCATE 5,62:PRINT " "
10025 LOCATE 6,19:PRINT " ":LOCATE 6,62:PRINT " "
10030 LOCATE 7,19:PRINT " ":LOCATE 7,62:PRINT " "
10040 LOCATE 8,19:PRINT " ":LOCATE 8,62:PRINT " "
10050 LOCATE 9,19:PRINT " ":LOCATE 9,62:PRINT " "
10060 LOCATE 10,19:PRINT " ":LOCATE 10,62:PRINT " "
10070 LOCATE 11,19:PRINT " ":LOCATE 11,62:PRINT " "
10075 LOCATE 12,19:PRINT " ":LOCATE 12,62:PRINT " "
10080 LOCATE 13,19:PRINT " ":LOCATE 13,20:PRINT STRING$(42," "):
      LOCATE 13,62:PRINT " "
10090 LOCATE 5,20:COLOR 12,0:PRINT "          STANFORD UNIVERSITY"
10100 LOCATE 6,20:PRINT "          PETROLEUM RESEARCH INSTITUTE"
10110 LOCATE 8,20:PRINT "          3 DIMENSIONAL STEAM INJECTION MODEL"
10115 LOCATE 9,20:PRINT "          DATA LOGGING PROGRAM by BIROL DEMIRAL"
10117 LOCATE 11,20:PRINT "          REVISED by BAKUL SHARMA, DEC 1994"
10118 '
10120 ' CREATE AND OPEN DATA FILE
10130 '
10140 COLOR 9,0

```

```
10150 LOCATE 16,9:PRINT " ":LOCATE 16,10:PRINT STRING$(61," "):  
      LOCATE 16,71:PRINT" "  
10160 LOCATE 17,9:PRINT "  
      "  
10170 LOCATE 18,9:PRINT " ":LOCATE 18,10:PRINT STRING$(61," "):  
      LOCATE 18,71:PRINT" "  
10180 LOCATE 18,10:PRINT STRING$(61," ")  
10190 LOCATE 17,11:COLOR 10,0:PRINT "PLEASE ENTER THE NAME OF  
      TODAY'S DATA FILE  
10200 LOCATE 17,54:COLOR 12,0:INPUT FILENAME$  
10210 COLOR 15,0  
10220 OPEN FILENAME$ FOR APPEND AS #1  
10225 CLS  
10230 RETURN  
10240 END
```

APPENDIX D. COMPUTER PROGRAM FOR DATA PREPARATION FOR
SECTIONAL TEMPERATURE DISTRIBUTIONS

File Name: Sections.f

This FORTRAN program is available on the PC located in the combustion lab. The data logger output file serves as its input.

C CALCULATION OF AREAL TEMPERATURE DISTRIBUTION

C AUTHOR: BAKUL SHARMA

```

C
C
C
C
parameter(N=40)
real T(N)
real ST(N,N)
open(UNIT=10, FILE='adata.in', STATUS='old')
open(UNIT=11, FILE='asectiona.out', STATUS='new')
open(UNIT=12, FILE='asectionb.out', STATUS='new')
open(UNIT=13, FILE='asectionc.out', STATUS='new')
open(UNIT=14, FILE='asectiond.out', STATUS='new')
open(UNIT=15, FILE='asectione.out', STATUS='new')
open(UNIT=16, FILE='asectionf.out', STATUS='new')
read(10,*) (T(I), I=1,39)
do 500 k=1,6
do 150 I=1,3
if (k.EQ.1) go to 99
if (k.EQ.2) go to 109
if (k.EQ.3) go to 119
if (k.EQ.4) go to 129
if (k.EQ.5) go to 139
if (k.EQ.6) go to 149
99 ST(19,37-(I-1)*12) = T(10*I)+(T(10*I)-T(10*I+1))/4.0
ST(1,37-(I-1)*12) = T(10*I+3)+(T(10*I+3)-T(10*I+4))/4.0
go to 150
109 ST(19,37-(I-1)*12) = T(10*I)-(T(10*I)-T(10*I+1))/4.0
ST(1,37-(I-1)*12) = T(10*I+3)-(T(10*I+3)-T(10*I+4))/4.0
go to 150
119 ST(19,37-(I-1)*12) = T(10*I+1)+(T(10*I)-T(10*I+1))/4.0
ST(1,37-(I-1)*12) = T(10*I+4)+(T(10*I+3)-T(10*I+4))/4.0
go to 150
129 ST(19,37-(I-1)*12) = T(10*I+1)-(T(10*I+1)-T(10*I+2))/4.0
ST(1,37-(I-1)*12) = T(10*I+4)-(T(10*I+4)-T(10*I+5))/4.0
go to 150
139 ST(19,37-(I-1)*12) = T(10*I+2)+(T(10*I+1)-T(10*I+2))/4.0
ST(1,37-(I-1)*12) = T(10*I+5)+(T(10*I+4)-T(10*I+5))/4.0
go to 150
149 ST(19,37-(I-1)*12) = T(10*I+2)-(T(10*I+1)-T(10*I+2))/4.0
ST(1,37-(I-1)*12) = T(10*I+5)-(T(10*I+4)-T(10*I+5))/4.0
150 continue
do 300 I=1,4

```

```

    if (k.EQ.1) go to 160
    if (k.EQ.2) go to 165
    if (k.EQ.3) go to 170
    if (k.EQ.4) go to 175
    if (k.EQ.5) go to 180
    if (k.EQ.6) go to 185
160  ST(10,43-(I-1)*12) = T(10*I-4)-(T(10*I-4)-T(10*I-3))/4.0
    go to 300
165  ST(10,43-(I-1)*12) = T(10*I-3)+(T(10*I-4)-T(10*I-3))/4.0
    go to 300
170  ST(10,43-(I-1)*12) = T(10*I-3)-(T(10*I-3)-T(10*I-2))/4.0
    go to 300
175  ST(10,43-(I-1)*12) = T(10*I-2)+(T(10*I-3)-T(10*I-2))/4.0
    go to 300
180  ST(10,43-(I-1)*12) = T(10*I-2)-(T(10*I-2)-T(10*I-1))/4.0
    go to 300
185  ST(10,43-(I-1)*12) = T(10*I-1)+(T(10*I-2)-T(10*I-1))/4.0
300  continue
310  do 315 I=43,7,-12
    write(10+k,*) 50-I,10,ST(10,I)
315  continue
    do 319 I=37,13,-12
    write(10+k,*) 50-I,19,ST(19,I)
    write(10+k,*) 50-I,1,ST(1,I)
319  continue
500  continue
    stop
    end

```

APPENDIX E. COMPUTER PROGRAMS FOR 2-PHASE and 3-PHASE SATURATION MEASUREMENTS

File Name: wf.imp (for 2-Phase) and 3phsat.imp (for 3-Phase)

Author: Bakul Sharma

These programs are written for image processing, and are available for use on the PC located in the CT scanner control room. infile_a and infile_b are the names of the image files to be processed.

Program For 2-Phase Saturation Measurements

```
infile_a
infile_b
outfile subt1.fl

print " starting Process"

process begin
#
# Enter Your Calcs Below:

out = ina - inb

# End of Calcs
#
process end

infile_a
infile_b
outfile subt4.fl

print " starting Process"

process begin
#
# Enter Your Calcs Below:

out = ina - inb
out = out / 0.9

# End of Calcs
#
process end

infile_a subt1.fl
infile_b subt4.fl
outfile subt5.fl
```

```
tiff so5.tif

window = 1.00
level = 0.50

print " starting Process"

process begin
#
# Enter Your Calcs Below:

inb = inb + .0001
out = ina / inb

# End of Calcs
#
process end

infile_a subt5.flr
outfile subt6.flr

tiff sw6.tif

window = 1.00
level = 0.50

print " starting Process"

process begin
#
# Enter Your Calcs Below:

out = 1.0 - ina

# End of Calcs
#
process end

exit
```

Program For 3-Phase Saturation Measurements

```
infile_a
infile_b
outfile subt1.flt

print " starting Process"

process begin
#
# Enter Your Calcs Below:

out = ina - inb

# End of Calcs
#
process end

infile_a
infile_b
outfile subt2.flt

print " starting Process"

process begin
#
# Enter Your Calcs Below:

out = ina - inb
out = out / 0.9

# End of Calcs
#
process end

infile_a
infile_b
outfile subt3.flt

print " starting Process"

process begin
#
# Enter Your Calcs Below:

out = ina - inb

# End of Calcs
#
```

```
process end

infile_a
infile_b
outfile subt4.fl

print " starting Process"

process begin
#
# Enter Your Calcs Below:

out = ina - inb

out = out / 0.9

# End of Calcs
#
process end

infile_a
infile_b
outfile subt5.fl

print " starting Process"

process begin
#
# Enter Your Calcs Below:

out = ina - inb

# End of Calcs
#
process end

infile_a
infile_b
outfile subt6.fl

print " starting Process"

process begin
#
# Enter Your Calcs Below:

out = ina - inb

# End of Calcs
#
```

```
process end

infile_a subt5.fl
infile_b subt2.fl
outfile subt7.fl

print " starting Process"

process begin
#
# Enter Your Calcs Below:

out = ina * inb

# End of Calcs
#
process end

infile_a subt6.fl
infile_b subt4.fl
outfile subt8.fl

print " starting Process"

process begin
#
# Enter Your Calcs Below:

out = ina * inb

# End of Calcs
#
process end

infile_a subt7.fl
infile_b subt8.fl
outfile subt9.fl

print " starting Process"

process begin
#
# Enter Your Calcs Below:

out = ina - inb

# End of Calcs
#
process end
```

```

infile_a subt1.flit
infile_b subt2.flit
outfile subt10.flit

print " starting Process"

process begin
#
# Enter Your Calcs Below:

out = ina * inb

# End of Calcs
#
process end

infile_a subt3.flit
infile_b subt4.flit
outfile subt11.flit

print " starting Process"

process begin
#
# Enter Your Calcs Below:

out = ina * inb

# End of Calcs
#
process end

infile_a subt10.flit
infile_b subt11.flit
outfile subt12.flit

print " starting Process"

process begin
#
# Enter Your Calcs Below:

out = ina - inb

# End of Calcs
#
process end

infile_a subt12.flit
infile_b subt9.flit

```

```

outfile subt13.flr
tiff sg13.tif

window = 1.00
level = 0.50

print " starting Process"

process begin
#
# Enter Your Calcs Below:

inb = inb + .0001
out = ina / inb

# End of Calcs
#
process end

infile_a subt1.flr
infile_b subt6.flr
outfile subt14.flr

print " starting Process"

process begin
#
# Enter Your Calcs Below:

out = ina * inb

# End of Calcs
#
process end

infile_a subt3.flr
infile_b subt5.flr
outfile subt15.flr

print " starting Process"

process begin
#
# Enter Your Calcs Below:

out = ina * inb

# End of Calcs

```

```

#
process end

infile_a subt14.flr
infile_b subt15.flr
outfile subt16.flr

print " starting Process"

process begin
#
# Enter Your Calcs Below:

out = ina - inb

# End of Calcs
#
process end

infile_a subt16.flr
infile_b subt9.flr
outfile subt17.flr

tiff so17.tif

window = 1.00
level = 0.50

print " starting Process"

process begin
#
# Enter Your Calcs Below:

inb = inb + .0001
inb = 0 - inb
out = ina / inb

# End of Calcs
#
process end

infile_a subt13.flr
infile_b subt17.flr
outfile subt18.flr

tiff sw18.tif

window = 1.00
level = 0.50

```

```
print " starting Process"
```

```
process begin
```

```
#
```

```
# Enter Your Calcs Below:
```

```
ina = 1 - ina
```

```
out = ina - inb
```

```
# End of Calcs
```

```
#
```

```
process end
```

```
exit
```

